Computational Aspects of Spectral Invariants

Michael Bironneau

Doctoral Thesis

submitted in partial fulfillment of the requirements for award of

Doctor of Philosophy of Loughborough University

August 30th, 2014

Abstract. The spectral theory of the Laplace operator has long been studied in connection with physics. It appears in the wave equation, the heat equation, Schrödinger's equation and in the expression of quantum effects such as the Casimir force. The Casimir effect can be studied in terms of spectral invariants computed entirely from the spectrum of the Laplace operator. It is these spectral invariants and their computation that are the object of study in the present work.

The objective of this thesis is to present a computational framework for the spectral zeta function $\zeta(s)$ and its derivative on a Euclidean domain in $\mathbb{R}^2$, with rigorous theoretical error bounds when this domain is polygonal. To obtain error bounds that remain practical in applications an improvement to existing heat trace estimates is necessary. Our main result is an original estimate and proof of a heat trace estimate for polygons that improves the one of van den Berg and Srisatkunarajah ([**75**]), using finite propagation speed of the corresponding wave kernel. We then use this heat trace estimate to obtain a rigorous error bound for $\zeta(s)$ computations. We will provide numerous examples of our computational framework being used to calculate $\zeta(s)$ for a variety of situations involving a polygonal domain, including examples involving cutouts and extrusions that are interesting in applications.

Our second result is the development a new eigenvalue solver for a planar polygonal domain using a partition of unity decomposition technique. Its advantages include multiple precision and ease of use, as well as reduced complexity compared to Finite Elemement Method. While we hoped that it would be able to contend with existing packages in terms of speed, our implementation was many times slower than MPSPack when dealing with the same problem (obtaining the first 5 digits of the principal eigenvalue of the regular unit hexagon).

Finally, we present a collection of numerical examples where we compute the spectral determinant and Casimir energy of various polygonal domains. We also use our numerical tools to investigate extremal properties of these spectral invariants. For example, we consider a square with a small square cut out of the interior, which is allowed to rotate freely about its center.

Acknowledgements. First and foremost, I would like to thank my supervisor Dr. Alexander Strohmaier for giving me the opportunity to undertake this research and for his steadfast and energetic support as well as his devotion to excellence. I would also like to thank other members of our research group who were always there to answer questions and help me learn.

Everyone else who helped me on the way: you know who you are and how you helped, and you know I am grateful for it.

Contents

Part 1

Background

CHAPTER 1

Introduction

1.1. Historical context

In this thesis we study the spectral theory of the Laplace operator on a planar domain. The Laplace operator Δ has been a popular object of study in mathematics since the early 19th century, when Pierre-Simon de Laplace first used it to study celestial mechanics. Since then, it has appeared in many areas of mathematics and physics. Laplace's equation, $\Delta f = 0$, has far-reaching applications in applied mathematics. Laplace's operator often appears in spectral theory, where it is studied via the equation $(\Delta - \lambda)f = 0$ for a function f that does not uniformly vanish on its domain. The values of λ that allow a solution of this equation to be found - called the eigenvalues of Δ -have physical interpretations in both classical and quantum mechanics. For this reason their properties have been extensively analyzed.

The solutions of the equation $(\Delta - \lambda)f = 0$ depend of course on the boundary conditions (if any) that one imposes on f. It is then natural to ask: what information can we deduce about the geometry of the boundary from the spectrum of Δ? As has been shown long ago by Hermann Weyl ([**77**]), the area contained within this boundary can be deduced from the spectrum. Under certain assumptions we can also recover a wealth of other information such as the length of the boundary and certain functions of its curvature (see eg. [**33**]). For a class of analytic domains, Steve Zelditch has even shown that one can reconstruct the domain entirely just from the spectrum and knowledge of an isolated periodic orbit (see [**80**]).

In 1967, Mark Kac ([**45**]) asked how far this relationship extends in his famous paper "Can one hear the shape of a drum?". The question asks whether it is impossible for two manifolds to have the same Laplacian spectrum whilst having different geometries - that is, whether it is impossible for two geometries to be isospectral but not isometric. John Milnor, very soon after Kac asked the question, constructed two higher dimensional isospectral tori, demonstrating that it was actually quite possible. Notwithstanding, it remained an open problem whether examples could be found in lower dimensions until 1992, when Gordon, Webb, and Wolpert ([**34**]) constructed two polygons that had different shapes but the same eigenvalues.

In the present paper we consider special quantities constructed from the spectrum called "spectral invariants". These are constants that depend only on the spectrum that we will define precisely later on. In particular, we use the spectral zeta function to create such invariants. We are interested in the forward problem, that is, how the geometry affects these spectral invariants. We will focus our attention on two spectral invariants that have extensive applications in physics: the spectral determinant and the Casimir energy.

The spectral determinant is in some sense a generalization of the determinant of a matrix. Because the Laplace operator can have (and, in our setting, does

have) infinitely many eigenvalues, it does not make sense to consider the usual determinant that is obtained by taking the product of all eigenvalues. However, as we will see, it is possible to construct a function whose derivative is formally equal to this product at some point and which we can analytically continue to the entire complex plane, therefore allowing us to regularize the infinite product. This regularization method, mainly invented by Hardy and Littlewood in 1916 (see for example Theorem 2.12 in [**38**]), preserves a wealth of geometric information owing to the geometric interpretation of the heat invariants used to construct it.

The main physical application of the spectral determinant in quantum physics lies in the computation of the effective action, a quantum analogue of the action, which associates to each path in a system a real number. The effective action accounts for quantum-mechanical corrections. We do not focus on the physics of the problem but on its analytical and computational aspects, providing an automated tool to compute the spectral determinants of planar domains, with rigorous error bound for polygons. As one application of our tool we will investigate the extremal properties of the spectral determinant for irregular n-sided polygons of a fixed area, providing evidence that the spectral determinant is maximized by the regular polygon in that class.

The extremal properties of the determinant have been studied by some authors. Namely, Phillips, Osgood, and Sarnak showed that within a conformal class, the round metric maximizes the spectral determinant (see [**58**]). Klein, Kokotov and Korotkin investigated extremal properties of the determinant in moduli spaces (see [**47**]). Aurell and Salomonson investigate the limiting behavior of the spectral determinant in regular polygons, as the number of sides becomes very large but the area remains constant (see [**5**]). They conclude that the spectral determinant of the disk is a supremum of the spectral determinants of the n-sided regular polygons of fixed area as n tends to infinity. It is an open problem to show that the regular polygon maximizes the spectral determinant within the class of n-sided polygons of a fixed area.

The second spectral invariant that we will focus on is the Casimir energy. In simple terms, the Casimir effect is a force that arises between two perfectly conducting metallic plates, separated by micrometers in a vaccum. Its name is due to its discoverer, Hendrik Casimir, who first studied it in 1947 shortly after publishing a paper on intermolecular forces ([**19**]). It was first observed in a laboratory setting in 1958 (see [**65**]) and is now a very active object of experimental study in quantum physics (see eg. [**?, 83, ?**]). As of now the dependence of the Casimir energy on the geometry of the domain remains an open question, and this is important in several fields related to nanoengineering, one of them being microelectronics (see eg. [**16, 51, 62**]). Indeed, as electronics are manufactured on smaller scales, forces on the micro scale such as the Casimir force become more important in considering circuit and component design (see eg. [**83**] for a discussion of the influence of the geometry of a silicone chip on the Casimir forces affecting it). Shape optimization with regards to the Casimir force and by extension, extremal properties of Casimir energy, is therefore an interesting subject to physics, and to identify attractors between which there is negative Casimir energy density, a theoretical possibility, remains an open problem (see [**29**]). We will apply our novel computational tools to problems that have remained difficult using standard methods.

Currently, there are several "standard" frameworks to compute the Casimir energy of arbitrary geometries (see eg. [**4**] for a detailed discussion). However, none of them have rigorous theoretical error bounds and they suffer from numerical instabilities when dealing with particularly narrow geometries (for example, when a hole in a domain approaches a boundary), as described for example in [**66**]. Nonetheless, these tools have proved useful in geometric optimization problems, where one tries to find the best "shape" to minimize Casimir interactions (see eg. [**56**], [**43**] and the recent pre-print [**3**]).

1.2. Motivation and Structure

Our objective in this paper is to provide a method for rigorous computation of the spectral determinant and Casimir energy in polygonal domains (and indeed, a general framework for the computation of the spectral zeta function and its derivative). We will also provide a semi-rigorous approach that works for more general domains (Lipschitz and piecewise smooth boundary). Moreover we provide an automated method of making such computations in Matlab and Mathematica using the freely available package MPSPack by Alex Barnett. This package is based on the Method of Particular Solutions, revived recently by Timo Betcke and Lloyd Trefethen (see [**14**]). To aid in our task we develop an improved estimate of the small-time heat trace in polygons using finite propagation speed of the wave kernel, building on the work of van den Berg and Srisatkunarajah ([**75**]). We also verify our spectral determinant computations for examples of polygonal domains using a formula of Aurell and Salomonson for the spectral determinant (see [**5**]). This formula also allows us to evaluate how sharp our error estimates are.

Finally, we use our computational framework to conduct some numerical investigations into the Casimir energy of cutouts, that is, of a polygon with another smaller polygon excluded from its interior, with Dirichlet boundary conditions throughout. In particular we are interested in investigating the extremal behavior of the Casimir energy for rotating cutouts, that is, to see how it behaves when the interior domain is rotated around its center. This problem is interesting to physics and nanoengineering.

The structure of this thesis will be as follows. First, we set out the foundation in functional analysis and spectral theory that are necessary for a coherent understanding of this thesis. Next, we perform a calculation to express the spectral zeta function in terms of the heat trace and the spectrum (Theorem 3.7 and Theorem 3.9). The spectrum will be computed by numerical methods. There are three sources of errors in our computation of $\zeta(s)$:

(1) **Eigenvalue error**: The error caused by using approximate eigenvalues instead of their real values. This can be explicitly controlled in principle, using interval arithmetic. Our package of choice MPSPack, provides eigenvalues along with semi-rigorous theoretical error estimates.
(2) **Spectrum truncation error**: The error caused by using only finitely many eigenvalues. This can be controlled using eigenvalue estimates (we use the Li-Yau estimate, Theorem 2.46).
(3) **Heat expansion error**: The error caused by replacing the heat trace by the heat expansion, for small time. This can be controlled in polygonal domains using known heat trace estimates for polygons (eg. Theorem 2.55).

We aim to both give explicit expressions for these errors, and to make the bounds as sharp as possible.

The results section of this thesis will be structured as follows: Chapter 4 deals with an original, new method for solving the Helmholtz equation on polygonal domains using a **partition of unity decomposition**. The main result is a proof-of-concept eigenvalue solver that computes the principal eigenvalue of a regular hexagon of unit side length to 12 decimal places. We have not found our method to be advantageous in efficiency compared to other solvers (such as Alex Barnett's MPSPack), despite our expectations, however, it may be easier to implement for multiply connected domains. It is also very easy to control the decomposition for domains with problematic geometries, placing different types of basis functions where they are most needed.

In Chapter 5 we present an L^∞ **estimate** for the eigenfunctions of the Dirichlet Laplace operator in a polygonal domain. The proof for this estimate relies on Zaremba's principle rather than heat equation methods, and thus differs from others proofs in the literature (see eg. [**25**]). This idea was proposed by Daniel Grieser (see [**36**]) for a general smooth domain, where the constant cannot be obtained analytically without having more information on the boundary. We focus on polygonal domains and obtain the constant.

Chapter 6 states **theoretical error bounds** for the computation of the spectral determinant and $\zeta(-\frac{1}{2})$. The methods used in the derivations of the estimates in this chapter are not novel but contribute to our computational framework.

Chapter 7 improves the **remainder term of the heat expansion** for a polygonal domain. We first prove a novel derivation of a "not feeling the boundary"-type estimate using finite propagation speed, which improves on Kac's original estimate ([**45**]) and produces a similar estimate to van den Berg's improved not-feeling-the-boundary estimate ([**74**]). We then use this estimate to improve the heat trace remainder estimate for a polygonal domain derived by van den Berg and Srisatkunarajah in [**75**], leading to an original estimate that, as we will explain in Chapter 8, improves our theoretical error bound for spectral zeta function computations by a factor of 5-10.

Finally, in Chapter 8 we will present a collection of numerical examples, some of which are highly applicable to nanophysics (such as cutouts). We will show how our error bounds can be applied to rigorously calculate the Casimir energy of different domains, as well as provide evidence for the conjecture that within the class of n-sided polygons of a fixed area, the regular polygon maximizes the spectral determinant.

CHAPTER 2

Functional Analysis and Spectral Theory

2.1. Notation

Throughout this thesis we will denote the complex numbers, real numbers, natural numbers, and integers using the standard conventions $\mathbb{C}$, $\mathbb{R}$, $\mathbb{N}$, and $\mathbb{Z}$. When we wish to include zero in the set of natural numbers we will denote this as $\mathbb{N}_0$. Intervals in $\mathbb{R}$ will be denoted by round parentheses when the endpoints are not included and square parentheses when they are, for example, $[0, 1)$ means that 0 is included in the set but 1 is not. We will normally denote open sets by capital letters from U upwards. For $U \subset \mathbb{R}^n$ we will denote its boundary by ∂U. We will denote its closure as $\overline{U}$. Complements will be denoted by a minus sign, eg. $(0, \infty) = \mathbb{R} - (-\infty, 0]$. Union and intersection will be denoted by $\cup$ and $\cap$, respectively. Disjoint union will be denoted by $\sqcup$.

Functions will be denoted with lowercase letters beginning with f. Derivatives of a function $f \in C^1(U)$ will be denoted using the standard notation $\frac{df}{dx}$, or, where there is no cause for ambiguity, by a prime, eg. $f'(x)$. Likewise, integrals will be denoted using standard notation like so: $F(b) - F(a) = \int_a^b f(x)dx$.

Metrics will normally be denoted by a lowercase d_X, the subscript X relating to the metric space to which the metric refers to. When it is clear from context we will omit the subscript. Norms will be denoted with double bars, i.e. $\|$, and when necessary the space of the norm will appear in the subscript after the closing bar, for example: $\|f\|_{L^2(\mathbb{R})}$. If clear from context we will sometimes omit the subscript, but most of the time it will be included for the sake of readability. In a metric space (M, d), we will denote an open ball of radius r centered at a point x as $B_x(r)$. When dealing with an inner product space, the inner product will be represented by angled brackets, eg. $\langle x, y \rangle$.

We now define some function spaces that we intend to use:

(1) $L^p(U)$ consists of the functions on an open set U whose p-th powers are integrable on U.
(2) $C^m(U)$ consists of the continuous functions on an open set U with continuous m-th derivatives. When $m = \infty$ the functions will be arbitratily often differentiable.
(3) $C_0^\infty(U)$ consists of arbitarily often differentiable functions on an open set U whose support is a compact subset of U.
(4) $C^\infty(\overline{U})$ for an open set $U \subset \mathbb{R}^d$ consists of the restrictions of members of $C^\infty(\mathbb{R}^d)$ to $\overline{U}$.
(5) $C_d(U)$, where U is bounded, consists of functions that vanish on ∂U.

To simplify formula used in multivariable calculus, we will sometimes use multi-index notation. A **multi-index** is an n-tuple $\alpha = (\alpha_1, \alpha_2, \cdots, \alpha_n)$ of non-negative

integers on which one can define compoment-wise operations such as sum, difference, and, most importantly for this work, higher-order weak or partial differentiation. Namely, we define

$$\partial^\alpha := \partial^{\alpha_1}\partial^{\alpha_2}\cdots\partial^{\alpha_n},$$

where $\partial_{x_k}^{\alpha_k} := \frac{\partial^{\alpha_k}}{\partial x_n^{\alpha_k}}$.

Finally, we define some geometric notation. Namely, if U is an open, bounded subset of $\mathbb{R}^d$, then $\mathrm{Vol}(U)$ will denote the d-dimensional Euclidean volume of U. For example, in $\mathbb{R}^2$, this will denote area. Provided ∂U is piecewise smooth we will use $|\partial U|$ to denote the length of the boundary, that is, its $d-1$-th dimensional Euclidean volume: $|\partial U| := \mathrm{Vol}(\partial U)$.

2.2. Setting

In this chapter we give some background on the theory of partial differential equations and spectral theory. We introduce definitions and standard results that we will use later on, starting with a brief overview of Sobolev spaces and elliptic regularity, and then discussing the spectral theory of unbounded operators, leading to the construction of the continuous functional calculus with examples useful to us. Then we review some properties of solutions of the heat equation, in particular its fundamental solution (the heat kernel). Finally, we define the spectral zeta function and show how its meromorphic continuation and spectral theory can be used to study it.

We will generally be dealing with open, bounded, and connected subsets of $\mathbb{R}^2$ with Lipschitz boundary. For completeness, we recall what this means below:

Definition 2.1. Let (X, d_X) and (Y, d_Y) be two metric spaces. A function $f : X \mapsto Y$ is called **Lipschitz continuous** if there exists a real constant $K \geq 0$ such that, for all $x_1, x_2 \in X$, we have

$$d_Y(f(x_1), f(x_2)) \leq K d_X(x_1, x_2).$$

An open, bounded set $U \subset \mathbb{R}^n$ with boundary ∂U is said to have **Lipschitz boundary** if, for every point $p \in \partial U$, there exists a radius $r > 0$, $Q \subset \mathbb{R}^n$ and a map $h_p : B_p(r) \to Q$ such that

(1) h_p is a bijection;
(2) h_p and h_p^{-1} are both Lipschitz continuous;
(3) $h_p(\partial U \cap B_p(r)) = \{(x_1, \cdots, x_n) \in B_1(0) | x_n = 0\}$
(4) $h_p(U \cap B_p(r)) = \{(x_1, \cdots, x_n) \in B_1(0) | x_n > 0\}$.

In particular, a Lipschitz function is absolutely continuous. The converse is however not true, as one can take any integrable function of unbounded variation $f(x)$ on some interval; then its primitive will be absolutely continuous but not Lipschitz. One can think of the boundary of a Lipschitz domain as the "graph" of a Lipschitz function. A more detailed exploration of Lipschitz continuity can be found in [**23**] and [**2**].

Definition 2.2. An open, bounded set $U \subset \mathbb{R}^2$ is called a **polygonal domain** with vertices v_i, $i = 1 \cdots m$ provided $v_i \neq v_j \, \forall i \neq j$ and if ∂U can be expressed as the union of line segments between v_i and $v_{(i+1) \bmod m}$ for $i = 1 \cdots m$.

Note that our definition excludes piecewise linear domains where a vertex can intersect more than two line segments, such as two triangles joined at a vertex. These domains do not necessarily satisfy a Lipschitz condition (the example of the two triangles does not).

PROPOSITION 2.3. *Let U be a polygonal domain with vertices $v_i, i = 1 \cdots m$ in $\mathbb{R}^2$. Then U has Lipschitz boundary.*

PROOF. We verify conditions 1-4 of Definition 2.1 directly. It is clear that for all $x \in \partial U \setminus \{v_i\}$, the Lipschitz condition is satisfied because at those points ∂U is smooth. It therefore suffices to verify the conditions at the vertices. Let $y \in v_i$ and suppose that the interior angle formed by the two line segments of this corner is given by α, $0 \leq \alpha < 2\pi$. This angle is unambiguous by definition of a polygonal domain since each vertex touches only two line segments. Define polar coordinates (r, θ) such that $r = 0$ at y and $\theta = 0$ along one of the edges of the two line segments meeting y. Then the map $h_y(r, \theta) = (r, \frac{\alpha}{\pi}\theta)$ defines a bijection from $B_\rho(y)$ to $B_0(\rho)$ (even at the origin), for ρ chosen small enough so that no vertex other than y is included in $B_0(\rho)$. It is trivial that the map is Lipschitz away from the origin. When $r = 0$, we have $|h_y(0, \theta + \epsilon) - h_y(0, \theta)| = |(0, \frac{\alpha}{\pi}\epsilon)|$ in the theta-direction and $|h_y(\epsilon, \theta) - h_y(0, \theta) = |\epsilon|$ in the r-direction so it follows that the map is Lipschitz there, too. The conditions 3-4 are satisfied by construction of h_y. □

2.3. Sobolev Spaces and the Fourier Transform

Here we recall some basic facts about the Fourier transform and Sobolev spaces and the maps that differential operators induce between these spaces. The arguments we use can be found, for the most part, in [**2**] or [**71**]. Our proof of Proposition 2.15 is motivated by some exercises in [**71**]; an alternative proof can be found in [**2**]. We begin by reviewing some theory of distributions and the Fourier transform.

DEFINITION 2.4. Let U be an open, bounded subset of $\mathbb{R}^d$ with piecewise smooth, Lipschitz boundary. A linear functional $S : C_0^\infty(U) \to \mathbb{R}$ is called a (real-valued) **distribution** if for any convergent sequence $\phi_n \to \phi$ in $C_0^\infty(U)$,

$$\lim_{n\to\infty} S(\phi_n) = S(\phi).$$

The space of distributions is denoted by $D'(U)$.

Convergence $\phi_n \to \phi$ in above definition means the following: There exists a compact subset $K \subset \mathbb{R}^d$ such that $\text{supp}(\phi_n) \subset K$ for all n and

$$\|\phi - \phi_n\|_{C^k} \to 0 \quad \forall k.$$

Distributions do not automatically admit a strong derivative, since they are not required to be differentiable (or even continuous). However, they do admit a weak derivative:

DEFINITION 2.5. Let $S \in D'(U)$. The n the **weak derivative** of S, denoted $\partial^\alpha S$ for a multi-index α, is the linear functional defined by

$$\langle \partial^\alpha S, \phi \rangle = (-1)^{|\alpha|} \langle S, \partial^\alpha \phi \rangle$$

for all $\phi \in C_0^\infty(U)$.

If $S \in C_0^1(U)$, then the definition of the weak derivative coincides with the definition of the strong derivative, as can be seen from integrating by parts.

DEFINITION 2.6. A linear map $L : D(L) \to L^2(U)$ is called a **linear differential operator** of order m if it admits the representation

$$Lf = \sum_{|\alpha| \leq m} \lambda_\alpha(x) \partial^\alpha f$$

for a multi-index α and where the $\lambda_\alpha \in C^\infty(U)$ are called the coefficients of L and $f \in D(L)$.

Perhaps the most basic example of a linear differential operator is the differentiation map $D : C^1(\mathbb{R}) \to C(\mathbb{R})$ given by $Df = \frac{df}{dx}$.

DEFINITION 2.7. Let U be an open subset of $\mathbb{R}^2$. A function $f : U \to \mathbb{R}$ is said to be a **Schwartz** function (or equivalently, a rapidly decreasing function on U) if $f \in C^\infty(U)$ and $\sup_{x \in U} |x^\alpha \partial^\beta f(x)| < \infty$ for any α, β multi-indices. The space of Schwartz functions on U is called **Schwartz space** and denoted $S(U)$. A **Schwartz distribution** ϕ on U is a continuous linear functional on $S(U)$. We denote the space of Schwartz distributions on U as $S'(U)$.

In particular, any $f \in L^1_{loc}(U)$ can be viewed as a distribution by the Cauchy-Schwarz inequality. We may now define the Fourier transform.

DEFINITION 2.8. Let $f \in S(\mathbb{R}^n)$. Then the **Fourier transform** of f, denoted $\hat{f}$, is defined to be

$$\hat{f}(\lambda) := \frac{1}{(2\pi)^{n/2}} \int_{\mathbb{R}^n} \mathrm{e}^{-i\langle x, \lambda \rangle} f(x) dx,$$

where $\langle x, \lambda \rangle := \sum_{i=1}^n x_i \lambda_i$. The **inverse Fourier transform** of f, denoted by $\check{f}$, is defined to be

$$\check{f}(\lambda) := \frac{1}{(2\pi)^{n/2}} \int_{\mathbb{R}^n} \mathrm{e}^{i\langle x, \lambda \rangle} f(x) dx.$$

Because every function in $S(\mathbb{R}^n)$ is in $L^1(\mathbb{R}^n)$, the integrals above make sense. Below, we recall some facts on the Fourier transform that we will using in this thesis.

THEOREM 2.9. *(Mapping Properties of the Fourier Transform) Let $f \in S(\mathbb{R}^n)$.*

1. *The Fourier transform is a linear bicontinuous map from $S(\mathbb{R}^n)$ onto $S(\mathbb{R}^n)$. Its inverse map is the inverse Fourier transform.*
2. *The Fourier transform is a one-to-one linear bijection from $S'(\mathbb{R}^n)$ to $S'(\mathbb{R}^n)$ which is the unique weakly continuous extension of the Fourier transform on $S(\mathbb{R}^n)$ (that is, if $T_n \to T$ in $S'(\mathbb{R}^n)$, then $\hat{T}_n \to \hat{T}$).*
3. *If α and β are multi-indices, then*
$$((i\lambda)^\alpha \partial^\beta \hat{f})(\lambda) = \partial^\alpha (\widehat{(-ix)^\beta f(x)}).$$
4. *We have the following equality (also known as Plancherel's Theorem):*
$$\int_{\mathbb{R}^n} |f(x)|^2 \, dx = \int_{\mathbb{R}^n} \left| \hat{f}(\lambda) \right|^2 d\lambda.$$

PROOF. In [**61**], claim 1 is proved in Theorem IX.1 in , claim 2 in Theorem IX.2, claim 3 in Lemma IX.1, and claim 4 in the Corollary to Theorem IX.1.

The Fourier transform maps convolution to multiplication, in the following sense: □

THEOREM 2.10. *(Convolution properties of the Fourier transform) Let $f, g, h \in S(\mathbb{R}^n)$. Then*

(1) *We have that $g \to f \star g$ is a continuous map of $S(\mathbb{R}^n)$ into $S(\mathbb{R}^n)$.*
(2) $\widehat{fg} = (2\pi)^{-n/2} \hat{f} \star \hat{g}$ and $\widehat{f \star g} = (2\pi)^{n/2} \hat{f}\hat{g}$

PROOF. Theorem IX.3 in [**61**]. □

Having now stated some basic properties of the Fourier transform, we state the well-known Poisson summation formula.

THEOREM 2.11. *(Poisson summation formula) Let f be a positive, continuous, decreasing, integrable function on $[0, \infty)$. Then*

$$\sum_{n=-\infty}^{\infty} f(n) = \sum_{k=-\infty}^{\infty} \hat{f}(k).$$

PROOF. See [**42**]. □

We are now ready to define the Sobolev spaces.

DEFINITION 2.12. Let $s \in \mathbb{R}$ and $n \in \mathbb{N}$. Then the Sobolev space $H^s(\mathbb{R}^n)$ is defined as

$$H^s(\mathbb{R}^n) = \{f \in S'(\mathbb{R}^n) : (1 + |\xi|^2)^{s/2} \hat{f} \in L^2(\mathbb{R}^n)\}.$$

We now give the corresponding definition for U.

DEFINITION 2.13. Let $U \subset \mathbb{R}^n$ be open. Then we define the set $H^k(U)$ to be

$$H^k(U) := \{u \in L^2(U) \quad s.t. \quad \partial^\alpha u \in L^2(U) \quad \forall 0 < |\alpha| < k\},$$

where $\partial^\alpha u$ is the weak derivative of u and we define $H_0^s(U)$ to be the closure of $C_0^\infty(U)$ in the space $H^k(U)$.

There are two properties of Sobolev spaces that we wish to prove: The first concerns the mapping properties of a differential operator. The second concerns the smoothness of the functions in a Sobolev space for high enough s. We first prove it for $\mathbb{R}^d$, then for a bounded subset.

PROPOSITION 2.14. *Let D^p be a p-th order differential operator with constant coefficients and $f \in H^s(\mathbb{R}^d)$. Then $D^p(f) \in H^{s-p}(\mathbb{R}^d)$.*

PROOF. We have that

$$\|D^p(f)\|_{H^{s-p}(\mathbb{R}^d)} \leq C \| \langle \xi \rangle^p \hat{f}\|_{H^{s-p}(\mathbb{R}^d)},$$

where C depends on the coefficients of D^p. But

$$\| \langle \xi \rangle^p \hat{f}\|_{H^{s-p}(\mathbb{R}^d)} \leq \|f\|_{H^s(\mathbb{R}^d)} < \infty$$

by assumption, proving the claim.

For a bounded domain, the proof is slightly different. □

PROPOSITION 2.15. *Let $p \in \mathbb{N}_0$ and D^p be a p-th order differential operator with constant coefficients and $f \in H^s(U)$ for U open and bounded with ∂U piecewise smooth and Lipschitz. Then $D^p(f) \in H^{s-p}(U)$.*

PROOF. First we prove the proposition true for $f \in H_0^s(U)$. Let $\phi_i \in C_0^\infty(\mathbb{R}^n)$ be a sequence converging to f in the H^s-induced topology. Let $F(U)$ be the subset of functions $g \in L^2(U)$ that have support in U. Let $E : F(U) \to L^2(\mathbb{R}^n)$ be extension by zero. It is clear that E and D^p commute. Note that because $H_0^s(U)$ embeds continuously into $H^s(\mathbb{R}^n)$, the map E is a natural injection.

We wish to prove that the sequence $D^p(E\phi_i)$ converges to D^pEf in the H^{s-p} norm:

$$\begin{aligned}\lim_{i\to\infty} \|D^p(E(\phi_i)) - D^p(E(f))\|_{H^{s-p}(U)} &= \lim_{i\to\infty} \|[D^p(E\phi_i - Ef)]\|_{H^{s-p}(\mathbb{R}^n)} \\ &= \lim_{i\to\infty} \|(|\xi|^p)\widehat{(E\phi_i - Ef)}\|_{H^{s-p}(\mathbb{R}^n)} \\ &\leq \lim_{i\to\infty} \|\widehat{E\phi_i} - \widehat{Ef}\|_{H^s(\mathbb{R}^n)}.\end{aligned}$$

Now by our earlier definition of Sobolev norms this is just

$$\begin{aligned}\lim_{i\to\infty} \|\widehat{E\phi_i} - \widehat{Ef}\|_{H^s(\mathbb{R}^n)} &= \lim_{i\to\infty} \|(1+|\xi|^2)^{s/2}\widehat{(E\phi_i - Ef)}\|_{L^2(\mathbb{R}^n)} \\ &= \lim_{i\to\infty} \|(1+|\xi|^2)^{s/2}[E\phi_i(-\xi) - Ef(-\xi)]\|_{L^2(\mathbb{R}^n)}\end{aligned}$$

by duality of the Fourier transform. Because $E\phi_i$ and Ef are supported in U, we can write this norm as an integral over U:

$$\lim_{i\to\infty} \|(1+|\xi|^2)^{s/2}[E\phi_i(-\xi) - Ef(-\xi)]\|^2_{L^2(\mathbb{R}^n)} = \lim_{i\to\infty} \int_U \left[(1+|\xi|^2)^{s/2}[\phi_i(-\xi) - f(-\xi)]\right]^2 d\xi,$$

where we can drop the E since it coincides with the identity operator inside U. By the Cauchy-Schwarz inequality, we have

$$\lim_{i\to\infty} \int_U \left[(1+|\xi|^2)^{s/2}[\phi_i(-\xi) - f(-\xi)]\right]^2 d\xi \leq \lim_{i\to\infty} \left\{\int_U \left[(1+|\xi|^2)^{s/2}\right]^2 d\xi\right\} \left\{\int_U [\phi_i(-\xi) - f(-\xi)]^2 d\xi\right\}.$$

The first integral is bounded and the second converges to zero. This proves the proposition true for $f \in H_0^s(U)$.

Let us now prove the proposition for $f \in H^s(U)$. To do so, consider a bounded open set V containing U with the property that $d(x, \partial V) > 0$ for any $x \in U$ and where d can be taken to be the standard Euclidean metric. Consider the set G of functions $g \in H_0^s(V)$ such that $g = f$ on U. It is clear that this set is non-empty as we can simply take a cutoff function with value 1 on $\overline{U}$ and value 0 on ∂V. We can apply the proposition to any such g to find that $D^pg \in H_0^{s-p}(V)$ and then restrict g to a function $\tilde{g}$ on U to obtain that $D^p\tilde{g} \in H^{s-p}(U)$. But $\tilde{g} = f$. Because we

assumed U to have piecewise smooth boundary, the restriction $R : H_0^s(V) \to H^s(U)$ is surjective, and this completes the proof. □

The next fact we wish to establish is the differentiability in a classical sense of Sobolev functions.

PROPOSITION 2.16. *If $s > n/2$, then each $u \in H^s(U)$ is continuous and bounded.*

PROOF. Using the same reasoning as in the previous proof, it will be sufficient to show the proposition true for $u \in H^s(\mathbb{R}^n)$, for we can always extend u as in the previous proof while preserving its Sobolev regularity. To prove boundedness, by the Fourier inversion formula, we just need to prove that $\hat{u}(\xi) \in L^1(\mathbb{R}^n)$. We have

$$\int |\hat{u}(\xi)| d\xi \leq \left(\int |\hat{u}(\xi)|^2 (1+|\xi|^2)^s d\xi \right)^{1/2} \cdot \left(\int (1+|\xi|^2)^{-s} d\xi \right)^{1/2}.$$

Making a change of variables in the second integral to multidimensional polar coordinates, we obtain

$$C_n \int (1+|r|^2)^{-s} r^{n-1} dr$$

and this converges precicely when $s > \frac{n}{2}$. This proves boundedness. To prove continuity, let $s = n/2 + \alpha$, for $0 < \alpha$, and again use the Fourier inversion formula to write

$$\begin{aligned} |u(x+\epsilon) - u(x)| &\leq (2\pi)^{-n/2} \left| \int \hat{u}(\xi) \mathrm{e}^{ix\cdot\xi} (\mathrm{e}^{i\epsilon\cdot\xi} - 1) d\xi \right| \\ &\leq C \left(\int |\hat{u}(\xi)| \langle \xi \rangle^{n+2\alpha} d\xi d\xi \right)^{\frac{1}{2}} \left(\int |\mathrm{e}^{i\epsilon\cdot\xi} - 1|^2 \langle \xi \rangle^{-n-2\alpha} d\xi \right)^{\frac{1}{2}}. \end{aligned}$$

If $|\epsilon| \leq 1/2$, then

$$\int |\mathrm{e}^{i\epsilon\cdot\xi} - 1|^2 \langle \xi \rangle^{-n-2\alpha} d\xi \leq C \int_{|\xi| \leq \frac{1}{|\epsilon|}} |\epsilon|^2 |\xi|^2 \langle \xi \rangle^{-n-2\alpha} d\xi + 4 \int_{|\xi| \geq \frac{1}{|\epsilon|}} \langle \xi \rangle^{-n-2\alpha} d\xi.$$

Again using polar coordinates, we can bound the RHS by

$$C|\epsilon|^2 + C|\epsilon|^2 \frac{|\epsilon|^{2\alpha-2} - 1}{2\alpha - 2} + C|\epsilon|^{2\alpha}$$

provided $\alpha \neq 1$. Therefore, for $|\epsilon| < 1/2$,

$$|u(x+\epsilon) - u(x)| \leq C_\alpha |\epsilon|^\alpha,$$

which proves continuity, and Lipschitz continuity if $\alpha \neq$. If $\alpha = 1$, then one gets the modified estimate

$$|u(x+\epsilon) - u(x)| \leq C|\epsilon| \left(\log \frac{1}{|\epsilon|} \right)^{1/2},$$

which means that u is continuous (but not necessarily Lipschitz continuous, see (1.19) of Chapter 4 in[**71**] for a counterexample). □

COROLLARY 2.17. *If $s > \frac{n}{2} + k$ then $H^s(U) \subset C^k(U)$.*

PROOF. This follows directly from applying the two previous results. □

A very powerful result concerning the embedding of Sobolev spaces is the Rellich-Kondrachov Theorem, which is very useful for proving that certain operators are compact.

THEOREM 2.18. *(Rellich-Kondrachov Compactness Theorem) Suppose that U is an open, bounded subset of $\mathbb{R}^d$ with piecewise smooth, Lipschitz boundary. If $t > s$, then the inclusion $i : H^t(U) \to H^s(U)$ is compact. That is, i maps bounded sets of $H^t(U)$ to precompact sets of $H^s(U)$.*

PROOF. Theorem 1.22 of [**63**]. □

Sobolev Spaces are often used to study partial differential equations. Therefore, one might sometimes ask about the boundary value of a Sobolev function $f \in H^s(U)$. If $f \in C(U)$, then obviously one can restrict f to the boundary. If this is not known, then it is not clear how one can restrict the function to the boundary since the boundary is a set of measure zero. The following Theorem answers this question:

THEOREM 2.19. *(Trace Theorem) Assume U is open and bounded with Lipschitz boundary and $s > \frac{1}{2}$. Then there exists a linear operator $T : H^s(U) \to H^{s-\frac{1}{2}}(U)$ such that*

$$Tu = u|_{\partial U}, \quad u \in H^s(U) \cap C(\overline{U})$$

$$\|Tu\|_{H^{s-\frac{1}{2}}(\partial U)} \leq C\|u\|_{H^s(U)},$$

where C only depends on U.

PROOF. Theorem 5.22 of [**2**]. □

In other words, this Theorem says that if the boundary is sufficiently nice then the set of functions with trace zero in $H^s(U)$ can be approximated by smooth functions with compact support. There is also the question of whether it is possible to extend a Sobolev function beyond the boundary. Obviously if $f \in H_0^s(U)$, then we can extend it by zero. Even if this is not the case, we can usually still extend $f \in H^s(U)$ to a function $f \in H^s(\mathbb{R}^n)$. The condition is given by the following Theorem.

THEOREM 2.20. *Assume U is open and bounded with Lipschitz boundary. Then there exists an extension operator $T : H^s(U) \to H^s(\mathbb{R}^n)$ and a constant $K = K(s, U) > 0$ with the following properties:*

$$Tf(x) = f(x) \quad a.e. \quad \text{in} \quad \text{U}$$

$$\|Tf\|_{H^s(\mathbb{R}^n)} \leq K(s, U)\|f\|_{H^s(U)}.$$

PROOF. Theorem 4.26 of [**2**]. □

These two theorems combined allow us to think of a function in $H^s(U)$ as a function on the whole of $\mathbb{R}^2$, provided that ∂U is Lipschitz.

2.4. Spectral Theory of Unbounded Operators

The operator that we want to study, the Laplacian, has the property that it is not bounded. Here we recall some facts about unbounded operators and their spectral theory.

DEFINITION 2.21. A linear operator $A : \mathrm{Dom}(A) \mapsto \mathcal{H}_2$ from a subspace $\mathrm{Dom}(A) \subseteq \mathcal{H}_1$ to a Hilbert space $\mathcal{H}_2$ is called **bounded** if there exists a constant C such that for any $f \in \mathrm{Dom}(A)$, we have $\|Af\|_{\mathcal{H}_2} \leq C\|f\|_{\mathcal{H}_1}$, where the norms are those induced by the inner products of $\mathcal{H}_1$ and $\mathcal{H}_2$, respectively. Otherwise we call A **unbounded**. If $\mathrm{Dom}(A)$ is dense in $\mathcal{H}_1$, then we say that A is **densely defined**.

If a densely defined operator is bounded on $\mathrm{Dom}(A)$, then it extends to a bounded operator on the whole of $\mathcal{H}_1$. Indeed, one can construct such an extension via continuity. An operator can be associated with a distribution known as its **kernel** by the Schwartz Kernel Theorem, which we state below:

THEOREM 2.22. *(Schwartz Kernel Theorem) Let U be open. Every $K \in \mathcal{D}'(U \times U)$ defines according to*

$$\langle T\phi, \psi\rangle = K(\psi \otimes \phi); \quad \psi \in C_0^\infty(U), \quad \phi \in C_0^\infty(U) \tag{2.4.1}$$

a linear map T from $C_0^\infty(U)$ to $\mathcal{D}'(U)$ which is continuous in the sense that $T\phi_j \to 0$ in $\mathcal{D}'(U)$ if $\phi_j \to 0$ in $C_0^\infty(U)$. Conversely, to every such linear map T there is one and only one distribution K such that (2.4.1) is valid. One calls K the kernel of T.

PROOF. 5.2.1 in [**42**]. □

When we say a distribution is unique, such as above, this is meant in the sense of maps: for example, if two kernels $\phi_1 \in \mathcal{D}'(\mathbb{R})$ and $\phi_2 \in \mathcal{D}'(\mathbb{R})$ exist for some operator T acting on $C_0^\infty(\mathbb{R})$, then it would be true that for every $f \in C_0^\infty(\mathbb{R})$, $\phi_1(f) = \phi_2(f)$, which means $\phi_1 = \phi_2$.

DEFINITION 2.23. The **graph** of a linear operator $A : \mathrm{Dom}(A) \mapsto \mathcal{H}_2$ from a subspace $\mathrm{Dom}(A) \subseteq \mathcal{H}_1$ to a Hilbert space $\mathcal{H}_2$ is the linear subspace

$$\Gamma(A) = \{(v, w) \in \mathcal{H}_1 \times \mathcal{H}_2 | v \in \mathrm{Dom}(A), w = A(v)\}.$$

If $\Gamma(A)$ is closed in $\mathcal{H}_1 \times \mathcal{H}_2$ (with respect to the norm induced by the inner product of the direct sum), then we say that A is **closed**. If this is not true but there exists a closed extension of A, then we say that A is **closable**.

In this work, when we write that two operators are equal, this will always mean that their graphs are equal.

DEFINITION 2.24. Suppose that A is a closed operator from a Hilbert space $\mathcal{H}$ to itself. We define the **resolvent set** $\rho(A)$ of A to be the set of points $\lambda \in \mathbb{C}$ such that $R_\lambda := (A - \lambda \mathrm{Id})^{-1}$ exists, is a bounded linear operator, and is defined on a dense subset of $\mathcal{H}$. For $\lambda \in \rho(A)$, we call R_λ the **resolvent operator** (or simply resolvent) of A. We define the **spectrum** of A to be the set $\sigma(A) = \mathbb{C} \backslash \rho(A)$.

We can now define adjointness of an operator.

DEFINITION 2.25. Suppose that A is a closed, densely defined operator from a Hilbert space $\mathcal{H}$ to itself and denote the inner product on $\mathcal{H}$ by $\langle \cdot, \cdot \rangle$. Define the operator A^* on $\mathcal{H}$ as the operator with $\mathrm{Dom}(A^*)$ containing elements $f \in \mathcal{H}$ for which there exists $g \in \mathcal{H}$ such that for all $h \in \mathrm{Dom}(A)$, we have

$$\langle Ah, f \rangle = \langle f, g \rangle.$$

Then define $A^* f = g$ for a given f. The operator A^* is called the **adjoint** of A, and if $A^* = A$ (recall that equality here is meant in the graph sense), then we say that A is **self-adjoint.** For self-adjoint operators, we can ask: for which f is $f(A)$ defined and what does this expression even mean? Clearly, if $f(x) = x$ then we would like $f(A) = A$, and similarly if f is a polynomial then we would like $f(A)$ to be an operator equal to a sum of powers of A. In particular, we will be interested in the case when $f(A) = \mathrm{e}^{-At}$. The result that allows this expression to be meaningful and well-defined even if A is unbounded is a Theorem called Continuous Functional Calculus (if A is bounded then it can be written as a convergent infinite series).

THEOREM 2.26. *(Continuous Functional Calculus) Let A be a self-adjoint operator on a separable Hilbert space $\mathcal{H}$. Then there is a unique map ϕ from the bounded Borel functions on $\mathbb{R}$ into the bounded operators on H so that:*

- ϕ is an algebraic $*-$homomorphism, that is: $\phi(fg) = \phi(f)\phi(g)$, $\phi(\lambda f) = \lambda\phi(f)$, $\phi(1) = I$, $\phi(\overline{f}) = \phi(f)^*$.
- ϕ is continuous, that is $\|\phi(f)\|_{\mathcal{L}(\mathcal{H})} \leq C\|f\|_\infty$
- Let $h_n(x)$ be a sequence of bounded Borel functions with $h_n(x) \to x$ for each x and $|h_n(x)| \leq x$ for all x and n. Then, for any $\psi \in D(A)$, $\lim_{n\to\infty} \phi(h_n)\psi = A\psi$.
- If $h_n(x) \to h(x)$ pointwise and if the sequence $\|h_n\|_\infty$is bounded, then $\phi(h_n) \to \phi(h)$ strongly.
- In addition, if $A\psi = \lambda\psi$, then $\phi(h)\psi = h(\lambda)\psi$.
- If $h \geq 0$, then $\phi(h) \geq 0$ (in the sense of operator positivity).

PROOF. Theorem VIII.5 in [**61**]. □

Therefore, for any bounded continuous function f we can define $f(A)$ unambiguously by using spectral mapping properties guaranteed by the Continuous Functional Calculus.

We now make a few final defintions before stating the Spectral Theorem for unbounded operators. This Theorem will be very important to us insomuch as it is a generalisation of the analogous result for matrices, which states that under certain conditions one can diagonalize a matrix.

Recall that a **Borel-measurable** subset of $\mathbb{R}$ is one that that is in the Borel σ-algebra of $\mathbb{R}$, that is, one that is formed by countable union and intersection of the open intervals and their complements.

DEFINITION 2.27. Let $S \subset \mathbb{R}$ be a Borel-measurable subset of $\mathbb{R}$. A **projection valued measure (p.v.m)** $\{E_A : \mathcal{H} \mapsto \mathcal{H}\}$ on a Hilbert space H is a family of operators with the following properties

(1) Each P_S is self adjoint and for any two Borel measurable subsets of $S_1, S_2 \subseteq \mathbb{R}$, $P_{S_1} P_{S_2} = P_{S_1 \cap S_2}$.
(2) $P_\emptyset = 0$ and $P_{(-\infty,\infty)} = \mathrm{Id}$.

(3) Suppose $S = \cup_{n=1} S_n$ and the S_n are pairwise disjoint. Then $P_A = \lim_{N\to\infty} \sum_{n=1}^{N} P_{S_n}$ in the strong operator topology. That is, the real-valued sequence
$$x_n = \|P_{S_n} f - P_A f\|$$
converges to zero.

From now on we will denote $P_\lambda := P_{(-\infty,\lambda)}$.

One can integrate against a projection-valued measure by using the inner product on $\mathcal{H}$. More precisely, if P_λ is a p.v.m, then for any $f \in \mathcal{H}$,$\langle f, P_S f\rangle$ is an ordinary measure (see eg. VII.3 of [**61**]). Under certain assumptions, projection valued measures allow one to define the value of an operator valued function, for example, $\sin(A)$.

THEOREM 2.28. *(Spectral Theorem for unbounded operators) Let A be a (possibly unbounded) self-adjoint operator on a Hilbert space $\mathcal{H}$ and that $f \in \mathrm{Dom}(A)$. Then there exists a unique p.v.m P_S on $\mathcal{H}$ with*
$$\langle f, Af\rangle = \int_{-\infty}^{\infty} \lambda d\langle f, P_\lambda f\rangle$$
and if g is a real-valued Borel-measurable function on $\mathbb{R}$, then
$$\langle f, g(A)f\rangle = \int_{-\infty}^{\infty} g(\lambda) d\langle f, P_\lambda f\rangle .$$
Moreover, the operator $g(A)$ thus defined is self-adjoint on the domain
$$\mathrm{Dom}(g(A)) = \left\{ f \in \mathcal{H} \quad s.t. \quad \int_{-\infty}^{\infty} g(\lambda)^2 d\langle f, P_\lambda f\rangle < \infty \right\}.$$

PROOF. Theorem VIII.6 in [**61**]. □

Recall that an operator is said to be **compact** if it maps bounded sets to sets with compact closure. Equivalently, a compact operator maps weakly convergent sequences to norm convergent sequences. In the case that A happens to be compact, we can say even more:

THEOREM 2.29. *(Hilbert-Schmidt Theorem) Let A be a compact self-adjoint operator on a separable Hilbert space $\mathcal{H}$. Then there exists a complete orthonormal basis $\{\phi_n\}$ for $\mathcal{H}$ so that $A\phi_n = \lambda_n \phi_n$ and $\lambda_n \to 0$ as $n \to \infty$.*

PROOF. Theorem VI.16 of [**61**]. □

Moreover, the eigenfunctions ϕ_n can be used to express the p.v.m guaranteed by Theorem 2.28. It follows immediately from the previous two Theorems that

COROLLARY 2.30. *Let A be a compact self-adjoint operator on a separable Hilbert space $\mathcal{H}$, $f \in \mathrm{Dom}(A)$ and P_λ be the unique p.v.m associated with A (guaranteed by Theorem 2.28). Then*
$$d\langle f, P_\lambda f\rangle = \sum_{n=1}^{\infty} \delta_{\lambda-\lambda_n} f \langle \phi_n, f\rangle \phi_n$$
or, equivalently,

$$A = \sum_{n=1}^{\infty} \lambda_n \langle \phi_n, \cdot \rangle \phi_n,$$

where convergence is in the strong sense, and where ϕ_n are the eigenfunctions of A.

Given a closed operator A, we defined its resolvent operator R_λ earlier. If the resolvent is compact for all $\lambda \in \rho(A)$, then we say that A has **compact resolvent**. The following Theorem shows that for a positive operator, this requirement is equivalent to asking that $(A+I)^{-1}$ is compact:

THEOREM 2.31. *Let A be a closed operator with resolvent set $\rho(A)$ and R_λ be its resolvent for $\lambda \in \rho(A)$. If $R_{\tilde{\lambda}}$ is compact for some $\tilde{\lambda} \in \rho(A)$, then R_λ is compact for all $\lambda \in \rho(A)$.*

PROOF. Proposition 8.8 in [**71**]. □

DEFINITION 2.32. Let A be a self-adjoint operator that has compact resolvent. Denote by λ_n the eigenvalues of A with $\lambda_1 < \lambda_2 \leq \lambda_3 \cdots$ (with multiple eigenvalues represented according to their multiplicities). The **counting function** of A, which we denote by $N(\lambda)$, is the number of eigenvalues of A lying below λ:

$$N_A(\lambda) := \#\{j \in \mathbb{N} : \lambda_j \leq \lambda\}.$$

Note that the principal eigenvalue of the Dirichlet Laplacian is always simple, i.e. $\lambda_1 < \lambda_2$ (see eg. [**61**]). When we write $N(\lambda)$, omitting the subscript "A", this will always denote the counting function of the Dirichlet Laplacian.

We also wish to define the so-called "spectral function" of A that has close ties with the counting function. We will be using a result of Safarov on the spectral function to obtain L^∞ estimates for eigenfunctions that will be crucial to our work (Corollay 5.2).

DEFINITION 2.33. Let U be an open, bounded subset of $\mathbb{R}^n$ with piecewise smooth, Lipschitz boundary, A be a self-adjoint operator with compact resolvent, with domain $\mathrm{Dom}(A) \subset L^2(U)$ and e_j be an orthonormal basis of $L^2(U)$ consisting of eigenfunctions of A. Order the e_j by eigenvalue, i.e. if λ_j are the ordered eigenvalues of A then e_j is the eigenfunction corresponding to λ_j. Then we define the **spectral function** of A, which we denote $e(x, y, \lambda)$, by

$$e(x, y, \lambda) := \sum_{\lambda_j \leq \lambda} e_j(x) e_j(y).$$

2.5. Quadratic Forms and Boundary Elliptic Regularity

In the rest of this work, we will be concerned with a special class of operators known as elliptic differential operators. In particular, it will be very important for our work that the eigenfunctions of the Laplace operator are sufficiently smooth. In what follows we state an elliptic boundary regularity theorem for Lipschitz domains. It is not true that regularity results from domains with smooth boundaries are easily generalizable to domains with piecewise smooth boundaries. For example, it is well known that Laplace's equation $\Delta u = f$ with Dirichlet boundary conditions on a domain with smooth boundary has a smooth solution u provided that f is smooth.

However, the same equation on a non-convex polygon may fail to have a solution in $H^1(\overline{U})$, even for smooth f (the solution actually lies in a weighted Sobolev space, see [**37**] for details).

Before we make this definition, note that any linear differential operator can be written in divergence form, that is, if L is a linear differential operator it admits the representation

$$(Lu)(x) = \sum_{0\leq|\alpha|,|\beta|\leq k} (-1)^{|\alpha|} D^\alpha (A_{\alpha\beta}(x) D^\beta u(x)).$$

This is not difficult to show using the chain and product rules of calculus. The workhorse that allows one to prove existence to a wide class of elliptic problems is the Babuska-Lax-Milgram Theorem. Recall that a bilinear form q on a Hilbert space H is called **coercive** if there exists a number $c > 0$ (the **coercivity constant** of q) such that

$$q(x, x) \geq c\|x\|\|$$

for all $x \in$ H. For example, the inner product on H is an example of a bounded and coercive form.

THEOREM 2.34. *(Babuska-Lax-Milgram Theorem) Let q be a coercive bilinear form on a Hilbert space* H. *Then there exists a unique solution $u = u_f \in$ H to the weak problem*

$$q(u_f, v) = \langle f, v\rangle$$

for all $v \in$ H. Moreover, the solution depends continuously on given datum, that is:

$$\|u_f\| \leq \frac{1}{c}\|u\|,$$

where c is the coercivity constant of q.

PROOF. Pages 324 in [**7**]. □

While this Theorem usually requires weak coercivity (a weaker condition than above), we will only be dealing with coercive forms, and further results rely on coercivity. Therefore there is no reason to bloat the present with added definitions.

The importance of this statement is that one can often express a differential operator as a coercive bilinear form on a Hilbert space, and this Theorem guarantees that the solution to a wide range of problems involving the operator in question are guaranteed to lie in the same Hilbert space. However, sometimes one would like the solution to lie in a subspace of H which is "better" in a sense of regularity. For example one might consider $q(f, g) = \langle \nabla f, \nabla g\rangle$, the quadratic form associated with the Laplace operator, on $H^1_0(U)$. As we will see shortly, the solution to the problem $\Delta u = f$, for $f \in H^k(U), k \in \mathbb{N}$, lies in $H^{k+2}_0(U) \subset H^1_0(U)$ provided that ∂U is sufficiently smooth. To prove this, the Babuska-Lax-Milgram lemma is not enough and one needs to make use of ellipticity, a condition that encodes the invertibility of an operator.

DEFINITION 2.35. A linear differential operator

$$(Lu)(x) = \sum_{0\leq|\alpha|,|\beta|=k} (-1)^{|\alpha|} D^\alpha (A_{\alpha\beta}(x) D^\beta u(x))$$

of order $2k$ is called **uniformly elliptic** if there exists a $c > 0$ such that for all $x \in m$ and every non-zero $\xi \in \mathbb{R}^n$, we have

$$\sum_{|\alpha|,|\beta|=k} \xi^\alpha A_{\alpha\beta}(x)\xi^b > c|\xi|^{2m}.$$

For an elliptic linear differential operator L, the following Theorem holds:

THEOREM 2.36. *(Elliptic Regularity) Let U be an open bounded subset of $\mathbb{R}^n$. Suppose L is an uniformly elliptic linear differential operator of order $2m$ for $m \in \mathbb{N}$ and that $f \in H^k(U)$ for $k \in \mathbb{N}$. Then there exists a unique solution $u \in H_0^1(U)$ of the system of equations $Lu = f$, $u(x) = 0, x \in \partial U$ and $u \in H_{k+2}(U)$. Moreover, if ∂U is smooth, then $u \in H^{k+2}(\overline{U})$.*

PROOF. The existence proof uses the Lax-Milgram lemma and does not require smooth boundary (Theorem 1 of Section 6.2.1 of [**30**]). The proof of interior regularity is a local statement that also does not require smooth boundary, and is Proposition 1.6 of [**71**]. The proof of boundary regularity, where the smooth boundary condition is essential (or one that is at least C^2), can be found in section 6.3.2 of [**30**], or a more direct proof using a parametrix construction in the case that L is a Laplace-type operator can be found in [**71**]. □

In our setting, where U may contain corners, regularity up to the boundary does not hold. In fact, if U is piecewise linear (polygonal) then $Lu = f$ may fail to have a solution in $H^1(\overline{U})$, even if $f \in C_0^\infty(U)$. Intuitively, what fails is the ability to "extend" u through a singular point - indeed, it is not even clear what this might mean. This question has been thoroughly examined by Kondratiev and Grisvard among others (see eg. [**37**] and [**32**]), and while elliptic regularity up to the boundary may not hold in a Sobolev space, we can still assess it in a different space. While we will not be stating or making use of these results, we will briefly mention for completeness that in a polygonal domain with corners r_c, the solution of an elliptic differential equation of order $2m$ with sufficiently smooth data cannot behave "worse" than $\frac{1}{d(x,r_c)}^m$ near a corner r_c. One example of such behavior is of the Green's function for the bilaplacian Δ^2 for a domain in $\mathbb{R}^3$ that is smooth apart from a single corner (see [**48**]).

2.6. The Laplace Operator

As we have written after stating the Lax-Milgram Lemma, sometimes it is possible to associate an operator with a quadratic form. This statement is precisely the Lax-Milgram Theorem:

THEOREM 2.37. *(Lax-Milgram Theorem) Let $\mathcal{H}$ be a Hilbert space and q be a bilinear form on $\mathcal{H}$ that is bounded and coercive. Then the maps $L_1 : \mathcal{H} \to \mathcal{H}^*$ and $L_2 : \mathcal{H}^* \to \mathcal{H}$ defined by $L_1 := q(v, \cdot)$ and $L_2 := q(\cdot, v)$, respectively, are linear and bounded (respectively) conjugate linear and linear isomorphisms of Hilbert spaces.*

One consequence of this Theorem is the following:

COROLLARY 2.38. *Let q be a bounded coercive bilinear form as in the previous Theorem. Further assume that the inclusion map $i : \mathcal{H} \to \mathcal{H}_0$ is bounded and let L_0 and L_1 be the unbounded linear operators defined by*

$$\mathrm{Dom}(L_0) := \{v \in \mathcal{H} : w \in \mathcal{H} \to q(v,w) \quad \text{is} \quad \mathcal{H}_0 \quad \text{continuous}\}$$

$$\mathrm{Dom}(L_1) := \{v \in \mathcal{H} : w \in \mathcal{H} \to q(w,v) \quad \text{is} \quad \mathcal{H}_0 \quad \text{continuous}\}$$

and for $v \in \mathrm{Dom}(L_0)$ *and* $w \in \mathrm{Dom}(L_1)$ *define* $L_0 v \in \mathcal{H}_0$ *and* $L_1 w \in \mathcal{H}_0$ *by requiring*

$$q(v,\cdot) = (L_0 v, \cdot)$$

and

$$q(\cdot, w) = (\cdot, L_1 w).$$

Then $\mathrm{Dom}(L_0)$ *and* $\mathrm{Dom}(L_1)$ *are dense subspaces of* $\mathcal{H}$ *and hence of* $\mathcal{H}_\prime$. *Moreover, the operators* L_0^{-1} *and* L_1^{-1} *are bounded as operators on* $\mathcal{H}_\prime$. *Finally,* $L_0^* = L_1$ *and* $L_1^* = L_0$. *In particular, both* L_0 *and* L_1 *are closed operators.*

Proof. See Lemma 5.13 of[**32**] for a proof using the Theorem. The statement that both L_0 and L_1 are both closed follows from the fact that the adjoint of an operator is always closed (see eg. [**49**]) . □

Corollary 2.39. *If* q *in the previous Theorem is furthermore assumed symmetric, then* L_0 *is self adjoint, i.e.* $\mathrm{Dom}(L_0) = \mathrm{Dom}(L_1)$.

Proof. Follows directly from the Theorem. □

For the remainder of this work, the operator we will be concerned with is the Dirichlet Laplacian Δ. In what follows we define this operator and state some of its desirable properties.

Definition 2.40. Let U be an open, bounded subset of $\mathbb{R}^d$ with piecewise smooth, Lipschitz boundary. We denote by $C_d^\infty(U)$ the space of smooth functions satisfying Dirichlet boundary conditions at ∂U.

Note the inclusions $C_0^\infty(U) \subset C_d^\infty(U) \subset H^1(U)$. Also note that $C_d^\infty(U)$ is not complete in any $H^k(U)$ norm. Consider the quadratic form $q(f,g) = \langle \nabla f, \nabla g \rangle$ for $f \in H_0^1(U) \cap H^2(U)$. This form is bounded with respect to the $H^2(U)$ norm. Because $f \in H_0^1(U)$ we can extend it by zero to $f_0 \in H_0^2(\mathbb{R}^2)$ and write

$$\langle \nabla f, \nabla f \rangle_{H^2(U)} = \|\nabla f_0\|^2_{H^2(\mathbb{R}^2)} \geq \inf_{\xi \in \mathbb{R}^2} |(1 + \|\xi\|^2)| \|f_0\|^2_{H^2(\mathbb{R}^2)} \geq \|f\|^2_{H^2(U)}$$

so in particular q is coercive with coercive constant 1. Therefore by the Lax-Milgram Theorem there exists an operator $\Delta : H_0^1(U) \cap H^2(U) \to L^2(U) \cap H^{-1}(U)$ that is bounded in the sense that $\|\Delta f\|^0_H(U) \leq C \|f\|^2_H(U)$ for all $f \in H_0^1(U) \cap H^2(U)$ and such that $q(f,\cdot) = (\Delta f, \cdot)$. Moreover, because q is symmetric, the Laplace operator that we have defined is self-adjoint.

Theorem 2.41. *Let* U *be a bounded open subset of* $\mathbb{R}^2$. *Let* Δ *be the operator associated with the* H^2*-norm closure of the bilinear form* $q(f,g) := \langle \nabla f, \nabla g \rangle$ *for* $f, g \in C_0^\infty(U)$ *via Corollary 2.38. Then* Δ *is self-adjoint with* $\mathrm{Dom}(\Delta) = H_0^1(U) \cap H^2(U)$.

It follows immediately from the expression of the Laplacian as a quadratic form that $\Delta f = (\nabla \cdot \nabla) f$, and so the definition we have given, when written in two-dimensional Cartesian coordinates, is equivalent to the familiar expression:

$$\Delta f = -\frac{\partial^2}{\partial x^2} f - \frac{\partial^2}{\partial y^2} f.$$

Now that we have shown self-adjointness, we wish to prove another property of the Laplacian: That in our setting, that is, for $\overline{U}$ compact, the inverse operator of the Laplacian is a compact operator. However, we have not even proven that the inverse exists and is well-defined, so we shall do this first. To begin, note that

$$\|\Delta u\|_{H^0(U)} \geq C \|u\|_{H^2(U)}$$

for $u \in H_0^2(U)$ (this is eq. 1.6 in [**71**]). This implies that Δ is injective with closed range. It is also surjective: if this were not the case, then we could find $u_0 \in H_0^2(U)$ with

$$(\Delta u, u_0) = 0$$

for all $u \in H_0^2(U)$. But setting $u = u_0$ implies $u_0 = 0$. Thus the inverse $\Delta^{-1} : L^2 \to H_0^1(U) \cap H^2(U)$ is uniquely determined.

By the Rellich-Kondrakov Theorem (Theorem 2.18), it follows that Δ^{-1} must be a compact operator. What we have proved is the following:

THEOREM 2.42. *Let U be a bounded, open subset of $\mathbb{R}^2$. Then Δ_U^{-1} is uniquely determined and a bounded operator from $L^2(U)$ to $H_0^1(U) \cap H^2(U)$. Moreover, $H_0^1(U) \cap H^2(U)$ can be compactly embedded into $L^2(U)$, so Δ_U has compact resolvent.*

COROLLARY 2.43. *The spectrum of Δ_U is a discrete set of real numbers $\{\lambda_n\}$ with no finite accumulation point. There exists a complete orthonormal basis $\{\phi_n\}$ for $L^2(U)$ so that $\Delta_U \phi_n = \lambda_n \phi_n$ and $\lambda_n \to \infty$ as $n \to \infty$.*

PROOF. This follows from applying the Hilbert Schmidt Theorem (Theorem 2.29) to Δ^{-1} and then using the continuous functional calculus for $f(\lambda) = \frac{1}{1+\lambda}$. Because $\lambda \geq 0$ for $\lambda \in \sigma(\Delta)$, then f is continuous on the spectrum and so we can use the Continuous Functional Calculus (Theorem 2.26) . □

We can say more about the asymptotics of λ_n as $n \to \infty$. Namely, Weyl's law says that how fast the eigenvalues grow depends inversely on the area of U:

THEOREM 2.44. *(Weyl's law) Let $N(\lambda) := \#\{\mu \in \sigma(\Delta_U) | \mu \leq \lambda\}$ and U be an open bounded subset of $\mathbb{R}^n$ with piecewise smooth, Lipschitz boundary. Then*

$$N(\lambda) \sim (2\pi)^{-n} \omega_n \lambda^{n/2} \mathrm{vol}(U) \quad \text{as} \quad \lambda \to \infty,$$

where ω_n is the volume of the unit ball in $\mathbb{R}^n$.

PROOF. See[**77**]. The requirement for a piecewise smooth, Lipschitz boundary is not necessary for domains in $\mathbb{R}^2$. Using heat equation methods, it is not difficult to show that the formula holds for any open set U with finite volume. □

The Dirichlet Laplacian satisfies a special property known as domain monotonicity, that allows us to estimate its eigenvalues by those of a Dirichlet Laplacian of a different domain. We will use this property later.

THEOREM 2.45. *(Domain Monotonicity) Let U and V be two open, bounded subsets of $\mathbb{R}^n$ with such that $U \subset V$ and $\mathrm{Vol}(V) < \infty$. Let λ_j be the eigenvalues of Δ_U and μ_j the eigenvalues of Δ_V. Then*

$$\mu_j \leq \lambda_j, \quad j = 1, 2, \cdots$$

PROOF. See [**61**]. □

It will be useful later on to record a well-known estimate of the counting function for the Dirichlet Laplacian:

THEOREM 2.46. *(Li-Yau) Let U be a connected, open bounded subset of $\mathbb{R}^n$ and $N(\lambda)$ the counting function of the Dirichlet Laplacian. Then for any $\lambda > 0$,*

$$N(\lambda) \leq \frac{1}{(2\pi)^n}(1 + 2/n)^{n/2}\omega_n \mathrm{Vol}(U)\lambda^{n/2},$$

where ω_n is the measure of the unit ball in $\mathbb{R}^n$.

PROOF. See [**53**]. □

Finally, we record a useful Theorem sometimes called the "generalized maximum principle" or "Zaremba's principle". It will play a crucial part in one of our later proofs.

THEOREM 2.47. *(Zaremba's principle) Let U be an open, bounded subset of $\mathbb{R}^n$ with piecewise smooth, Lipschitz boundary. Suppose u is a Dirichlet eigenfunction of Δ_U with eigenvalue λ^2 and that v is twice-differentiable, positive function on the strip*

$$S = \{x \in U : d(x, \partial U) \leq \lambda^{-1}\} \subset U$$

with

$$(\Delta_U + \lambda^2)v \leq 0$$

then

$$\max_S \frac{|u|}{v} \leq \max_{\partial S} \frac{|u|}{v}.$$

PROOF. Theorem 10 in [**59**]. □

2.7. The Heat Equation

In this section will recall some properties of the heat equation and the heat operator as well as some special solutions to it known as heat kernels. These objects are crucial to our work and therefore we will take some time to state some of their properties. As before, U will be a domain with Lipschitz boundary and Δ_U the (self-adjoint) Dirichlet Laplacian on U with domain $H_0^1(U) \cap H^2(U)$. The partial differential equation known as the **heat equation** is the following:

$$(\frac{\partial}{\partial t} + \Delta_U)u = 0, \quad u \in (H_0^1(U) \cap H^2(U), C^1(\mathbb{R}^+)). \tag{2.7.1}$$

$$u(0, x) = f(x), \quad f \in L^2(U) \tag{2.7.2}$$

We now aim to give a description of the solutions of this equation, but first we must recall some theory.

DEFINITION 2.48. A **fundamental solution** to the heat equation is a distribution $k : U \times U \times \mathbb{R} \to \mathbb{R}$ that satisfies (2.7.1) in the first and third variable and moreover has the following property:

$$\lim_{t\to 0} k(x, y; t) = \delta_x \quad \text{in} \quad S'(U)$$

where $\delta_x \in S'(U)$ is the so-called delta distribution whose action is defined as $\delta_x f = f(x)$. In the sense of kernels, this means that if we pair each side with a rapidly-decreasing function $f \in S(U)$ and integrate over U, then we obtain

$$\lim_{t\to 0} \int_U k(x, y; t) f(y) dy = \delta_x(f) = f(x) \quad \text{in} \quad S'(U).$$

We can associate to the heat equation the operator known as the **heat operator** because it is the so-called solution operator to the heat equation. This operator is uniquely defined as $L_U := \mathrm{e}^{-\Delta_U t}$ by the Continuous Functional Calculus. It is called the solution operator because $L_U f$ satisfies (2.7.2) by construction and (2.7.1), as we now show. With U an open, bounded set with piecewise smooth, Lipschitz boundary, we denote by ψ_n the eigenfunctions of Δ_U and λ_n the corresponding eigenvalues (existence and orthonormality were shown in Corollary 2.43). From the Continuous Functional Calculus and Corollary 2.43, we obtain:

$$\begin{aligned}
(\frac{\partial}{\partial t} - \Delta_U)(e^{-\Delta_U t} f) &= (\frac{\partial}{\partial t} - \Delta_U) \sum_{n=1}^{\infty} e^{-\lambda_n t} \langle \psi_n, f \rangle \psi_n \\
&= \sum_{n=1}^{\infty} (\frac{\partial}{\partial t} - \Delta_U) e^{-\lambda_n t} \langle \psi_n, f \rangle \psi_n \\
&= \sum_{n=1}^{\infty} \left[-\lambda_n e^{-\lambda_n t} \langle \psi_n, f \rangle \psi_n + \lambda_n e^{-\lambda_n t} \langle \psi_n, f \rangle \psi_n \right] \\
&= 0,
\end{aligned}$$

where in the second line we have used uniform convergence to move $(\frac{\partial}{\partial t} - \Delta_U)$ inside the sum. By Domain Monotonicity (Theorem 2.45) we can bound the eigenvalues λ_n by those of a rectangle, and thus the infinite sum will be dominated by a convergent geometric series. It follows from this calculation that the fundamental solution to the heat equation on U is precisely

$$k(x, y; t) = \sum_{n=1}^{\infty} e^{-\lambda_n t} \psi_n(x) \psi_n(y)$$

and moreover by taking derivatives, we can see that all derivatives of the RHS will be in L^2, proving membership to a Sobolev space of arbitrarily high exponent, and thus that this sum converges in any C^k norm for $t > 0$. We will not prove that ϕ converges to δ in $S'(U)$ but this can be seen by noting that ϕ forms a $\delta-$family. The action of this solution, as a distribution is given by

$$\phi(f)(x) = \int_U \sum_{n=1}^{\infty} e^{-\lambda_n t}\psi_n(x)\overline{\psi_n(y)}f(y)dy.$$

DEFINITION 2.49. We say that an operator A acting on a Hilbert space $\mathcal{H}$ of functions on U is **smoothing** if $Tf \in C^\infty(U)$.

An operator is smoothing if and only if its kernel is smooth, in fact sometimes this is taken as the definition of smoothing (see eg. [**61**]). The heat kernel is the unique fundamental solution of the heat equation with at most polynomial growth (see eg. [**30, 33**]). Therefore we have proved:

THEOREM 2.50. *Let U be an open, bounded subset of $\mathbb{R}^2$ with piecewise smooth, Lipschitz boundary. The kernel of the heat operator L_U is given by*

$$k(x,y;t) = \sum_{n=1}^{\infty} e^{-\lambda_n t}\psi_n(x)\overline{\psi_n(y)}.$$

Moreover, $k(x,y;t) \in C^\infty(U \times U \times \mathbb{R}^+)$. Therefore, the heat operator is smoothing.

We call the kernel of the heat operator the **heat kernel**. This object is central to many areas in mathematics because of the geometric information that it encodes. We will explain what we mean by this shortly. While we have been working on bounded domains, we will need to know the heat kernel on $\mathbb{R}^n$ later on. Let us show that it does indeed satisfy the conditions for being a fundamental solution of the heat equation.

EXAMPLE 2.51. The fundamental solution of the heat equation for the free Laplacian Δ acting on smooth, compactly supported functions in $\mathbb{R}^d$ is

$$k_0(x,y;t) = \frac{1}{(4\pi t)^{d/2}}\mathrm{e}^{-d(x,y)^2/4t}.$$

We call this function the **free-space heat kernel** or **Euclidean heat kernel** to reflect the fact that it does not satisfy any boundary conditions (note that it is intended as an example of a heat kernel, but not an example on a bounded domain). It is very easy to prove that the Euclidean heat kernel satisfies (2.7.1). To prove that it satisfies the appropriate initial condition, namely, that $\lim_{t\to 0} k_0(x,y;t) = \delta_x$, we need to show that it converges to δ_x in the sense of distributions. Let $s_n(x,y) = \frac{n^{d/2}}{(4\pi)^{d/2}}\mathrm{e}^{-nd(x,y)^2/4}$. First, note that due to the factor of $\left(\frac{1}{4\pi t}\right)^{d/2}$, we have that $\int_{\mathbb{R}^d} s_n(y)dy = 1$. Next, suppose that $f \in \mathcal{S}(\mathbb{R}^d)$. Then

$$\begin{aligned}\int_{\mathbb{R}^d} s_n(x,y)f(y)dy &= \int_{B_{\frac{1}{n}}(x)} s_n(x,y)f(y)dy + \int_{\mathbb{R}^d - B_{\frac{1}{n}}(x)} s_n(x,y)f(y)dy \\ &= \int_{B_{\frac{1}{n}}(x)} s_n(x,y)f(y)dy + O(n^{d/2}\mathrm{e}^{-\frac{nd(x,\mathrm{supp}f)^2}{4}}).\end{aligned}$$

The second term obviously decays as $n \to \infty$. To evaluate the first term, note that

$$\int_{B_{\frac{1}{n}}(x)} s_n(x,y)f(y)dy = \int_{B_{\frac{1}{n}}(x)} s_n(x,y)f(x)dy + \int_{B_{\frac{1}{n}}(x)} s_n(x,y)\left[f(y) - f(x)\right]dy$$

but the second term vanishes as $n \to \infty$ by continuity of f since

$$\left| \int_{B_{\frac{1}{n}}(x)} s_n(x,y)\,[f(y)-f(x)]\,dy \right| \leq \left| \int_{B_{\frac{1}{n}}(x)} s_n(x,y)\,[f(y)]\,dy - f(x)\int_{B_{\frac{1}{n}}(x)} s_n(x,y)dy \right| \sup_{\|y\|<1/n} |f(y)-f(x)|.$$

Therefore we have proved that s_n converges to δ_x in the sense of distributions.

DEFINITION 2.52. A bounded, linear operator A on a separable Hilbert space $\mathcal{H}$ is called **trace class** if for some (and hence all) orthonormal basis f_n of $\mathcal{H}$ the sum of terms

$$\|A\|_1 := \sum_k \left\langle (A^*A)^{\frac{1}{2}} f_k, f_k \right\rangle$$

is finite. In this case, the sum

$$\mathrm{Tr}(A) := \sum_k \langle Af_k, f_k \rangle$$

is called the **trace** of A, is absolutely convergent, and is independent of the choice of orthonormal basis (see eg. [**61**]).

Note that A^*A is self-adjoint and therefore the square root can be defined using the continuous functional calculus (Theorem 2.26).

PROPOSITION 2.53. *Let U be an open, bounded subset of $\mathbb{R}^2$. Then L_U, the heat operator on U, is trace class for $t > 0$.*

PROOF. In the following we denote the trace of L_U by $\mathrm{Tr}(L_U)(t)$, to highlight the dependence on t. By the Hilbert-Schmidt Theorem and the Continuous Functional Calculus (see Corollary 2.43), the eigenfunctions of the Laplace operator form an orthonormal basis of $L^2(U)$. Therefore it is sufficient to consider

$$\begin{aligned} \mathrm{Tr}(L_U)(t) &= \textstyle\sum_k \int_U \mathrm{e}^{-\lambda_k t} |\psi_k(x)|^2 dx \\ &= \sum_k \mathrm{e}^{-\lambda_k t}. \end{aligned}$$

By Domain Monotonicity, the eigenvalues λ_k can be bound by those of a rectangle of smaller area than U, and therefore the sum is dominated by a convergent geometric series for $t > 0$. Therefore the last line is finite for $t > 0$. This completes the proof. □

The trace of the heat operator is constructed from the eigenvalues of the Laplace operator. It is not surprising, therefore, that it contains much geometric information, but one cannot recover information such as the area of U simply by evaluating the trace since the sum is over all the eigenvalues. However, if one looks at the behavior of $\mathrm{Tr}(L_U)(t)$ for very small t, then one can recover in its asymptotics precious information about the geometry of U. Namely, there is the following result:

THEOREM 2.54. *Let U be an open bounded subset of $\mathbb{R}^2$ with piecewise smooth Lipschitz boundary ∂U. The heat trace $\mathrm{Tr}(L_U)(t)$ has a full asymptotic expansion as $t \to 0^+$. Namely,*

$$\mathrm{Tr}(L_U)(t) \sim \sum_{k=1}^{\infty} a_{-1+\frac{k}{2}} t^{-1+\frac{k}{2}} \quad , t \to 0^+$$

Moreoever, if ∂U, the first few constants are given by $a_{-1} = \frac{\mathrm{Vol}(U)}{4\pi}$, $a_{-1/2} = -\frac{1}{8\sqrt{\pi}}|\partial U|$, and, if ∂U is smooth, $a_0 = \frac{1-N_H}{12}$, where $|\partial U|$ denotes the length of the boundary and N_H is the number of holes.

PROOF. See [**33**]. An alternative proof as well as a derivation of the first four coefficients can be found in [**28**]. For further information on the case when U has cusp singularities, see [**67**]. □

The coefficients a_n are called the **heat trace coeffients.** It follows from the asymptotic formula that aside from the first three terms, all other terms decay polynomially as $t \to 0$ and do not contribute. For domains with polygonal boundary, M. van den Berg and S. Srisatkunarajah proved even more in [**75**]: the other terms decay exponentially. The statement of their result is as follows:

THEOREM 2.55. *Let U be a polygonal domain in $\mathbb{R}^2$. Then we have*

$$|\mathrm{Tr}(L_U)(t) - \frac{\mathrm{Vol}(U)}{4\pi t} + \frac{|\partial U|}{8(\pi t)^{1/2}} - \sum_{k=1}^{n} \frac{\pi^2 - \gamma_k^2}{24\pi\gamma_k}| \leq \left(5n + \frac{20\mathrm{Vol}(U)}{R^2}\right) \frac{1}{\gamma^2} \mathrm{e}^{-(R\sin\gamma/2)^2/(16t)}$$

where γ_k are the angles of U, γ the smallest angle of U, n the number of sides of U, and R a constant depending on the geometry of U (but which can be chosen to be equal to half the length of its smallest side, though this is not always optimal)

PROOF. Theorem 1 of [**75**]. □

This result relies on an estimate known in the literature as "not feeling the boundary". Basically, this result states that for points far enough from the boundary, the heat kernel behaves like the Euclidean heat kernel, that is, it doesn't "feel" the boundary. Although van den Berg and Srisatkunarajah states this result in more generality (that is, for a regular boundary), we will only use it in the case that U is piecewise polygonal so we state it in this context only as it avoids having to define barrier functions required for an understanding of a "regular" boundary.

THEOREM 2.56. *(Not feeling the boundary) Let U be a Euclidean domain in $\mathbb{R}^2$ and $k_U(x, y; t)$ the Dirichlet heat kernel on U. Then for any $x, y \in \overline{U}$ and $t > 0$,*

$$|k_U(x, y; t) - k_0(x, y; t)| \leq \frac{1}{\pi t} \mathrm{e}^{-(2\sqrt{2}-3)d(x,\partial U)^2/2t}.$$

The proof is achieved by approximating the heat kernel on U with the heat kernel of a unit square, which can be written explicitly, and comparing it with the Euclidean one. In fact, all that is really required by the proof is the so-called "domain monotonicity" property of heat kernels, that is, if $U \subset V$, then $k_u \leq k_v$.

Finally, note that if one integrates $k_U(x,y;t)$ over the diagonal and takes the limit as $t \to 0$, then by a Tauberian Theorem we can recover Weyl's law. Therefore the asymptotics of the heat trace are closely linked to those of the counting function.

The first objective of this work will be to improve the estimate of Theorem 2.56 using finite propagation speed. We will then substitute this result into the intermediate results in [**75**] to obtain an improvement on Theorem 2.55. Of course, the heat equation does not have finite propagation speed - in fact, no matter how localized the initial distribution of heat on a surface, after any time $t > 0$ the smoothing character of the heat operator will have propagated small but non-zero amounts of the heat throughout the surface. In what follows we recall some results about the wave equation and its link with the heat equation; then we will be in a position to use finite propagation speed of the wave equation on U to obtain results relating to the heat equation on U.

2.8. The Wave Equation

In this section we recall some basic properties of the wave equation and how one can extend properties of the wave equation to the heat equation via integral transforms. In particular we set up the machinery to show what consequences finite propagation speed has for the heat equation in the next section. If U is an open, subset of $\mathbb{R}^2$, and $f \in L^2(U)$, then the initial value problem for the wave equation on U is:

$$\left(\frac{\partial^2}{\partial t^2} - \Delta_U\right) u(x,t) = 0, \quad x \in \overline{U}, t > 0, u \in \mathrm{Dom}(\Delta_U) \tag{2.8.1}$$

$$u(x,0) = f(x), \quad x \in \overline{U} \tag{2.8.2}$$

The existence and uniqueness of weak solutions follows from applying the Babuska-Lax-Milgram Lemma (Theorem 2.34) to $q(f,g) := \langle \nabla f, \nabla g \rangle$ and using the Continuous Functional Calculus for $\cos(\lambda^{\frac{1}{2}} t)$ to relate this to (2.8.1).

If U is bounded with piecewise smooth, Lipschitz boundary, we may impose boundary conditions on u. Namely, we will require Dirichlet boundary conditions, that is, $u(x,t) = 0$ whenever $x \in \partial U$.

We proceed as in the previous section, first identifying the fundamental solution of the wave equation in U, that is, when the initial condition is δ_x rather than a square integrable function. Using the same method as the previous section, we can show that the operator $\cos(\Delta_U^{1/2} t)$ is defined by the Continuous functional calculus and that its kernel provides a fundamental solution. Applying the Continuous Functional Calculus and Corollary 2.43 as in the previous section, we have therefore proved:

THEOREM 2.57. *Let U be an open, bounded subset of $\mathbb{R}^2$ with piecewise smooth Lipschitz boundary. The fundamental solution of (2.8.1) is given by*

$$w_U(x,y;t) = \sum_{n=1}^{\infty} \cos(\lambda_n^{1/2} t) \overline{\psi_n(y)} \psi_n(x).$$

The convergence of the sum is understood in the sense that for $\phi \in C_0^\infty(U)$, the partial sums $\psi_S(x) := \int_U \sum_{n=1}^{S} \cos(\lambda_n^{1/2} t) \overline{\psi_n(y)} \psi_n(x).\phi(y) dy$ converge with respect to S in any H^s norm.

The fundamental solution of the wave equation is known as the **wave kernel**.

EXAMPLE 2.58. The fundamental solution of the wave equation in $\mathbb{R}^2$ is known as the **Euclidean wave kernel**, and has the expression

$$w_U(x,y;t) = (it)(d(x,y)^2 - t^2)_-^{-3/2},$$

where the minus subscript means that $w_U(x,y;t) := 0$ whenever $t \leq 0$. The singularity at $d(x,y)^2 = t^2$ means that w_U is not locally integrable. However, it can be defined as the second weak derivative of a locally integrable function, using integration by parts, and can therefore be defined as a distribution (see section 7.8 of [**42**] for details). The main property that makes study of this object desirable is that of finite propagation speed: If the initial distribution function f is localized, then the support of the solution cannot grow arbitrarily fast in time. Physically, this means that the wavefront propagates at a finite speed. The precise statement is the following:

THEOREM 2.59. *(Finite Propagation Speed of wave operator) Let U be an open subset of $\mathbb{R}^2$. Then for any $f \in C_0^\infty(U)$, we have that the support of $\cos(\Delta_U^{1/2}t)f$ lies within a distance t of the support of f, that is:* $\operatorname{supp}\left(\cos(\Delta_U^{1/2}t)f\right) \subset \overline{\cup_{x\in\operatorname{supp} f} B_t(x)}$.

PROOF. Theorem 6 in [**30**]. □

Note that $\tilde{f}(x,t) = \cos(\Delta_U^{1/2}t)f$ satisfies

$$\left(\frac{\partial^2}{\partial t^2} - \Delta_U\right)\tilde{f} = 0, \quad \tilde{f}(x,0) = f, \quad \frac{d}{dt}\tilde{f}|_{t=0} = 0.$$

COROLLARY 2.60. *(Finite Propagation Speed of solutions to the wave equation) Let $x_0 \in U$, $R > 0$ be such that $B_R(x_0) \subset U$, and suppose that $f(x,t) \in C_t^2 L_x^2(\mathbb{R} \times U)$ is a solution of the wave equation on U such that $f(x,0) = 0$ for $x \in B_R(x_0)$ and $\frac{d}{dt}f(x,t)|_{t=0}$ also for $x \in B_R(x_0)$. Then $f(x,t) = 0$ for $x \in B_{R-d}(x_0)$ and for all $0 \leq t < d$.*

PROOF. See section 3.2 of [**39**]. □

COROLLARY 2.61. *Let $x_0, y_0 \in U$ and $d = 2\min(d(x_0,\partial U), d(y_0,\partial U)) > 0$. Then we have that for $\epsilon > 0$ and $t < d - \epsilon$, the restriction of the Dirichlet wave kernel, $w_U(\cdot,\cdot,t)$, to $B_{\epsilon/2}(x_0) \times B_{\epsilon/2}(y_0)$ is equal to the restriction of the free Euclidean wave kernel $w_0(\cdot,\cdot,t)$ to the same set.*

PROOF. Without loss of generality, suppose $d(x_0,\partial U) \leq d(y_0,\partial U)$. Let $f \in C_0^\infty(B_{\epsilon/2}(x_0))$, where $0 < \epsilon < \frac{d}{2}$. Consider the operator defined by the functional calculus

$$W(t)f := \cos(\Delta_U^{\frac{1}{2}}t)f - R_U \cos(\Delta_0^{\frac{1}{2}}t)f_0,$$

where f_0 denotes extension by zero and R_U denotes restriction to U. Note that $W(t)f \in L^2(U) \cap C^\infty(U)$. The Schwartz Kernel Theorem (Theorem 2.22) tells us that we can associate with this operator a unique kernel $w(x,y;t) \in \mathcal{D}'(U \times U \times \mathbb{R})$. Moreover, by linearity (and the Schwartz Kernel Theorem, again) this kernel can be understood as the difference of the distributions $w_U(x,y;t)$ and $w_0(x,y;t)$, where $w_0(\cdot,\cdot,t)$ is restricted to $U \times U$.

Define $g(x,t) = (W(t)f)(x)$. We will now show that $g(x,t)$ satisfies an ordinary differential equation and initial conditions that force it to vanish for $t < \frac{d}{2} - \frac{\epsilon}{2}$. First, the Theorem says that for all $t < \frac{d}{2} - \frac{\epsilon}{2}$, the supports of $\cos(\Delta_U^{\frac{1}{2}}t)f$ and $R_U \cos(\Delta_0^{\frac{1}{2}}t)f_0$ lie within distance $\frac{d}{2} - \frac{\epsilon}{2}$ of $B_{\epsilon/2}(x_0)$, and therefore $g(\cdot,t) \in C_0^\infty(U)$. Moreover, because $\cos(\Delta_U^{\frac{1}{2}}t)f$ and $\cos(\Delta_0^{\frac{1}{2}}t)f_0$ satisfy the wave equation,

$$\frac{\partial^2}{\partial t^2}(g(x,t)) = \Delta_U g(x,t) - \Delta_0 g(x,t),$$

where the Laplacians are in the first variable. However, the RHS is zero as Δ_U and Δ_0 coincide when restricted to $C_0^\infty(U)$. Therefore, for $t < \frac{d}{2} - \frac{\epsilon}{2}$, we have $\frac{\partial^2}{\partial t^2}(g(x,t)) = 0$. Note also that $g(x,0) = f - f = 0$. Furthermore, using the functional calculus,

$$\begin{aligned}\left[\frac{\partial}{\partial t}g(x,t)\right]_{t=0} &= \Delta_U^{\frac{1}{2}} \sin(\Delta_U^{\frac{1}{2}}(0))f - \Delta_0^{\frac{1}{2}} \sin(\Delta_0^{\frac{1}{2}}(0))f \\ &= 0.\end{aligned}$$

Any function satisfying $\frac{\partial^2}{\partial t^2}(g(x,t)) = 0$, $g(x,0) = 0$, and $\left[\frac{\partial}{\partial t}g(x,t)\right]_{t=0} = 0$ is by necessity the zero function, that is, for $t < \frac{d}{2} - \frac{\epsilon}{2}$ and for all $x \in U$, $g(x,t) = 0$.

Now let $0 < t_0 < \frac{d}{2} - \frac{\epsilon}{2}$ and define

$$h(x,t) := W(t+t_0)f(x).$$

Note that $h(x,t)$ satisfies $h(x,0) = 0$ for all $x \in U$. Indeed, $h(x,0) = g(x,t_0)$ but $t_0 < \frac{d}{2} - \frac{\epsilon}{2}$ so by the previous paragraph, $h(x,0) = 0$. The same reasoning gives $\lim_{t\to 0-}\left[\frac{\partial}{\partial t}h(x,t)\right] = \lim_{t\to t_0-}\left[\frac{\partial}{\partial t}g(x,t)\right] = 0$ for all $x \in U$. Because $g(x,t)$ is differentiable, we must have $\lim_{t\to t_0-}\left[\frac{\partial}{\partial t}g(x,t)\right] = \lim_{t\to t_0+}\left[\frac{\partial}{\partial t}g(x,t)\right] = 0$. Thus $\left[\frac{\partial}{\partial t}h(x,t)\right]_{t=0} = 0$. Furthermore, because $\cos(\Delta_U^{\frac{1}{2}}t)f$ and $\cos(\Delta_0^{\frac{1}{2}}t)f_0$ satisfy the wave equation,

$$\frac{\partial^2}{\partial t^2}h(x,t) = \Delta_U h(x,t).$$

In particular, we have $h(x,0) = 0$ for $x \in B_{\frac{d}{2}}(y_0)$ because $d(y_0, \partial U) > \frac{d}{2}$. Therefore the first corollary tells us that $h(x,t) = 0$ for $x \in B_{\frac{d}{2}-\frac{\epsilon}{2}}(y_0)$. Note that there is nothing inherently special about the point y_0, except that $d(y_0, \partial U) > \frac{d}{2}$. If this property were not satisfied, then $x \in B_{\frac{d}{2}}(y_0)$ would not be contained in U, which would prevent us from applying the corollary. Therefore with our choice of y_0, we conclude that $h(x,t) = 0$ for $x \in B_{\frac{d}{2}-\frac{\epsilon}{2}}(y_0)$.

By definition of $h(x,t)$, this means that $W(t)f$ vanishes when restricted to $B_{\frac{\epsilon}{2}}(y_0)$ for all $0 < t < d - \epsilon$. Translated to integral kernels, this is precisely the statement of the corollary. Namely, for $f \in C_0^\infty(B_{\frac{\epsilon}{2}}(x_0))$ and $g \in C_0^\infty(B_{\frac{\epsilon}{2}}(y_0))$ as previously defined, we have

$$\begin{aligned}\langle g, W(t)f\rangle &= \int_U\int_U w_U(x,y;t)f(y)g(x)dydx - \int_U\int_U w_0(x,y;t)f(y)g(x)dydx \\ &= \int_{B_{\frac{\epsilon}{2}}(y_0)}\left(\int_U w_U(x,y;t)f(y)g(x)dx\right)dy - \int_{B_{\frac{\epsilon}{2}}(y_0)}\left(\int_U w_0(x,y;t)f(y)\right)g(x)dxdy \\ &= 0\end{aligned}$$

for $0 < t < d - \epsilon$ as we have already shown that $W(t)f$ vanishes when restricted to $B_{\frac{\epsilon}{2}}(y_0)$ for all $0 < t < d - \epsilon$. It follows that for $0 < t < d - \epsilon$, the restriction of $w_U(\cdot,\cdot,t)$ to $B_{\frac{\epsilon}{2}}(y_0) \times B_{\frac{\epsilon}{2}}(x_0)$ is equal to the restriction of $w_0(\cdot,\cdot,t)$ to $B_{\frac{\epsilon}{2}}(y_0) \times B_{\frac{\epsilon}{2}}(x_0)$, as required. □

What this corollary tells us is essentially that for small enough time, knowing the Euclidean wave kernel is equivalent to knowing the wave kernel of Δ_U. Moreover, in contrast to the hitting time of the stochastic formulation we discussed in the last section, where the Brownian process stops whenever it hits the boundary, here the path γ is allowed to hit the boundary and come back - meaning that we "know" the wave kernel for twice as long. This point of view allows us to improve Theorem 2.56, as we will see later on.

We finish this section by recording the relationship between the wave and heat kernels. First, however, we will need the following well-known formula for the Fourier transform of a Gaussian wavepacket:

LEMMA 2.62. *Let $\alpha > 0$. We have the following identity:*

$$\int_{\mathbb{R}} e^{-\alpha x^2}e^{i\xi x}dx = \sqrt{\frac{\pi}{\alpha}}\mathrm{e}^{-\frac{\xi^2}{4\alpha}}$$

PROOF. See for example the appendix of [**46**]. □

THEOREM 2.63. *Let U be a bounded open subset of $\mathbb{R}^2$. Then we have the following equality where the convergence is in the norm:*

$$\frac{1}{2\sqrt{\pi t}}\int_{-\infty}^{\infty}\cos(\Delta_U^{\frac{1}{2}}s)e^{-\frac{s^2}{4t}}ds = e^{-\Delta_U t}.$$

PROOF. First note that

$$\int_{-\infty}^{\infty}\|\cos(\Delta_C^{\frac{1}{2}}s)e^{-\frac{s^2}{4t}}\|ds \quad\leq\quad \int_{-\infty}^{\infty}\|e^{-\frac{s^2}{4t}}\|ds = 2\sqrt{\pi t}$$

so it follows that the integral exists and converges in the norm. Using Corollary 2.43, we have:

$$\begin{aligned}
&\operatorname{Tr}\left(\frac{1}{2\sqrt{\pi t}}\int_{-\infty}^{\infty}\cos(\Delta_U^{\frac{1}{2}}s)e^{-\frac{s^2}{4t}}ds\right) \quad = \\
&\frac{1}{2\sqrt{\pi t}}\left(\operatorname{Tr}\int_{-\infty}^{\infty}\sum_{n=1}^{\infty}\cos(\lambda_n^{1/2}s)e^{-\frac{s^2}{4t}}\overline{\psi_n(y)}\psi_n(x)ds\right) \\
&= \frac{1}{2\sqrt{\pi t}}\int_U Re[\int_{-\infty}^{\infty}\sum_{n=1}^{\infty}e^{is\lambda_n^{\frac{1}{2}}}e^{-\frac{s^2}{4t}}\overline{\psi_n(y)}\psi_n(x)ds]dxdy \\
&= \frac{1}{2\sqrt{\pi t}}\int_U Re[\sum_{n=1}^{\infty}\int_{-\infty}^{\infty}e^{is\lambda_n^{\frac{1}{2}}}e^{-\frac{s^2}{4t}}\overline{\psi_n(y)}\psi_n(x)ds]dxdy,
\end{aligned}$$

where the interchange of limits is allowed due to absolute convergence of the sum due to Corollary 2.30. Note that the eigenfunctions ψ_n can be chosen to be real (because Δ_U is self-adjoint) and normalized. Upon a change of variables to make use of Lemma 2.62, we obtain that

$$\begin{aligned}
\operatorname{Tr}\left(\frac{1}{2\sqrt{\pi t}}\int_{-\infty}^{\infty}\cos(\Delta_U^{\frac{1}{2}}s)e^{-\frac{s^2}{4t}}ds\right) &= \int_U Re[\sum_{n=1}^{\infty}e^{-t\lambda_n}\overline{\psi_n(y)}\psi_n(x)]dxdy, \\
&= \int_U\sum_{n=1}^{\infty}e^{-t\lambda_n}\overline{\psi_n(y)}\psi_n(x)dxdy, \\
&= \sum_{n=1}^{\infty}\int_U e^{-t\lambda_n}\overline{\psi_n(y)}\psi_n(x)dxdy \\
&= \sum_{n=1}^{\infty}e^{-t\lambda_n}
\end{aligned}$$

which is precisely $\operatorname{Tr}(\mathrm{e}^{-\Delta t})$, as required. We made use of the fact that $\mathrm{e}^{-t\lambda_n}$ is dominated by $\mathrm{e}^{-t\lambda_1}$, which is a convergent integrand, to apply Dominated Convergence and interchange summation and integration again. □

2.9. Pettis Integration

As part of a later construction we make use of the theory of integrals taking values in Banach spaces. We need two concepts for this: one a "strong" integral and one a "weak" one. We will use Bochner's criterion of integrability as a definition of Bochner integrability, as it avoids having to define a Bochner integral in the first place.

Definition 2.64. Let B be a Banach space with dual space B' and (X,Σ,μ) a measure space. A function $f: X\to B$ is called Bochner integrable if

$$\int_X \|f\|_B d\mu < \infty.$$

In particular we will be using the Pettis integral, also known as the "weak" integral. This will also require the notion of a weakly measurable function:

DEFINITION 2.65. Let (X, Σ, μ) be a measure space and B a Banach space over a field K that is either $\mathbb{R}$ or $\mathbb{C}$. Then $f : X \to B$ is called weakly measurable if for every continuous linear functional $g : B \to K$, the function

$$g \circ f : X \to K : x \mapsto g(f(x))$$

is a measurable function w.r.t Σ and the usual Borel σ-algebra on K.

Now we can define a Pettis integral.

DEFINITION 2.66. Let B be a Banach space with dual space B' and (X, Σ, μ) a measure space. Suppose that $f : X \to B$. Let $E \in \Sigma$. If there exists $A \in B$ such that for all $v \in B'$, we have

$$\langle v, A \rangle = \int_E \langle v, f(t) \rangle \, d\mu(t)$$

then we say that A is the Pettis integral of f over E and we write

$$A = \int_E f(t) d\mu(t).$$

We now examine the convergence properties of Pettis integrals. To begin, it follows from the previous definition that

DEFINITION 2.67. Let X be a topological vector space. Let I be an index set and $x_i \in X$ for all $i \in I$. The series $\sum_{i \in I} x_i$ is called unconditionally convergent to $x \in X$ if

- The indexing set $I_0 := \{i \in I : x_i \neq 0\}$ is countable and
- for every permutation of I_0, the relation holds: $\sum_{i=1}^{\infty} x_i = x$.

The statement of representation of Pettis integrals as unconditionally convergent sums is as follows:

THEOREM 2.68. **[17]***Let (X, Σ, μ) be a measure space and B a Banach space. Let $f : S \to X$ be a Pettis integrable function. Then f can be represented in the form $f = g + h$ almost everywhere w.r.t μ, where g is a bounded Bochner integrable function and h assumes at most countably many values in B. If one writes h in the form $h = \sum_{i=1}^{\infty} x_i 1_{E_i}$, where the measurable sets E_i are disjoint, then*

$$\int_E f(t) d\mu = \int_E g(t) d\mu + \sum_{i=1}^{\infty} x_i \mu(E_i \cap E),$$

where the last series converges unconditionally for each $E \in \Sigma$. It converges absolutely if and only if f is Bochner integrable.

A Bochner integrable function is Pettis integrable. The difference between Bochner measurability and weak measurability is explained by Pettis' Theorem. It is not straightforward to construct a function that is Pettis measurable but not Bochner integrable without referring to the Dvoretsky-Rogers Theorem (see e.g. **[27]**). The Dvoretsky-Rogers Theorem states that every infinite-dimensional Banach space contains one unconditionally convergent series that is not absolutely convergent. Using this Theorem, one can construct the example as follows:

COROLLARY 2.69. *Suppose B is infinite dimensional and let $\sum_n x_n$, $x_n \in B$ be a series that is unconditionally convergent but not absolutely convergent. Let E_n be a partition of X into sets of strictly positive measure. Then the function $f : X \to B$ given by*

$$f(\cdot) = \sum_{n=1}^{\infty} \frac{x_n}{\mu(E_n)} 1_{E_n}(\cdot)$$

is Pettis integrable, but not Bochner integrable.

PROOF. First, f is weakly measurable: If $y \in B'$, then because E is a partition, and therefore the E_n are pairwise disjoint,

$$\begin{aligned} \sup_{y \in B'} \int_X |y(f)| d\mu &= \sup_{y \in B'} \int_X |y \left(\sum_{n=1}^{\infty} \frac{x_n}{\mu(E_n)} 1_{E_n}(\cdot) \right)| d\mu \\ &\leq \|y\|_{B'} \|\{x_n\}\|_{l^\infty}. \end{aligned}$$

The existence of the Pettis integral is also clear as f is a sum of simple functions. It is also clear that f takes on countably many values in B (by construction) and so that the g in the representation formula can be set to vanish identically. Suppose that f is also Bochner measurable. Then the Theorem states that the x_n are absolutely convergent, which we assumed was not the case. Therefore f cannot be Bochner measurable. □

REMARK 2.70. Weak measurability does not imply Pettis integrability. A necessary condition for Pettis integrability is not only that for any $x^* \in B'$, $x^* f$ be measurable, but also the existence of an element $\int_E f d\mu$ that satisfies $\langle x^*, \int_E f d\mu \rangle = \int_E x^*(f) d\mu$ for all $x*$. Geitz showed that in a finite perfect measure space, a function is Pettis integrable if and only if there exists a bounded sequence of simple functions f_n such that $\lim_{n\to\infty} x^* f_n = x^* f$ almost everywhere for each $x^* \in B'$. We will make limited application of this result since the Lebesgue measure is finite on Euclidean domains and the measure space is perfect in this case since the Lebesgue measure is Radon and all Radon measure spaces are perfect.

We conclude this section with a simple but highly relevant example.

EXAMPLE 2.71. Let B be the Banach space of bounded operators acting from $L^2(\mathbb{U})$ to itself. Consider a norm-continuous family of smoothing operators $A(t) \in B$, $t \in \mathbb{R}$. Then if the Pettis integral

$$B = \int_0^1 A(t) dt$$

exists, then it converges to an element $\tilde{A} \in B$ in the weak operator topology as the Pettis norms coincide with the weak topology norms. If $\int_0^1 \|A(t)\| dt < \infty$ then the integral converges in the strong sense, which implies convergence in the Pettis sense. This convergence implies an equality of kernels: If $a_t(x, y)$ is the integral kernel of $A(t)$ and $b(x, y)$ is the kernel of B, then we have

$$\begin{aligned}\langle B, v\rangle &= \int_0^1 \langle A(t), v\rangle \, dt \\ &= \int_0^1 \int_{\mathbb{R}} a_t(x,y)v(y)dydt\end{aligned}$$

by Pettis convergence but also

$$\langle B, v\rangle := \int_{\mathbb{R}} b(x,y)v(y)dy.$$

Equating these two formulae results in

$$\int_0^1 \int_{\mathbb{R}} a_t(x,y)v(y)dydt = \int_{\mathbb{R}} b(x,y)v(y)dy.$$

Because the $A(t)$ are smoothing we can use Fubini's Theorem to interchange the order of integration on the LHS and obtain

$$\int_{\mathbb{R}} \int_0^1 a_t(x,y)v(y)dydt = \int_{\mathbb{R}} b(x,y)v(y)dy.$$

Therefore, we can translate the Banach-valued integral to an equality in terms of integral kernels.

CHAPTER 3

Spectral Invariants

In this chapter, we explain what are spectral invariants, give some examples, and show how knowledge of the heat trace coefficients can be used to compute them. We will end the chapter by outlining our proposed method for high accuracy computation of the Casimir energy, a spectral invariant with numerous applications to physics and microelectronics.

DEFINITION 3.1. Let $\mathcal{S}$ denote the set of all Euclidean domains. A function $f : \mathcal{S} \mapsto \mathbb{R}$ is called a **spectral invariant** if and only if for every pair of isospectral domains D_1 and D_2, we have $f(D_1) = f(D_2)$.

By construction, such a function is invariant under a spectrum-preserving map, leading to the name "spectral invariant". Further note that not all spectrum-preserving maps between polygonal domains in $\mathbb{R}^2$ are isometries, so a spectral invariant is not always the same as a metric invariant (see **[69]** for some famous isospectral domains that are not isometric).

EXAMPLE 3.2. The quantity $\lambda_1(U)$, the principal Dirichlet eigenvalue of U, is a spectral invariant, as is $D(U) = \text{Area}(U) + |\partial U|^2$. Indeed, heat trace asymptotics (Theorem 2.54) imply that both the area and length of boundary can be recovered from spectral data. Another example is given by the heat trace - it depends only on the spectrum and thus is also a spectral invariant.

3.1. The Spectral Zeta Function

The spectral invariants that are studied in the present report all have in common that they can be expressed in terms of the spectral zeta function. In this section we define this function, its analytical continuation, and explain its relationship to Riemann's zeta function.

Consider an invertible, diagonalizable $n \times n$ complex matrix A with eigenvalues λ_n. One can define the function

$$\zeta_A(s) = \sum_{k=1}^{n} \frac{1}{\lambda_n^s},$$

and because the sum is finite and none of the λ_n are zero, it can be defined for all $s \in \mathbb{C}$. Now suppose that we consider not A a matrix, but the Dirichlet Laplacian Δ_U on a bounded open set $U \subset \mathbb{R}^2$.

PROPOSITION 3.3. *Let U be a bounded, open set in $\mathbb{R}^2$ with piecewise smooth Lipschitz boundary ∂U. Then the function*

$$\zeta_U(s) = \sum_{n=1}^{\infty} \frac{1}{\lambda_n^s}$$

is analytic and well-defined provided that $\Re(s) > 1$.

PROOF. The sum is dominated by the geometric series $C\sum_{n=1}^{\infty}(k^{-1})^s$ by the Li-Yau estimate (Theorem 2.46), which converges when $\Re(s) > 1$. □

For a moment, consider the Laplacian on smooth functions on $[0, \pi]$. The eigenvalues are precisely squares of the integers and so $\zeta_U(2s)$ is none other than the well-known Riemann zeta function $\zeta_R(s) = 2\sum_{n=1}^{\infty}\frac{1}{n^s}$. In this sense, a spectral zeta function generalises the Riemann zeta function.

It is a basic result of complex analysis that an analytic function that vanishes on an open subset of a connected domain must vanish everywhere. It follows that:

PROPOSITION 3.4. *Let* V *be a non-empty open subset of* $\mathbb{C}$ *and* $U \supset V$ *also a non-empty open subset of* $\mathbb{C}$. *Let* $f_1 : U \to \mathbb{C}$ *and* $f_2 : U \to \mathbb{C}$ *be analytic functions such that* $f_1(z) = f_2(z)$ *for* $z \in V$. *Then* $f_1(z) = f_2(z)$ *for all* $z \in U$.

PROOF. Let $g = f_2 - f_1$. Then g vanishes on V, an open set, and g is analytic. Therefore, it must vanish everywhere. □

Suppose now that we are given $f : V \to \mathbb{C}$ and $g : \mathbb{C} \to \mathbb{C}$ with f and g analytic so that f and g agree on V. Then g is called an **analytic continuation** of f. By Proposition 3.4 analytic continuations are unique. We wish to construct an analytic continuation of the spectral zeta function. This method of continuation was first used by Minakshisundaram and Pleijel in 1949 (see [**60**]).

THEOREM 3.5. *(Analytic Continuation of Spectral Zeta Function) Let* U *be an open, bounded, connected subset of* $\mathbb{R}^2$ *with piecewise smooth Lipschitz boundary* ∂U *and denote by* $\mathrm{Tr}(\mathrm{e}^{-\Delta_U t})$ *the trace of the Dirichlet heat kernel on* U. *Then the function*

$$\tilde{\zeta}_U(s) = \frac{1}{\Gamma(s)}\int_0^{\infty} t^{s-1}(\mathrm{Tr}(\mathrm{e}^{-\Delta_U t}))dt$$

agrees with $\zeta_U(s)$ *for* $\Re(s) > 1$ *and is meromorphic with poles at the negative half integers and* $s = \frac{1}{2}, 1$.

PROOF. Let $\Gamma(n)$ denote the Gamma function and consider the sum

$$\zeta(n) = \frac{1}{\Gamma(n)}\sum_{k=1}^{\infty}\frac{1}{\lambda_k^n}\int_0^{\infty} e^{-y}y^{n-1}dy. \tag{3.1.1}$$

Note that the integral on the RHS is just $\Gamma(n)$ and so cancels with the factor outside the sum, giving the usual definition of the Zeta function. Now we have

$$\frac{1}{\Gamma(n)}\sum_{k=1}^{\infty}\frac{1}{\lambda_k^n}\int_0^{\infty} e^{-y}y^{n-1}dy = \frac{1}{\Gamma(n)}\sum_{k=1}^{\infty}\int_0^{\infty} e^{-y}(\frac{y}{\lambda_k})^{n-1}\frac{dy}{\lambda_k^{1-n}}.$$

Make the substitution $u = y/\lambda_k$ so that $du = \frac{dy}{\lambda_k}$ to get

$$\frac{1}{\Gamma(n)}\sum_{k=1}^{\infty}\int_0^{\infty} e^{-y}(\frac{y}{\lambda_k})^{n-1}\frac{dy}{\lambda_k^{1-n}} = \frac{1}{\Gamma(n)}\sum_{k=1}^{\infty}\int_0^{\infty} e^{-\lambda_k u}u^{n-1}du.$$

Observe that we can re-write this as

$$\frac{1}{\Gamma(s)}\sum_{k=1}^{\infty}\int_0^{\infty} e^{-\lambda_k u}u^{s-1}du = \frac{1}{\Gamma(s)}\int_0^{\infty} t^{s-1}(\mathrm{Tr}(e^{-t\Delta_U}))dt.$$

The interchange can be justified using Fubini's Theorem since all terms are positive. The Li-Yau estimate implies that for large K, $\sum_{k=1}^{K} \frac{1}{\lambda_k^s} - \sum_{k=1}^{K} \frac{1}{k^s} \leq C\lambda_K$, for a positive constant C. Therefore the integral converges for $\Re(s) > 1$.We can partition the integral into two halves:

$$\zeta(s) = \frac{1}{\Gamma(s)} \int_1^\infty t^{s-1}(\mathrm{Tr}(e^{-t\Delta_U}))dt + \frac{1}{\Gamma(s)} \int_0^1 t^{s-1}(\mathrm{Tr}(e^{-t\Delta_U}))dt$$

and substitute the asymptotic expansion of the heat trace of Theorem 2.54 (valid for t near zero), which tells us that

$$\mathrm{Tr}(\mathrm{e}^{-\Delta_U t}) = (4\pi t^{-1}) \left[\sum_{k=0}^{N} t^{k/2} a_{k/2} + R_N(t) \right],$$

where

$$|R_N(t)| \leq C t^{N+1/2}.$$

Applying this gives:

$$\begin{aligned} \zeta(s) = \frac{1}{\Gamma(s)} \int_1^\infty t^{s-1}(\mathrm{Tr}(e^{-t\Delta_U}))dt + \frac{1}{\Gamma(s)} \int_0^1 t^{s-1}((4\pi t)^{-1} \sum_{k=0}^{N} t^{k/2} a_{k/2})dt \\ + \frac{1}{\Gamma(s)} \int_0^1 t^{s-1}(4\pi t)^{-1} R_N(t)dt. \end{aligned}$$

$$\begin{aligned} \frac{1}{\Gamma(s)} \int_0^1 t^{s-1}((4\pi t)^{-1} \sum_{k=0}^{N} t^{k/2} a_{k/2})dt &= \frac{1}{\Gamma(s)} \int_0^1 t^{s-1}(\frac{\alpha_0}{t} + \alpha_1 t^{-1/2} + \alpha_2 + \ldots + \alpha_n t^{(N-1)/2})dt \\ &= \frac{1}{\Gamma(s)} \sum_{n=-1}^{N} \alpha_{\frac{n+1}{2}} \int_0^1 t^{s-1} t^n dt \\ &= \frac{1}{\Gamma(s)} \sum_{n=-1}^{N} \alpha_{n/2+1} \left[\frac{t^{s+n/2}}{s+n} \right]_0^1 \\ &= \frac{1}{\Gamma(s)} \sum_{n=-1}^{N} \frac{\alpha_{n+1}}{n+s} \end{aligned}$$

Because the Gamma function has poles at all the negative integers and zero, $\frac{1}{\Gamma(s)}$ has first order zeros at all the negative integers and zero that cancel out with the first order poles of the above, leaving the ones at the negative half integers and $s = \frac{1}{2}, 1$.

We can proceed similarly with the last term, since $R_N(t)$ is bounded by $Ct^{N+1/2}$, to obtain that

$$\frac{1}{\Gamma(s)} \int_0^1 t^{s-1}(4\pi t)^{-1} R_N(t)dt \leq \tilde{C} \frac{1}{\Gamma(s)} \int_0^1 t^{s+N-5/2} dt$$

which converges if and only if $\Re(s + N - 5/2) > -1$, that is, in the half-plane $\Re(s) > 3/2 - N$. Because there exists a full asymptotic expansion of the heat trace

(see Theorem 2.54) we can take N as large as required to make the third term bounded in any half-plane.

For the first term, Theorem 2.50 implies that $\mathrm{Tr}(\mathrm{e}^{-\Delta_U t})$ is dominated by the convergent series

$$S(t) = \sum_{k=1}^{\infty} \mathrm{e}^{-kt} = \frac{1}{1-(\mathrm{e}^{-t})},$$

where λ_1 is the first Dirichlet eigenvalue of Δ_U. It therefore follows from Lebesgue's Dominated Convergence Theorem (see eg. [**54**]) that the summation and integration can be interchanged and that this term is in fact holomorphic. Therefore the function $\tilde{\zeta_U}$ is meromorphic and agrees with ζ_U whenever $\Re(s) > 1$ as required. □

We have therefore constructed an analytic continuation of $\zeta_U(s)$. We now use it to define the spectral determinant, a generalization of the determinant of matrices.

3.2. The Spectral Determinant

Suppose A is a self-adjoint $n \times n$ matrix. Then A has n eigenvalues λ_k and the determinant of A is defined as

$$\mathrm{Det}(A) := \prod_{k=1}^{k} \lambda_k.$$

Because the product has finitely many terms convergence is not an issue. Note furthermore that $\mathrm{Det}(A) = \mathrm{e}^{-\zeta_A'(0)}$, where $\zeta_A = \sum_{k=1}^{n} \frac{1}{\lambda_k^s}$ is a finite rank analogue of the zeta function we defined in the previous section. To see this, write

$$\zeta'(s) = \sum_{i=1}^{n} \frac{-\log \lambda_i}{\lambda_i^s}.$$

Therefore,

$$\zeta'(0) = \sum_{i=1}^{n} -\log \lambda_i.$$

It follows that

$$e^{-\zeta'(0)} = e^{\log \lambda_1 \log \lambda_2 \cdots}.$$

However, if we replace A by Δ_U, then the product defined above no longer converges. However, $\zeta(0)$ has an analytic extension that is analytic at $s = 0$ by Theorem 3.5. We can use this to make a definition of the determinant of an operator:

Definition 3.6. Let U be an open, bounded subset of $\mathbb{R}^2$ with Lipschitz boundary. Then the **spectral determinant** of U denoted $\mathrm{Det}(\Delta_U)$, is defined as

$$\mathrm{Det}(\Delta_U) := \mathrm{e}^{-\zeta_U'(0)}.$$

This definition was first proposed by Ray and Singer in a 1971 paper ([**60**]) and has subsequently been studied by mathematicians and physicists alike for its connections to Quantum Field Theory, among others (see [**58, 50, 6**] for more information). The analytical continuation of Theorem 3.5 is a convenient way to study the spectral determinant. We now express the spectral determinant in terms of the heat coefficients and the eigenvalues of the Laplacian.

THEOREM 3.7. *Let U be an open, bounded set in $\mathbb{R}^2$ with Lipschitz boundary. Denote the heat coefficients of U by $a_{n/2}$,$n = -2, -1, 0, 1, 2, \cdots, \infty$ and let $F(t) = \sum_{n=1}^{\infty} a_{\frac{n}{2}} t^{n/2}$. Let λ_n be the n-th Dirichlet Laplace eigenvalue of U. Then for any $\epsilon > 0$,*

$$-\text{logDet}(\Delta_U) = \log \text{Det}(\Delta_U)_\epsilon + \log \text{Det}(\Delta_U)_\infty + \int_0^\epsilon \frac{F(t)}{t} dt,$$

where

$$\log \text{Det}(\Delta_U)_\epsilon = -\frac{a_{-1}}{\epsilon} + (\gamma + \log \epsilon) a_0 - 2\frac{a_{-\frac{1}{2}}}{\sqrt{\epsilon}}$$

and

$$\log \text{Det}(\Delta_U)_\infty = \sum_{n=1}^{\infty} \int_\epsilon^\infty t^{-1} \text{e}^{-\lambda_n t} dt.$$

where $\gamma \approx 2.718\cdots$ is the Euler-Mascheroni constant.

PROOF. Before giving the full proof, we outline the main details. Namely, the idea of the proof is to separate the integral defining the analytical continuation of the zeta function into two parts: one that is localized to small time and another part that contains everything else. For small time, we will use our knowledge of the heat trace to say something about the spectral determinant. For large time, we simply re-write the heat trace in terms of the spectrum of Δ_U. For computational purposes, this separation will enable rapid and accurate computation of Δ_U once knowledge of the eigenvalues of Δ_U is attained.

In what follows, we calculate $\zeta'(0)$. By Theorem 3.5, the spectral zeta function $\zeta(s)$ admits a meromorphic extension to the entire complex plane with simple poles at the negative integers and $s = 1$. In particular, $s = 0$ is not a pole. More precisely, we have

$$\zeta(s) = \frac{1}{\Gamma(s)} \int_0^\infty t^{s-1} (\text{Tr} e^{-t\Delta_U}) dt.$$

Given ϵ, we can partition $\mathbb{R}^+$ into two intervals $(0, \epsilon)$ and $[\epsilon, \infty)$:

$$\frac{1}{\Gamma(s)} \int_0^\infty t^{s-1} (\text{Tr}(\text{e}^{-t\Delta_U})) dt = \frac{1}{\Gamma(s)} \left[\int_0^\epsilon t^{s-1} (\text{Tr}(\text{e}^{-t\Delta_U})) dt + \int_\epsilon^\infty t^{s-1} (\text{Tr}(\text{e}^{-t\Delta_U})) dt \right].$$

We compute the first term. Recall from Theorem 2.54 that the heat trace has a full asymptotic expansion for small time, namely

$$\text{Tr}(e^{-t\Delta_U}) - 1 = a_{-1} t^{-1} + a_{-\frac{1}{2}} t^{-1/2} + a_0 + F(t),$$

where $F(t)$ decays as $t \to 0$. Therefore we write the first term above as

$$\begin{aligned}\frac{1}{\Gamma(s)}\int_0^\epsilon t^{s-1}\mathrm{Tr}(e^{-t\Delta_U})dt &= \frac{1}{\Gamma(s)}\int_0^\epsilon t^{s-1}(\frac{a_{-1}}{t}+\frac{a_{-\frac{1}{2}}}{\sqrt{t}}+a_0)dt \\ &\quad +\frac{1}{\Gamma(s)}\int_0^\epsilon t^{s-1}F(t)dt \\ &= \frac{1}{\Gamma(s)}\left(\frac{1}{s-1}a_{-1}\epsilon^{s-1}+\frac{a_{-\frac{1}{2}}}{s-\frac{1}{2}}\epsilon^{s-1/2}+\frac{a_0}{s}\epsilon^s\right) \\ &\quad +\frac{1}{\Gamma(s)}\int_0^\epsilon t^{s-1}F(t)dt.\end{aligned}$$

We are interested in $\zeta'(0)$, that is,

$$\begin{aligned}\lim_{s\to 0}\frac{d}{ds}\left\{\frac{1}{\Gamma(s)}\int_0^\epsilon t^{s-1}(\mathrm{Tr}(e^{-t\Delta_U})-1)dt\right\} = \lim_{s\to 0}\Bigg\{&\left(\frac{\epsilon^{s-1}}{s-1}\frac{a_{-1}}{\Gamma(s)}\right)'+ \\ &+\left(\frac{\epsilon^{s-1/2}a_{-\frac{1}{2}}}{\Gamma(s)(s-1/2)}\right)'+\left(\frac{\epsilon^s a_0}{\Gamma(s)s}\right)'+\frac{d}{dt}\left[\frac{1}{\Gamma(s)}\int_0^\epsilon t^{s-1}F(t)dt\right]\Bigg\}.\end{aligned}$$

There is only one argument so the " $'$" is unambiguous. We now evalue these terms in order. To evalute the first term, recall that $\Gamma(s)$ has a pole of order one at $s=0$. Using its well-known Laurent series (see eg. [**1**]), one has

$$\lim_{s\to 0}\left(\frac{1}{\Gamma(s)}\right)' = \frac{1}{\mathrm{Res}\left[\Gamma(s)\right]_{s=0}} = 1.$$

For the second term, recall that by construction, the Gamma function has the property $\Gamma(s+1)=s\Gamma(s)$. Therefore we can write

$$\lim_{s\to 0}\left(\frac{1}{s\Gamma(s)}\right)' = \lim_{s\to 0}\left(\frac{1}{\Gamma(s+1)}\right)'.$$

Differentiating and applying the chain rule gives

$$\lim_{s\to 0}\left(\frac{1}{\Gamma(s+1)}\right)' = -\frac{\Gamma'(1)}{\Gamma(1)^2}.$$

Because the Gamma function agrees with the shifted factorial map at positive integers (i.e. $\Gamma(n)=(n-1)!$) we have $\Gamma(1)=1$ so

$$-\frac{\Gamma'(1)}{\Gamma(1)^2} = -\Gamma(1)'.$$

For subsequent calculations define the Euler-Mascheroni constant $\gamma := -\Gamma'(1)$. Combining these results, we can write

$$\begin{aligned}\lim_{s\to 0}\left(\frac{\epsilon^{s-1}}{s-1}\frac{1}{\Gamma(s)}\right)' a_{-1} &= \lim_{s\to 0}\frac{1}{\Gamma(0)}\left(-\frac{\epsilon^{s-1}}{(s-1)^2}+\frac{\epsilon^{s-1}\log\epsilon}{s-1}\right)-\frac{a_{-1}}{\epsilon} \\ &= \frac{\alpha}{\epsilon}\end{aligned}$$

because

$$\lim_{s\to 0}\frac{1}{\Gamma(s)} = 0.$$

Also,

$$\begin{aligned}\lim_{s\to 0}\left(\frac{\epsilon^s}{s\Gamma(s)}\right)' a_0 &= \gamma a_0 + \frac{a_0\log\epsilon}{\Gamma(1)}\\ &= a_0(\gamma+\log\epsilon).\end{aligned}$$

Similarly, we obtain that

$$\begin{aligned}\lim_{s\to 0}\frac{d}{dt}\left[\frac{1}{\Gamma(s)}\int_0^\epsilon t^{s-1}F(t)dt\right] &= \left(\frac{1}{\Gamma(s)}\right)'_{s=0}\int_0^\epsilon \frac{F(t)}{t}dt + \\ &\quad + \lim_{s\to 0}\left(\frac{1}{\Gamma(s)}\right)\frac{d}{ds}\int_0^\epsilon t^{s-1}F(t)dt\\ &= \int_0^\epsilon \frac{F(t)}{t}dt\end{aligned}$$

and

$$\lim_{s\to 0}\left(\frac{\epsilon^{s-1/2}a_{-\frac{1}{2}}}{\Gamma(s)(s-\frac{1}{2})}\right)' = -2\frac{a_{-1/2}}{\sqrt{\epsilon}}.$$

Combining these results, we have

$$\begin{aligned}\frac{1}{\Gamma(s)}\int_0^\epsilon t^{s-1}\mathrm{Tr}(e^{-t\Delta_U})dt = -\frac{a_{-1}}{\epsilon} + (\gamma+\log\epsilon)a_{-\frac{1}{2}}\\ - 2\frac{a_0}{\sqrt{\epsilon}} + \int_0^\epsilon \frac{F(t)}{t}dt.\end{aligned} \tag{3.2.1}$$

We now have left to evaluate the other part of the integral, namely

$$\int_\epsilon^\infty t^{s-1}(\mathrm{Tr}(e^{-t\Delta_U}))dt.$$

Using Theorem 2.50, we have:

$$\int_\epsilon^\infty t^{s-1}(\mathrm{Tr}(e^{-t\Delta}))dt = \frac{1}{\Gamma(s)}\int_\epsilon^\infty t^{s-1}\left(\sum_{i=1}^\infty e^{-\lambda_i t}\right)dt.$$

We wish to interchange summation and integration. Observe that each term of the series is integrable. Also, by Weyl's law, there can only be finitely many eigenvalues λ_j with $\lambda_j < 1$, and thus the terms of the series are eventually majorized by $t^{s-1}e^{-t}$, a series that converges uniformly on (ϵ,∞) for all $s\in\mathbb{R}$ so we can write:

$$\zeta_{sp}(s) := \int_\epsilon^\infty t^{s-1}(\mathrm{Tr}(e^{-t\Delta}))dt = \frac{1}{\Gamma(s)}\sum_{i=1}^\infty\int_\epsilon^\infty t^{s-1}e^{-\lambda_i t}dt.$$

Differentiating with respect to s at the point $s=0$:

$$\zeta'_{sp}(0) = \lim_{s\to 0}\frac{d}{ds}\frac{1}{\Gamma(s)}\left[\sum_{i=1}^\infty\int_\epsilon^\infty t^{s-1}e^{-\lambda_i t}dt\right].$$

Applying the product rule, we obtain:

$$\zeta'_{sp}(0) = \lim_{s\to 0}\left[\left(\frac{1}{\Gamma(s)}\right)'\sum_{i=1}^{\infty}\int_{\epsilon}^{\infty} t^{s-1}e^{-\lambda_i t}dt + \frac{1}{\Gamma(s)}\frac{d}{ds}\int_{\epsilon}^{\infty} t^{s-1}\left(\sum_{i=1}^{\infty} e^{-\lambda_i t}\right)dt\right].$$

Applying Weyl's law to the sequence $\{\lambda_n\}$ shows that one can use interchange summation and integration in the second term. But then $\sum_{i=1}^{\infty}\int_{\epsilon}^{\infty} t^{-1}e^{-\lambda_i t}dt$ is bounded, and $\frac{1}{\Gamma(s)} \to 0$ as $s \to 0$ so the second term must vanish at 0.

Therefore

$$\begin{aligned}\zeta'_{sp}(0) &= \lim_{s\to 0}\left(\frac{1}{\Gamma(s)}\right)'\sum_{i=1}^{\infty}\int_{\epsilon}^{\infty} t^{s-1}e^{-\lambda_i t}dt \\ &= \sum_{i=1}^{\infty}\int_{\epsilon}^{\infty} t^{-1}e^{-\lambda_i t}dt \qquad (3.2.2)\end{aligned}$$

where the last equality follows from $-\frac{\Gamma'(1)}{\Gamma(1)^2} = -\Gamma(1)'$. Because $\mathrm{Det}\Delta_U = \mathrm{e}^{-\zeta'(0)}$, the result follows. □

We could use van den Berg and Srisatkunarajah's result (Theorem 2.55) to obtain a straightforward estimate for $\int_0^{\epsilon}\frac{F(t)}{t}dt$ in the polygonal domain setting. However, we will be improving van den Berg and Srisatkunarajah's result later on, so we will use this improved result instead to obtain a better estimate for $\int_0^{\epsilon}\frac{F(t)}{t}dt$. For now, suffice to say that $\int_0^{\epsilon}\frac{F(t)}{t}dt$ is that it is possible to choose ϵ away from zero in such a way that makes it very small.

3.3. Casimir Energy

The Casimir Effect is a physical force produced by a quantized field that was first studied by H.B.G Casimir in a three-page paper dating back from 1948 ([**19**]). It is a very small force on an uncharged, source-free body due to variations in the zero-point energy associated with fluctuations in the quantum vacuum, or what are known in the literature as "virtual photons" ([**24**]). It cannot be explained by traditional intermolecular forces such as the Van der Waals force, and showing this was the object of Casimir's original paper. The typical example is given by two metallic plates, separated by a vacuum and placed micrometers apart. If there is no external field acting on the plates then classical theory would not predict that any measurable force act between the plates. However, quantum electrodynamics says that the plates affect the virtual photons, causing a force known as the "Casimir Force". These forces have been calculated in laboratory settings but only for simple geometries such as parallel plates ([**16**]) or spheres and plates (see [**57**], [**18**], [**15**]). This force depends on the geometry of the plates and how they are arranged. The Casimir Energy is a spectral invariant that assesses how the geometry of a plate affects the Casimir Force its interaction may cause.

There is a need for efficient computation of Casimir Energies in various fields, the most recent at the time of writing being microelectronics. A recent application of Casimir energy in this field has been in the design of a so-called "Casimir chip", that measures its own Casimir interaction and exploits it to create a stictionless

actuator ([**83**]). More information on the applications as well as extensive introductory material can be found in [**24**] and [**13**]. We will not give any details of the physics behind the Casimir force, as this is not the focus of the present work. For our purposes, suffice to say that the Casimir energy is related to $\zeta(-\frac{1}{2})$, of which we detail the regularization below. We will give a definition further on.

We use a cutoff $\epsilon > 0$ as before and write:

$$\begin{aligned}\zeta\left(-\frac{1}{2}\right) &= \frac{1}{\Gamma(-\frac{1}{2})}\int_0^\epsilon t^{-\frac{3}{2}}\sum_{j=1}^{\infty} a_{-1+\frac{j}{2}}t^{-1+\frac{j}{2}}dt + \frac{1}{\Gamma(\frac{1}{2})}\int_\epsilon^\infty t^{-\frac{3}{2}}\sum_{j=1}^{\infty}\mathrm{e}^{-\lambda_j t}dt \\ &= \frac{1}{\Gamma(-\frac{1}{2})}(I_1(\epsilon)+I_2(\epsilon)).\end{aligned}$$

As before, we can evaluate $I_2(\epsilon)$ in practice numerically using a Finite Element package or MPSPack. The integration and summation can be interchanged using dominated convergence and Weyl's law, and then the integration can be carried out explictly to give:

$$I_2(\epsilon) = \sum_{j=1}^{\infty}\left[\frac{2\mathrm{e}^{-\epsilon\lambda_j}}{\sqrt{\epsilon}} - 2\sqrt{\pi\lambda_j}\mathrm{Erfc}(\sqrt{\epsilon\lambda_j})\right].$$

For the small time term, we make use again of the asymptotic expansion of the heat trace, giving:

$$I_1(\epsilon) = \int_0^\epsilon t^{-\frac{3}{2}}\sum_{j=0}^{2} a_{-1+\frac{j}{2}}t^{-1+\frac{j}{2}}dt + \int_0^\epsilon a_{\frac{1}{2}}\frac{dt}{t} + F(\epsilon)$$

where $F(\epsilon)$ decays as $\epsilon \to 0$. We analytically continue the first term and integrate to give:

$$I_1(\epsilon) = a_{-1}\left(-\frac{2}{3\epsilon^{\frac{3}{2}}}\right) + a_{-\frac{1}{2}}\left(-\frac{1}{\epsilon}\right) + a_0\left(-\frac{2}{\sqrt{\epsilon}}\right) + \int_0^\epsilon a_{\frac{1}{2}}\frac{dt}{t} + F(\epsilon).$$

The logarithmic divergence obtained from the fourth term is precisely the energy of the scalar field and must be removed to obtain the Casimir energy of U (see [**13**] for a more detailed physical justification).

DEFINITION 3.8. Let U be an open bounded subset of $\mathbb{R}^2$ with Lipschitz boundary. Then the **Casimir Energy** of U is defined as

$$\mathrm{Cas}_U := \frac{1}{2}\zeta_{FP}\left(-\frac{1}{2}\right),$$

where the "FP" subscript indicates that the logarithmic divergence has been removed. Therefore we have proved the following Theorem:

THEOREM 3.9. *Let a_n be the heat trace coefficients of U, $n = -1, -\frac{1}{2}, , 0\cdots$ and λ_j be the eigenvalues of the Dirichlet Laplacian on U, Δ_U. Then the Casimir energy of U is given by*

$$\mathrm{Cas}(U) = \frac{1}{2\Gamma(-\frac{1}{2})}(I_1(\epsilon)+I_2(\epsilon)),$$

for any choice of $\epsilon > 0$*, where*

$$I_1(\epsilon) = a_{-1}\left(-\frac{2}{3\epsilon^{\frac{3}{2}}}\right) + a_{-\frac{1}{2}}\left(-\frac{1}{\epsilon}\right) + a_0\left(-\frac{2}{\sqrt{\epsilon}}\right) + F(\epsilon),$$

$$I_2(\epsilon) = \sum_{j=1}^{\infty}\left[\frac{2\mathrm{e}^{-\epsilon\lambda_j}}{\sqrt{\epsilon}} - 2\sqrt{\pi\lambda_j}\mathrm{Erfc}(\sqrt{\epsilon\lambda_j})\right],$$

and

$$F(\epsilon) = \int_0^{\epsilon} \frac{\mathrm{Tr}(\mathrm{e}^{-\Delta_U s}) - \sum_{j=0}^{2} a_{-1+\frac{j}{2}} s^{-1+\frac{j}{2}}}{s^{3/2}} ds,$$

where $F(\epsilon)$ *is decaying as* $\epsilon \to 0$*.*

In practice, we can easily and explicitly compute the first few heat trace coefficients of U. Moreover, if U is a polygon, then $F(\epsilon)$ is rapidly decreasing and $a_0 = a_{\frac{1}{2}} = 0$ (by Theorem 2.55). We can then adjust ϵ depending on the behavior of $F(\epsilon)$ and the number of eigenvalues we are able to calculate so that in some ϵ-region we can truncate the spectrum and omit $F(\epsilon)$ altogether with minimal error (the more eigenvalues we know, the smaller we can choose ϵ and the smaller the effect of $F(\epsilon)$). So this Theorem provides a practical method for computing the Casimir energy of a polygonal domain. Even in the case of most planar domains it is easy to compute heat trace coefficients and the first few hundred Dirichlet eigenvalues of the Laplacian.

Part 2

Results

The motivation of this thesis is to compute spectral zeta functions for domains in $\mathbb{R}^2$ with explicit theoretical error bounds for polygonal domains. In particular, we want to compute the spectral determinant and Casimir energy due to the number of interesting applications they present to physics and microelectronics. For this computation, we use Theorems 3.7 and 3.9. These require us to have knowledge of the spectrum, for which we use numerical methods (for example, Alex Barnett's MPSPack) and the analytical continuation of the zeta function. Three sources of errors arise.

(1) First, there are numerical errors from the eigenvalues themselves, as they are not known explicitly but only approximated. These can be controlled, in principle, using interval arithmetics. Namely in MPSPack, Barnett provides theoretical error bounds for every eigenvalue and it is therefore possible to track the propagation of these errors throughout our computation. Other packages provide similar possibilities and there is much literature on bounding the error of boundary element methods (see eg. [**79**] and [**78**] for a discussion of worse-case error bounds for the boundary element method). For the Method of Particular Solutions, that MPSPack is based on, we refer the reader to [**31**], the 1967 paper of Fox, Henrici, and Moler, who invented the method and derived theoretical error bounds for it, as well as the subsequent 2005 paper by Betcke and Trefethen that renewed interest in this method in ([**14**]).

(2) Because we cannot hope to numerically calculate the entire spectrum, the second source of error comes from truncating the spectrum and taking only finitely many eigenvalues into account for our computation. We will bound this error using the Li-Yau estimate (Theorem 2.46), which gives us an upper bound for the counting function. The counting function, in turn, can be used to give an upper bound for the heat trace, that we are approximating with a finite number of eigenvalues. Because each term involving an eigenvalue is positive, our approximation must be less than the real heat kernel, and therefore the maximal difference between the upper bound and our approximation can be taken as a theoretical error bound.

(3) Finally, we replace the true heat kernel by its asymptotic expansion, for small time, introducing another source of error. This error can be controlled by Theorems that estimate the remainder term of the heat expansion for polygonal domains. Namely, there is an explicit remainder term in the Theorem of van den Berg and Srisatkunarajah (Theorem 2.55). We improve upon this remainder term in Theorem 7.7, which allows us to provide a sharper error bound for our computation.

This thesis has three main parts. The first deals with a new method of solving the Helmholtz equation on a polygonal domain in $\mathbb{R}^2$, using domain decomposition and a partition of unity to reduce the problem of solving the Helmholtz equation in the domain to solving it in a half-plane and infinite wedge, where explicit solutions are known. The main result is a comparison with the usual MPS method (for example, MPSPack). While our implementation supports multiple-precision arithmetic and has rigorous theoretical error bounds that can be used to obtain an arbitrarily large number of digits in the computation of the eigenvalues, the speed and efficiency of the implementation is disappointing compared to MPSPack despite our original

expectations. However, one advantage of our method is that it may be easier to implement for multiply connected domains.

The second part of this thesis improves the remainder term of the heat expansion for polygonal domains. As a consequence we are able to obtain a sharper error bound for the error we make by replacing the heat trace with its expansion for small time, and this means that as a result we need less eigenvalues to obtain the same precision in our zeta function computation, compared with the original Theorem of van den Berg and Srisatkunarajah (Theorem 2.55). Because eigenvalue computation is the computational bottleneck of our algorithm, reducing the number of eigenvalues that we need for our computation for a given precision is the simplest way to improve its efficiency. Because our improvement deals with the constant in the exponent of the remainder term, it is especially useful for extremely small time, and namely, for high-precision computations. In the following chapter, we will give a practical example where our improvement leads to a reduction by 15% in the number of eigenvalues required to compute the spectral determinant of a unit regular hexagon to 7 significant digits, and a time gain of just over 10%. For higher precision computations the improvement would be even greater.

Finally, the third part of this thesis is a collection of numerical studies of different domains that have interesting applications in physics. Namely, we study some "cut outs", multiply connected polygonal domains where the holes can be moved to extremize the Casimir energy. Such objects are interesting in physics as numerical instabilities arise in standard methods when the holes come close to the boundary. We are able to tackle such examples and show what the stable configurations are.

CHAPTER 4

Partition of Unity Method of Particular Solutions

In this chapter, we describe a highly flexible method of finding eigenvalues of an elliptic operator defined on an appropriate function space on a Euclidean domain when one knows solutions of the partial differential equations in open regions satisfying some of the same boundary conditions. In particular we will be interested in solving the eigenvalue equation for the Dirichlet Laplacian in polygonal domains. Similar methods have been investigated before to solve the eigenvalue equation in Euclidean domains (see for example [**9**] and [**35**]). However, these methods combine partition of unity decompositions with the Finite Element Method (FEM), which is higher in complexity and more difficult to implement that our method. More recently in [**20**], a method was proposed that combines the partition of unity decomposition and the Method of Particular Solutions (MPS) developed by Fox, Henrici and Moler in [**31**] and recently implemented by Betcke and Trefethen in [**14**]. The method of [**20**] was used to solve the clamped wave equation. Here we use a similar method to find eigenvalues of the Dirichlet Laplacian of a polygonal domain U. First, we give some background to the numerical methods available to solve the eigenvalue problem.

4.1. Numerical Approaches to the Eigenvalue Problem

The Dirichlet eigenvalue problem on a two-dimensional Euclidean domain U is defined as follows: Find a pair $\lambda \in \mathbb{R}, u \in H^2(U)$ satisfying

$$(\Delta_U - \lambda)u = 0 \quad \text{in} \quad U$$

$$u = 0 \quad \text{on} \quad \partial U,$$

subject to the normalizing criterion that $\|u\|_{L^2} = 1$ (thereby discarding the trivial zero solution). Although exact solutions can rarely be found for an arbitrary domain, a vast amount of work has been done on obtaining approximate solutions numerically. The main numerical tools are the Finite Element Method (FEM) and the Boundary Element Method (BEM), which we now briefly introduce.

4.1.1. Finite Element Method. The FEM was first proposed by Richard Courant in 1943 ([**21**]), but subsequently forgotten until 1950, when it was first revived by engineers (see [**52**] for a survey), and then the 1960s, when Milos Zlamal first analysed the method in the mathematical sense ([**82**]). Since then, the method has grown to become one of the most general and powerful techniques available to approximate the solution of partial differential equations. Numerical methods of the finite element type are now widely used in applications.

All FEMs share the same underlying principle: the subdivision of a domain into simpler parts. The idea is to subdivide the domain into a grid (normally called a

"mesh"), usually consisting of triangles, where one represents the original equation by simper "element equations" that are easier to solve (for a detailed introduction, see eg. [**55**]). Then, one recombines all the local solutions into a system of global equations, where the techniques of linear algebra can be used to attempt to find a solution. The step of replacing the original equation by element equations is achieved by replacing the original equation by a weak formulation using the inner product and then replacing the original, usually infinite-dimensional solution space, by finite subsets of a Hilbert basis whose finite linear combinations are dense. Piecewise polynomial (or just piecewise linear functions) which have small support are often used as basis functions in FEM due to the low computational cost of evaluating them, but more complex basis functions can also be used (the method is then referred to as non-polynomial FEM). The advantage of more complex basis functions is that a wider mesh can sometimes be used to achieve the same accuracy as long as the geometry of the boundary is sufficiently simple.

The main methods of improving precision in polynomial FEMs are to subdivide the mesh and to increase the order of the basis. Indeed, one can show, for a convex domain (and under some fairly weak assumptions on the mesh), that if h is the diameter of the largest element in the mesh and N the highest order of the polynomial basis, then the error is bounded by Ch^{N+1}. For a non-convex domain, the power may not be $N+1$, though in general it is still an increasing function of N. There is a large body of work analyzing the convergence properties of FEMs, for example Babuska's classic paper and his collaboration with Melenk ([**8, 9**]).

To discuss the complexity of the FEM assumes that one has made a choice of linear algebraic method to combine the local solutions. One of the simplest and most common techniques used to do this is the least squares method (see eg. the introductory material of [**40**]). If there are N nodes, then a square stiffness matrix would be of size proportional to $N \times N$ and using Cholesky factorization (a typical bottleneck of Least Squares) requires $O(N^3)$ steps (see eg. [**9**]) . More details can be found in eg. [**8**],[**7**], [**55**] and [**81**].

4.1.2. Boundary Element Method. BEMs are fairly recent development compared to FEMs. The foundational work for the method was done by Jawson ([**44**]) and Symm ([**70**]) independently in 1963, and then developed further by Cruse and Rizzo in 1968 ([**22**]), although the name "Boundary Element Method" was not used for another decade. The BEM for the Dirichlet eigenvalue problem takes a different approach to FEM. Starting with a choice of solutions to the eigenvalue equation on $\mathbb{R}^2$ with no boundary conditions (known as the "basis" functions), one attempts to form a linear combination of such solutions that approximately satisfy the Dirichlet boundary conditions. This only requires evaluating the basis functions at a finite set of boundary points (the mesh) and hence affords a reduction of complexity compared to FEM (for a more detailed discussion see eg. [**12**]). Because the space of solutions to the free Helmholtz equation in $\mathbb{R}^2$ is dense in $L^2(U)$ for any compact U, it is possible to approximate the original solution to arbitrary accuracy provided that one chooses a suitably dense basis. In situations where the geometry of ∂U is simple, it is possible to choose the basis functions and the mesh to speed up computation (for an elaborate example, see [**40**]). As a simple example, when attempting to solve the eigenvalue equation on a regular polygon, one can use as a basis Bessel functions corresponding to Dirichlet eigenfunctions on discs of varying

radii, and therefore make use of the high level of symmetry in the problem. The more basis functions and mesh points are employed, the better the approximation.

4.1.3. The Method of Particular Solutions. For the case when U is polygonal and for the Helmholtz equation, the Method of Particular Solutions, first discovered by Fox, Henrici, and Moler in 1967 ([**31**]), is a combination of FEM and BEM that uses as a basis solutions to the Helmholtz equation in a wedge-like region (as opposed to a BEM basis of solutions that are not required to satisfy any boundary conditions), and then uses FEM-type least squares approximation to combine these solutions to form a global one. Of course, it is possible to translate and rotate the solutions on a wedge so that they satisfy not only the Helmholtz equation but also boundary conditions on two edges of the polygonal domain, and because the spectrum of the Laplacian on the infinite wedge is the whole positive real axis, these basis functions can be parametrized by spectral parameter. The convergence of the Method of Particular Solutions has been studied extensively, and numerous improvements have been made since its early days (for a short survey of these improvements see eg. [**14**]). We will be using a Matlab implementation of the MPS created by Alex Barnett and Timo Betcke called MPSPack (see [**12**]), for which we state the rate of convergence below. Given a polygonal domain U centered at the origin with vertices p_i, the elements E_i (where i is the corner parameter) consist of $B_{\rho_i}(V_i) \cap U$ for a positive ρ_i.

THEOREM 4.1. *Let U be a polygonal domain. Let u be an exact solution of the Helmholtz equation with spectral parameter λ (if it exists). Then if v is the approximate solution produced by the MPSPack algorithm with N_i local basis functions in element E_i, there exists $\tau_i > 1$ such that*

$$\|u - v\|_{L^\infty(E_i)} = O(\tau_i^{-N_i})$$

as $N_i \to \infty$.

PROOF. See Theorem 5.2 in [**12**]. □

A similar bound is proved for analytic domains in [**11**]. The constants are difficult to obtain for arbitrary geometries, and MPSPack does not provide theoretical error bounds for its errors. As explained in [**12**], the MPSPack algorithm chooses a suitable mesh and number of basis functions and identifies spectral intervals where there are likely to be eigenvalues. Once this is done, it performs a root-finding algorithm in each interval (the Boyd algorithm) to find the spectral parameter and coefficients that minimizes $\Delta_U - \lambda$ applied to the linear combination of basis functions. The error returned by the algorithm is the difference between the last two iterations of the rootfinding algorithm, before it detects that insufficiently many basis functions have been used to get more precision (while it is possible to see [**12**] for a brief discussion of the error estimate, inspecting the source code of MPSPack directly is very instructive).

The complexity of the MPS is different from traditional FEM because one can end up with rectangular matrices. Namely, the analogue of the stiffness matrix consists of the evaluations of the basis functions at boundary points, and we wish to construct a linear combination of basis functions that vanish at the boundary, but as there is no requirement that there be as many points as basis functions, we may obtain a rectagular matrix (see [**14**] for detailed examples). One then performs

relative Singular Value Decomposition (SVD) on a matrix of size $N \times M$, where $N \geq M$, which has a cost of $O(N^3 D^2)$, where $D = \log(\sigma_1/\sigma_n)$ and σ_n is the n-th largest singular value of the matrix ([**31**]). Intuitively, D measures how close to singular the matrix is (see eg. [**14**]). For a sparse matrix, where most of the entries are zero, efficient algorithms have been created that can do SVD in $O(N^3)$ (see eg. [**26**]). In MPS, the matrix does not satisfy a sparsity condition because the basis functions do not have compact support. In our method, however, the basis functions have compact support and the resulting matrix is sparse, making it possible for us to make use of these more efficient algorithms.

4.2. POUMPS Method

Recall that we wish to solve the following problem: Given a polygonal domain U we wish to approximate the solutions of

$$\Delta_U \psi = \lambda \psi, \quad \psi \in H^2(U), \quad \psi(x) = 0 \quad \forall x \in \partial U$$

to arbitrary accuracy. Given that solutions to the Helmholtz equation with Dirichlet boundary conditions on an open wedge, a half-space, and the whole space $\mathbb{R}^2$ are explictly known, and moreover, that given positive spectral parameter λ one can generate a L^2-basis of λ-eigenfunctions in each of the above regions, we now explain how one can combine such solutions to approximate the exact solution of the Helmholtz equation with Dirichlet boundary condtiions on U with spectral parameter λ to arbitrary accuracy (provided that λ is an eigenvalue of Δ_U). In what follows below $\lambda > 0$ will always denote the spectral parameter.

For an open wedge W_α of angle $\frac{\pi}{\alpha}$ with one ray $\theta = 0$ and the other $\theta = \frac{\pi}{\alpha}$, the Dirichlet eigenfunctions are fractional Bessel functions

$$u_l(r, \theta; \lambda) = J_{\alpha l}(\sqrt{\lambda} r) \sin \alpha l \theta, \quad \lambda > 0, l = 1, 2, 3 \cdots .$$

For a half-space $\mathbb{R}^+$ with boundary at $x = 0$, we use the eigenfunctions:

$$u_l(x, y; \lambda) = \sin(lx) \sin(\sqrt{\lambda - l^2} y) \quad l = 1, 2, 3, \cdots$$

and

$$u_l(x, y; \lambda) = \sin(lx) \cos(\sqrt{\lambda - l^2} y) \quad l = 1, 2, 3, \cdots$$

Finally, for free space we use radial basis functions (which also happen to satisfy Dirichlet boundary conditions on a disk):

$$u_l(r, \theta; \lambda) = J_l(\sqrt{\lambda} r)(\sin l\theta)$$

and

$$u_l(r, \theta; \lambda) = J_l(\sqrt{\lambda} r)(\cos l\theta).$$

Note that all basis functions are parametrized by mode number l and spectral parameter λ.

4.3. Partition of Unity Decompositions

The purpose of any Partition of Unity (POU) decomposition is to patch together a family of local solutions to generate a global one. We now explain what this means and how it is accomplished. For more detail see [**9**], the original paper by Babuska and Melenk where the POU method is first described.

DEFINITION 4.2. Let $U \subset \mathbb{R}^d$ be an open set and let $\{U_i\}$ be an open cover of U. Then $\{U_i\}$ is said to satisfy the bounded local overlap property if each $x \in U$ is contained in only finitely many of the U_i.

Note that if $\{U_i\}$ is a finite set, then the bounded local propety is automatically satisfied.

DEFINITION 4.3. A C^k partition of unity $\{\phi_i\}$, with $k \geq 2$ subordinate to the open cover $\{U_i\}$ satisfies the following properties:

(1) $\phi_i \in C^k(U) \forall i$
(2) $\Sigma_i \phi_i(x) = 1 \quad \forall i, \quad \forall x \in U$
(3) $\text{supp}\phi_i \subset \overline{U_i} \quad \forall i$
(4) $0 \leq \phi_i(x) \leq 1 \forall x \in U$
(5) There exist constants $C_1 > 0$ and $C_2 > 0$ such that for all $x \in U$ and $\forall i$, $\|\nabla \phi_i\|_{L^\infty(U)} < C_1$ and $\|\Delta \phi_i\|_{L^\infty(U)} < C_2$.

It is possible to explicitly construct partitions of unity when U is a polygon by using linear finite element basis functions (see eg. [**10**]). However, we use our knowledge of the explicit solutions stated earlier to obtain a superior and far less complex construction - indeed, finite element meshes can contain thousands of local approximation spaces to approximate an eigenfunction on a unit hexagon depending on the accuracy required, whereas our method employs significantly less (seven spaces is sufficient for any desired accuracy).

To create a $C^2(U)$ partition of unity (which is sufficient for our purposes), we first decompose a polygon U into corners, edges, and the interior (see fig.1 for an example on a regular octagon). Thus we obtain an open cover $\{U_i\}$. We then choose a partition of unity $\{\phi_i\}$ subordinate to this cover (this will be detailed later). That this construction is possible for any polygon is clear as we can take an arbitrarily large disc containing the polygon as an interior region. In our implementation we do place this restriction on the interior as this makes the programming far easier and it increases the efficiency (determining whether a point is within a disk is a very quick computation). Therefore in some convex cases (very thin rectangles, for example) and almost all non-convex cases, it may be necessary to have multiple interior regions to enable this decomposition. However symmetry considerations show that for all regular polygons, which we use to present a proof of concept eigenvalue solver, this construction can be done with just one interior region and one can even do it without any edge regions. That said we will not restrict ourselves to this case in the following, and the method that follows are valid for any polygonal domain, convex or otherwise.

Given a covering $\{U_i\}$ of U that decomposes the domain into corner, edge, and interior regions, the Method of Particular Solutions builds an approximate global solution

$$\psi_{app}(x, y) = \sum_{i,l} c_{i,l} \phi_i(x, y) \psi_{i,l}(x, y),$$

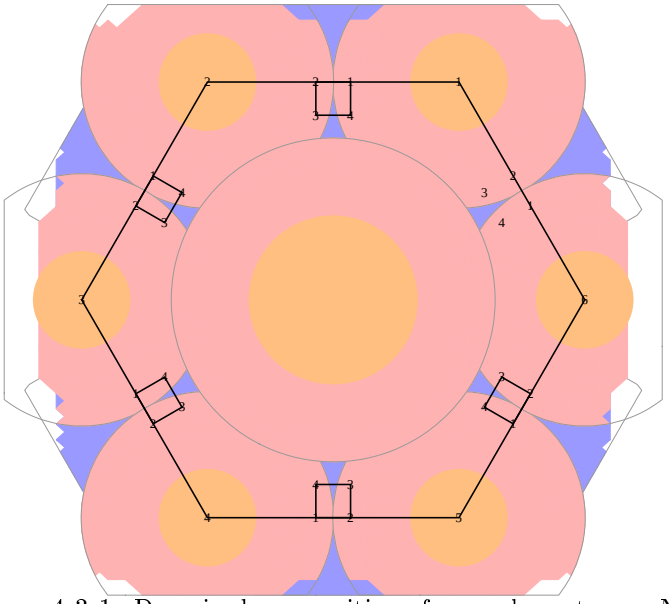

FIGURE 4.3.1. Domain decomposition of a regular octagon. Near corners we use an open wedge approximation with a fractional Bessel basis. In the rectangular regions we use rectangles (Fourier basis). In the interior we use radial basis functions.

where $c_{i,l}$ are constants, the ϕ_i form a C^2 partition of unity, and the $\psi_{i,l}, l \in 1 \cdots N_i$ are basis functions that satisfy

$$\Delta_U \psi_{i,l}(x,y,\lambda) = \lambda \psi_{i,l}(x,y,\lambda) \quad \forall (x,y) \in U_i \tag{4.3.1}$$

and also satisfy Dirichlet boundary conditions on $\partial U_i \cap U$ wherever $\phi_i(x,y) > 0$. The explicit solutions to the open wedge, rectangle, and disk problems form basis functions that satisfy the above requirements. Therefore, our approximation is essentially a sum of these solutions weighted by cutoff functions ϕ_i.

More details on how we choose the basis functions can be found and the end of the previous section. Optimizing the edge length and the radii of the various regions of the polygon (see Figure 4.3.1) can be accomplished using the CoverCheck.nb Mathematica notebook which can be downloaded at http://bit.ly/1xnTPX7. This computes various C^3 norms (the smaller the norm, the better, eg. see Theorem 4.11). It also checks that that radius of the inner region (The blue disk in Figure 4.3.1) is such that the boundary of the disk lies outside U.

PROPOSITION 4.4. *Suppose that $\lambda \in \sigma(\Delta_U)$. Then we have that*

$$\|(\Delta_U - \lambda)\psi_{app}\|_{L^\infty(U)} = \sum_{i,l} c_{i,l} \nabla\phi_i(x,y) \cdot \nabla\psi_{i,l}(x,y,\lambda) - \\ - 2\sum_{i,l} c_{i,l} \Delta_U \phi_i(x,y)\psi_{i,l}(x,y,\lambda)$$

PROOF. The statement is a straightforward computation. We have

$$\|(\Delta_U - \lambda)\psi_{app}\|_{L^\infty(U)} = \sum_{i,k} c_{i,l}\nabla\phi_i(x,y)\cdot\nabla\psi_{i,l}(x,y) - \\ - 2\sum_{i,l} c_{i,l}\psi_{i,l}(x,y,\lambda)\Delta_U\phi_{i,k}(x,y) - 2\sum_{i,l} c_{i,l}\Delta_U\psi_{i,l}(x,y,\lambda)\phi_i(x,y)$$

but the last term vanishes because the $\psi_{i,l}$ satisfy (4.3.1) . □

Therefore we must seek to find constants $c_{i,l}$ that minimize this error. To do this we will use Singular Value Decomposition.

4.4. Singular Value Decomposition Method

From the previous section arises a minimization problem. Indeed, based on Proposition 4.4, we seek to minimize

$$|\sum_{i,l} c_{i,l}\nabla\phi_i(x,y)\cdot\nabla\psi_{i,l}(x,y,\lambda) - 2\sum_{i,l} c_{i,l}\phi_i(x,y)\Delta_U\psi_{i,l}(x,y,\lambda)| \tag{4.4.1}$$

subject to the following normalization condition:

$$\|\sum_{i,l} c_{i,l}\phi_i\psi_{i,l}(\cdot,\cdot,\lambda)\|_{L^2(U)} = 1, \tag{4.4.2}$$

where equality is usually not achieved in practice, but rather, the idea is that ψ_{app} has a norm bounded from below by a strictly positive constant. The objective of the normalization condition is to remove spurious solutions that have very small norm, as these are approximations of the zero function (which trivially satisfies the Helmholtz equation and Dirichlet boundary conditions). With this in mind it is not important for the L^2-norm of ψ_{app} to be precisely one, just that it stays away from zero.

The minimization problem in its current form is all but untractable from a computational point of view as it implies the matching of conditions at an infinite set of points inside U. We therefore approximate the $L^2(U)$ norm by sampling points inside U and checking conditions at those points - the more points we take, the better the approximation. Denote this set of points by $\{(x_k, y_k)\}$ with $(x_k, y_k) \in U$. We need these points to satisfy some conditions related to geometry and linear algebra of the problem, namely:

Definition 4.5. Let $\{U_i\}$ be a polygonal domain decomposition of U, $\{\phi_i\}$ be a C^3 partition of unity subordinate to $\{U_i\}$ and $\psi_{i,l}$, $0 \leq l \leq N_i(\lambda)$, denote the polygonal basis functions associated with U_i and λ, and $X = \{(x_k, y_k)\}$ a set of points in U. We denote the number of members of X by $|X|$. We call X an **adequate mesh** if and only if for each ϕ_i, there are strictly more than N_i members of X with $\|\nabla\phi_i(x_k, y_k)\| > 0$.

We now explain the point of this constraint. Suppose $X = \{(x_k, y_k)\}$ is an adequate mesh. Then we may define the matrix $A(\lambda) = (A_{k,(i,l)}(\lambda))$,$k \in \{1, \cdots, k\}$ and $l \in \{1, \cdots, N_i(\lambda)\}$ă, which records the contribution the remainder term from Proposition 4.4 coming from each basis function $\psi_{i,l}$ evaluated at each point in X.

The rows of $A(\lambda)$ correspond to elements of X and the columns correspond to basis elements:

$$A_{k,\sum_{m<i} mN_m+k-1}(\lambda) = \nabla\phi_i(x_k,y_k)\cdot\nabla\psi_{i,l}(x_k,y_k,\lambda) - 2\Delta_U\phi_i(x_k,y_k)\psi_{i,l}(x_k,y_k,\lambda).$$

If λ is an eigenvalue and A happens to be a square matrix, then A has an eigenvector with small eigenvalue, and this eigenvector gives a vector of coefficients for which the error term is small, forming an approximate solution , i.e.

$$\sum_{i,l} c_{i,l}\nabla\phi_i(x_k,y_k)\cdot\nabla\psi_{i,l}(x_k,y_k,\lambda) - 2\sum_{i,l} c_{i,l}\Delta_U\phi_i(x_k,y_k)\psi_{i,l}(x_k,y_k,\lambda) = 0$$

can be solved for the $c_{i,l}$. Thus if we are close to an eigenvalue λ of the system, we expect the determinant of A to be small.

There are two problems with this approach. First of all, A is not actually a square matrix (see Prop 4.6 below). For rectangular matrices, one can look for small singular values instead small eigenvalues and this is the approach we take. Second, not every value of λ for which there exists a small singular value corresponds to a true eigenvalue of the system, because small singular values can correspond to singular vectors with very small norm, which approximate the zero solution. To get around this, we will use QR factorisation. In the remainder of this subsection, we see the theoretical basis of our method using these ideas.

PROPOSITION 4.6. *If $X = \{(x_k,y_k)\}$ is an adequate mesh, then the linear system*

$$\sum_{i,l} c_{i,l}\nabla\phi_i(x_k,y_k)\cdot\nabla\psi_{i,l}(x_k,y_k,\lambda) - 2\sum_{i,l} c_{i,l}\Delta_U\phi_i(x_k,y_k)\psi_{i,l}(x_k,y_k,\lambda) = 0$$

with unknown variables $c_{i,l}$ is overdetermined.

PROOF. The system has $|X|$ equations and $\sum_i N_i(\lambda)$ unknowns. Note that wherever $(x_k,y_k) \notin \{(x_k,y_k) \in U_i \quad s.t. \quad \|\nabla\phi_i(x_k,y_k)\| > 0\}$, the LHS vanishes and the resulting equation becomes trivial. Because the mesh $X = \{(x_k,y_k)\}$ is adequate, then by this definition for each region U_i we can find strictly more than $N_i(\lambda)$ points where the LHS does not vanish at all basis functions because $\|\nabla\phi_i(x_k,y_k)\| > 0$. Therefore there are strictly more than $\sum_i N_i(\lambda)$ non-trivial equations and only $\sum_i N_i(\lambda)$ unknowns, and the system is overdetermined. □

Note that whether X is an adequate mesh or not does not explicitly depend on λ. However, higher eigenvalues correspond to higher eigenfunctions, so we will need more modes to approximate these. Therefore, a finer mesh is needed to approximate a higher eigenfunction to the same degree of accuracy, as we will discuss in the following section regarding implementation.

Because the system is overdetermined, the matrix A is not square, but a rectangular matrix with more columns than rows. Therefore, we cannot use the determinant to check whether λ is a good candidate eigenvalue. Instead, we use singular values, an analogue of eigenvalues for non-square matrices.

DEFINITION 4.7. A non-negative real number σ is called a singular value for a complex $m \times n$ matrix M if and only if there exist unit-length vectors u in $\mathbb{C}^m$ and v in $\mathbb{C}^n$ such that

$$Mv = \sigma u$$

and

$$M^* u = \sigma v.$$

The vectors u and v are called left-singular and right-singular vectors for σ, respectively. It is a well known fact that the σ are eigenvalues of $\sqrt{M^* M}$ (see eg. [**72**]).

There is no reason to expect, for an arbitrary matrix, that we can always find left and right-singular vectors. However, the following well-known theorem of linear algebra says that in fact we can find m linearly independent left-singular vectors and n linearly independent right-singular vectors of any $m \times n$ matrix M.

THEOREM 4.8. *(Singular Value Decomposition) Suppose that M is an $m \times n$ matrix over the field K, where K is either the field of real or complex numbers. Then there exists a factorization of the form*

$$M = U \Sigma V^*$$

where U is a unitary $m \times m$ matrix over K, the matrix Σ is an $m \times n$ diagonal matrix with nonnegative real numbers on the diagonal, and V^* is an $n \times n$ matrix that is the conjugate transpose of V. The diagonal entries σ_i of Σ are the singular values of M. The m columns of U and the n columns of V are the left-singular vectors and right-singular vectors of M, respectively.

PROOF. See for example p.25 of [**72**]. □

It is clear from the definition that singular values are an analogue of eigenvalues for non-square matrices. Moreover, we can use the smallest singular value and its corresponding singular vectors to solve the constrained minimization problem we defined at the start of this section: We wish to find a unit vector such that the vector $\|Mu\|$ has a small norm. In fact, if u and v are the singular vectors corresponding to the singular value σ, then

$$\begin{aligned} \|Mv\| &= \|\sigma u\| \\ &= \sigma \|u\| \\ &= \sigma \end{aligned}$$

and furthermore u and v have unit norm. Therefore the solution $c_{i,k}$ to the minimization problem (4.4.1) subject to (4.4.2) is precisely given by the entries of the right-singular vector v corresponding to the smallest singular value σ of $A(\lambda)$. This leads us to expect that whenever the smallest singular value of $A(\lambda)$, σ_{min}, is very small, λ is very close to an eigenvalue of Δ_U.

However, there are cases in which σ_{min} could be very small without λ being close to an eigenvalue. We have already excluded the case where A is underdetermined in Proposition 4.6 by using an adequate mesh. However, we have not required that our basis functions be normalized with respect to the L^2 norm, and

in fact a simple calculation shows that the edge basis functions have very large norms for higher orders while the corner functions decrease in norm. Differences in these norms can (and does) lead to spurious detection of eigenvalues. While it is possible to analytically calculate the norm of the edge basis functions, this is not feasible for the corner and interior basis functions. We could implement it using numerical integration, but such computations would take a needless amount of time (and moreoever would need to be repeated at each evaluation of $A(\lambda)$ since the norms depend on λ). A more efficient way is to use QR decomposition.

THEOREM 4.9. *(QR Factorization Theorem) Let M be a complex $m \times n$ matrix. Then there exists a complex $m \times m$ unitary matrix Q and a complex $m \times n$ upper triangular matrix R such that*

$$M = QR$$

Moreover, Q has full rank if and only if M has full rank.

PROOF. See for example pg. 48 of [**72**]. □

Now, we adjoin to $A(\lambda)$ a matrix $B(\lambda)$ consisting of basis function evaluations at sample points. This will serve to exclude **spurious solutions**, that is, solutions approximating the zero function (which satisfies the Helmholtz equation but is not an eigenfunction by definition). Therefore each row of the resulting matrix $C(\lambda)$ contains $2n$ entries: The first half are evaluations of the Laplacians of the basis functions at the sample points. The second half are evaluations of the basis function values at the same sample points:

$$B_{l,\sum_{m<i} mN_m+k-1}(\lambda) = \phi_i(x_k, y_k)\psi_{i,l}(x_k, y_k, \lambda).$$

The columns and rows of the matrix Q from the QR decomposition of $C(\lambda)$ will be unit vectors (as Q is orthogonal by Theorem 4.9). If λ is close to an eigenvalue, then the first half of the columns of Q will be very small, so the norm of the sum of the second half of the column values in each row will be near one. This effectively forces a non-zero L^2-norm of the approximate eigenfunction, thereby discarding spurious solutions by construction. We then project onto the first half of the columns to obtain a matrix $S_{mat}(\lambda)$ consisting of a normalized version of $A(\lambda)$. It follows that if λ is an approximate eigenvalue because by virtue of Theorem 4.8 then $S_{mat}(\lambda)$ has a very small singular value σ_{min} (meaning that it "almost" does not have full rank), and there exists a singular vector v corresponding to σ_{min} such that

$$\begin{aligned} \|A(\lambda)v\| &= \sigma\|v\| \\ &= \sigma \end{aligned} \tag{4.4.3}$$

(the norm of v is one due to the QR normalization), and therefore as before we can construct an approximate eigenfunction over our mesh X:

$$\theta(x_k, y_k) = \sum_{i,l} c_{i,l}\phi_i\psi_{i,l}(x_k, y_k, \lambda),$$

where the coefficients $c_{i,k}$ are the entries of $R^{-1}v$, and now the approximation possesses the property that

$$\max_{(x,y)\in X} |(\Delta - \lambda)\theta(x,y)| \leq \sigma \tag{4.4.4}$$

by (4.4.3) and by construction of A. To see this note that $(\Delta - \lambda)\theta(x_k, y_k) = \sum_{i,l} c_{i,l} A(\lambda)_{k,\sum_{m<i} mN_l + l}$, and also that for any vector $w \in \mathbb{R}^n$ and $p \in \mathbb{N}$, we have that $\|w\|_\infty \leq \|w\|_p$. Therefore the LHS of (4.4.4) is bounded by the RHS of (4.4.3).

We wish to use the above facts to prove that (4.4.4) implies that λ is close to an eigenvalue if σ is close to zero. To do this we will require the following theorem.

THEOREM 4.10. *Let A be a linear operator on a Hilbert space H and let $\|A\|$ denote its operator norm. Then for all $\lambda \in \mathbb{C}$,*

$$\|(A - \lambda)^{-1}\| \leq \frac{1}{d(\lambda, \mathrm{spec}(A))}.$$

PROOF. This is (13.1) in [**61**]. □

This theorem implies the following:

COROLLARY 4.11. *Suppose that there exists a singular value σ of $S_{mat}(\lambda)$ such that (4.4.4) holds for the approximate eigenfunction $\theta(x,y)$. Let*

$$d_{\max} = \max_{p_0, p_1 \in X} d(p_0, p_1)$$

be the size of the largest "gap" in the mesh X. Then

$$d(\lambda, \mathrm{spec}(\Delta_{\mathrm{U}})) \leq \sigma \|\theta\|_{C^3} \frac{d_{\max}}{2}.$$

PROOF. Because θ is C^3 because it is the finite sum of C^3 functions, $(\Delta - \lambda)\theta(x,y)$ is C^1 and it follows that in any given neighborhood of a sampled point $(x,y) \in X$, we can use (4.4.4)

$$\sup_{d((\tilde{x},\tilde{y}),(x,y)) \leq d_{max}} |(\Delta - \lambda)\theta(x,y)| \leq \sigma \|\theta\|_{C^3} \frac{d_{max}}{2}.$$

To see this, observe that any function $f \in C^1([a,b])$ differentiable on some interval $[a,b]$ satisfies

$$\sup_{x \in [a,b]} |f(x)| \leq (b-a) \frac{\|f'\|_{C^1([a,b])}}{2}$$

and the piecewise linear function with slope $\|f'\|_{C^1([a,b])}$ from a to $(b-a)/2$ and slope $-\|f'\|_{C^1([a,b])}$ from $(b-a)/2$ to b is the extremizer (though it is clearly not in C^1 it is possible to construct a sequence of C^1 functions that converges to it in the C^1 norm). It therefore follows that for $\tilde{\theta}$ a restriction of θ to U,

$$\sup_{(x,y)\in U} |(\Delta_U - \lambda)\tilde{\theta}(x,y)| \leq \sigma \|\tilde{\theta}\|_{C^3} \frac{d_{max}}{2}.$$

The Theorem says that if we can find a lower bound for $\|(\Delta_U - \lambda)^{-1}\|$, we can find an upper bound for $d(\lambda, \mathrm{spec}(\Delta_U))$. With this in mind, we observe that

$$\|(\Delta_U - \lambda)^{-1}\| \geq \|(\Delta_U - \lambda)^{-1}\tilde{\theta}\|_{L^2(U)} \geq \|(\Delta_U - \lambda)^{-1}\tilde{\theta}\|_{L^\infty(U)},$$

since U has finite volume. Therefore, because $\|(\Delta_U - \lambda)^{-1}\|$ is bounded for λ not an eigenvalue,

$$\begin{aligned}\|(\Delta_U - \lambda)^{-1}\| &\geq \frac{1}{\|(\Delta - \lambda)\|} \\ &\geq \frac{1}{\|(\Delta - \lambda)\tilde{\theta}\|_{L^\infty(U)}}.\end{aligned}$$

Using that $\|\|(\Delta_U - \lambda)\tilde{\theta}(x,y)\|_{L^\infty(U)} \leq \sigma\|\tilde{\theta}\|_{C^3}\frac{d_{max}}{2}$ as shown above, we therefore have the required result. That is, using the Theorem and the above argument,

$$\begin{aligned}\frac{1}{d(\lambda, \mathrm{spec}(\Delta_U))} &\geq \|(\Delta_U - \lambda)^{-1}\| \\ &\geq \frac{1}{\sigma\|\tilde{\theta}\|_{C^3}\frac{d_{max}}{2}},\end{aligned}$$

which is precisely the statement of the corollary after re-arranging. □

The importance of the corollary is four-fold. First, given a λ and a mesh |X|, one can calculate θ and σ and thereby obtain an estimate of how far λ is from the spectrum. It is therefore possible to devise a stopping criteria for an eigenvalue-search algorithm. This is discussed further in the following section (4.5).

The second piece of information that one can deduce from the corollary is how to make a good choice of mesh. For example, the maximum "gap" size in the mesh appears as d_max, so in this sense it is helpful to have some regularity in the mesh to avoid making this constant too large (though this does not necessarily imply that uniform sampling is optimal). We have found that in practice, it is better to sample more points in regions where multiple regions overlap, since that is where θ will not automatically satisfy the Helmholtz equation - in regions only covered by one cutoff function, θ automatically satisfies the Helmholtz equation). This can also be seen from the corollary, since it is directly related to $\|A\|$, whose entries are essentially components of $(\Delta - \lambda)\theta$, and so where the points are sampled directly affects σ. From a strictly computational point of view, one wants to use as few mesh points as possible, therefore the corollary gives us justification for a choice of mesh that favors points in overlap regions but retains some regularity. Figure 4.5.3 illustrates this point and the CoverCheck.nb notebook available at http://bit.ly/1xnTPX7 helps make such choices without computing A by informing the user of the maximum norm of the cutoff functions and d_max.

The third use of the corollary is in determining whether one is making a good choice for the cover regions R_i. Due to the chain rule, the C^3 norm of θ is directly affected by the C^3 norm of the cutoff functions. In turn, the C^3 norm of the cutoff functions are governed by how "narrow" the intersections of the R_i are, and therefore the estimate tells us that we must make the intersections wide. Again, the CoverCheck.nb notebook can help make such choices based on this heuristic without the need to compute A.

The final piece of information that the corollary gives us is evidence for how much accuracy we can hope to gain by including more basis functions in the calculation. The size of the matrix S_{mat}, given $N(\lambda) = \sum_i N_i(\lambda)$ basis functions and a mesh of size $|X|$, is precisely $2|X| \times N$ (the factor of 2 accounts for the normalization

entries). The complexity of the QR decomposition of an $m \times n$ matrix scales like cube of the largest dimension (see eg. [**72**]), and the complexity of Singular Value Decomposition also scales like the cube of the largest dimension under a sparseness assumption. As those are the two bottleneck steps in our algorithm, we have that the complexity of the POUMPS is also $O(|X|^3)$, provided that the matrix S_{mat} is suitably sparse, which is guaranteed due to the use of cutoff functions. Assuming that the C^3 convergence of the singular vectors obtained by the algorithm is reasonable, the direct gain of precision obtained by adding mesh points is $\sqrt{|X|}$, and σ decreases with respect to the number of local basis functions like $O(\tau^{-N_i})$ for some $\tau > 1$ in the same way as the MPS (Theorem 4.1). This means that overall, the error of the method is expected to scale like $O(\tau^{-\tilde{N}}|X|^{-3/2})$, where $\tilde{N(\lambda)} = \min_i N_i(\lambda)$.

However, we stress that this last point is just a heuristic without a bound on $\|\theta\|_C^3$ that does not depend on X, while the bound from the corollary does depend on X. One would expect that if λ is near an eigenvalue then $\|\theta\|_{C^3}$ can be bounded by the C^3 norm of the eigenfunction, so such reasoning is plausible.

4.5. Implementation

Our implementation of the Partition of Unity Method was done in Mathematica. The goal of this implementation was to produce a proof-of-concept eigenvalue solver that could search over an interval (a, b) for eigenvalues, producing approximate eigenvalues accurate to multiple precision for any given convex polygon. Mathematica was the ideal tool for the implementation given its high level of abstraction, efficient implementation of Bessel functions (version 8+), built-in error propagation control, and the power of its symbolic language that allowed us to perform change of coordinates for the Helmholtz equation easily. In this section, we focus on an example where we applied this notebook to compute the first eigenvalue of a regular unit hexagon. This allowed us to simplify the procedure of choosing a mesh and number of basis functions, as the search interval (a, b) was fixed.

The procedure for selecting the starting number of basis functions in each region was semi-automated, using the Calibrator.nb notebook available at http://bit.ly/1xnTPX7. The procedure for this is to choose a fixed number of basis functions for corner and edge regions and try to expand a radial basis function using this many modes using a least squares do perform the curve fitting. If the error is too high, then more basis functions are selected and the process is repeated until a tolerance is met. For the interior region, where we already use radial basis functions, we used least squares on square eigenfunctions (sines and cosines) instead. This is of course not a rigorous process (nor does it need to be) but we found that it gives good results quickly.

The structure of the code is as follows. The inputs are a set of vertices for the polygon, the search interval (a, b), parameters specifying how fine the mesh is, that is, the set of points where the algorithm will attempt to solve the linear system to satisfy the Helmholtz equation, and finally, λ, the spectral parameter. In general, when the shape of the region is unknown, the notebook allows one to use basis functions of wedge, edge, and radial type, and this is required for example in thin rectangles or thin L-shaped domains, where wedge and radial basis functions alone are not enough. These geometries are particularly problematic as regions cannot

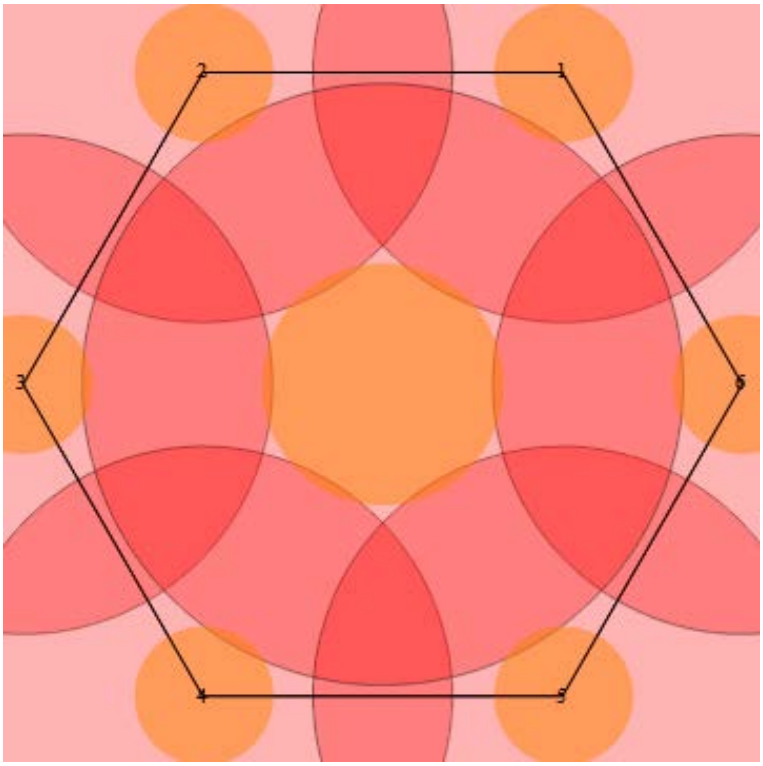

FIGURE 4.5.1. The decomposition chosen for a regular unit hexagon. Note the absence of rectangular "edge" functions, which are not required in this case and whose absence makes computations faster.

be made very large so the C^3 norms of cutoff functions is harder to control. In this case one could consider regions and basis functions of a different type: One could use basis functions for two rectangular cavities explicitly to compute those of an L-shaped region and avoid the problems above. However, we did not consider such basis functions.

As the main example for the proof-of-concept was to compute the principal eigenvalue of the regular hexagon, we assumed that $b - a$ was sufficiently small to fix the mesh size - whereas naturally the mesh size would need to increase with the spectral parameter as more basis functions would be needed to approximate higher eigenfunctions (and thus a finer mesh, to remain adequate). First, the geometry is decomposed into regions adjacent corners, edges, or the center of the polygon. Next the mesh is generated. These regions are stored and various objects encoding changes of coordinates for the Laplacian and values of cutoff functions are computed for each point in the mesh. So far, the computation does not depend on λ and values are therefore re-used for various λ, saving time.

We also developed Mathematica code to help evaluate the cover by computing the norms of the Laplacians of the basis functions in the overlap regions, when multiplied by the cutoffs. The error of the algorithm depended on this norm and

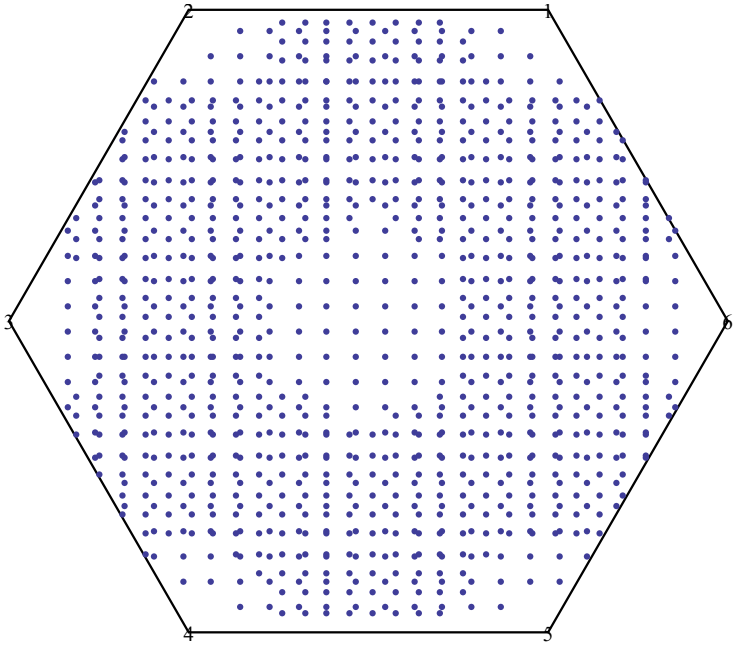

FIGURE 4.5.2. A typical "mesh" of the unit hexagon. The mesh selection algorithm allocates more points in the overlap regions, since this is where compatibility conditions need to be satisfied (they are automatically satisfied where there is no overlap). The additional points are used for normalization. This explains why the mesh is so irregular.

therefore it was essential to keep it as low as possible. In the above example, a plot of the norm is shown in Figure 4.3.3.

Once this computation is complete, values of the basis functions are computed for λ and each point in the mesh. These values and the pre-computed ones from the previous paragraph are then substituted into a large matrix that undergoes QR decomposition and SVD to identify potential small singular values (corresponding to eigenvalues) and singular vectors (corresponding to eigenvectors). The smallest singular value is returned.

The algorithm repeats this computation for various λ in a given range and follows a bisection minimization algorithm around suspected eigenvalues, stopping when a prescribed tolerance is met or when it detects that insufficiently many basis functions have been used to meet the required precision. This is done by considering the smallest singular value, which stops decreasing linearly as expected and can thereafter exhibit instability (this heuristic has been discussed eg. in [**68**]). A plot while the algorithm is running gives us this indication and we have not automated the process for the proof-of-concept. A way that this could be automated is to use a statistical indicator such as the Mean-Squared-Error (MSE) of a linear regression

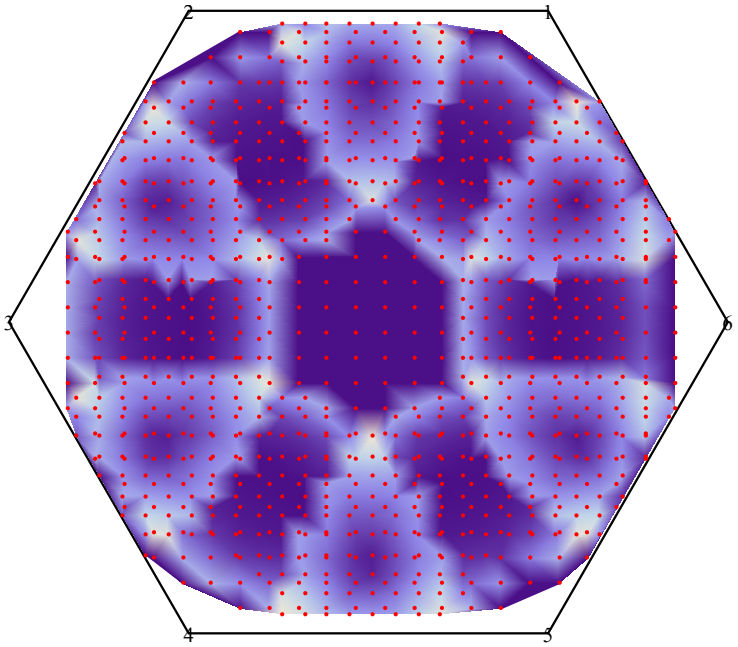

FIGURE 4.5.3. A contour plot of the norms of the Laplacians of the basis functions multiplied by their cutoff functions. The narrower the region, the higher the norm, and as our error estimate depended on it, it was essential to keep it as low as possible (and the regions large).

to measure how linear the smallest singular value was with respect to the spectral parameter, and then stop when a large change was detected. Because the singular value is expected to vary linearly with respect to the spectral parameter, we expect that this method would be effective.

The error bound that we give of the algorithm is semi-rigorous. Subject to the conditions of Corollary 4.11 being met and that the heuristic of linear descent of the smallest singular value is met, we can be assured that the distance of λ to is never greater than the error of the bisection method at that step. That is, if λ_M and λ_{M+1} are the spectral parameters of the approximate eigenvalue at steps M and $M+1$, respectively, then we can be sure that there is a true eigenvalue between λ_M and λ_{M+1}, and thus the error cannot be greater than $|\lambda_{M+1} - \lambda_M|$. This is very similar to the method used by Barnett to estimate MPSPack errors, where the returned error bounds are obtained as the difference between the spectral parameter between the last two iterations of the Boyd rootfinding algorithm (see section 4.1).

4.6. Numerical Results

The first check of our implementation was to compute eigenvalues of a geometry where the spectrum can be analytically computed. For this purpose chose a unit square. Upon successfully computing the first few eigenvalues to 10-digit accuracy, we then proceeded to check our implementation against MPSPack computations for a unit hexagon. Because MPSPack outputs error estimates, we expected our code to match MPSPack output to as many decimal places as our error estimate dictates that it should. Indeed, using sufficiently many basis functions (roughly 10 in each region for every digit of precision required), we observed that the eigenvalues produced by our code agreed with those produced by MPSPack. We computed the remainder term in each region and were able to use this information to allocate additional basis functions in regions where the remainder term was largest. We found that the interior region required more local basis functions than the corner regions, perhaps to be expected as it was larger.

At this stage we observed that our code was computationally inefficient in several ways and undertook to modify it to improve speed of execution. While we more than halved the execution time with these improvements it remains true that our code performed much slower than MPSPack for the same degree of accuracy. That said, our code was able to output results in multiple precision, whereas MPSPack could not. We attempted to modify MPSPack to output multiple precision results using a drop-in replacement for the double class called Multiple Precision Toolbox for Matlab, but this slowed down the computations so much that computations could not be completed in a reasonable amount of time.

Therefore, while our method allows one to compute eigenmodes of polygonal geometries to arbitrary precision, and at a lesser complexity than traditional finite element methods, the limitations of this method appear to lie in the speed of execution, that we have not been able to improve to match anything remotely similar to MPSPack.

As a quick basis for comparison, we note the following example of the computation of the principle eigenvalue of a regular unit hexagon. Given a range of length 0.5 in which to search, our code was able to compute the eigenvalue to 6 digits of precision in 3.5 minutes on a quad core Intel i7 vPro. On the same machine, MPSPack was able to compute the first 150 eigenvalues to 6-8 digit precision in this same time span. A plot of the convergence is shown below:

As a proof of concept we also computed the principal eigenvalue of the unit regular hexagon to 12 significant figures. We point out that unlike our other error estimates, this is only semi-rigorous. What we mean by this is that the error bound produced comes from the error of the bisection algorith, which assumes that sufficiently many basis functions have been used to meet the required accuracy, as seen by the heuristic of linear descent (see section 4.5 for a detailed discussion). This computation, which took several hours on the aforementioned machine, produced an answer of 7.155339133926. The domain decomposition used by the algorithm can be found in Figure 4.4.2. Additionally, the Mathematica source code needed to replicate the result can be downloaded at http://bit.ly/192guiR. The first 8 digits agree with the computation produced by MPSPack, as expected.

In conclusion, while our partition-of-unity method is able to produce high-accuracy results with relatively low complexity, the speed of its implementation

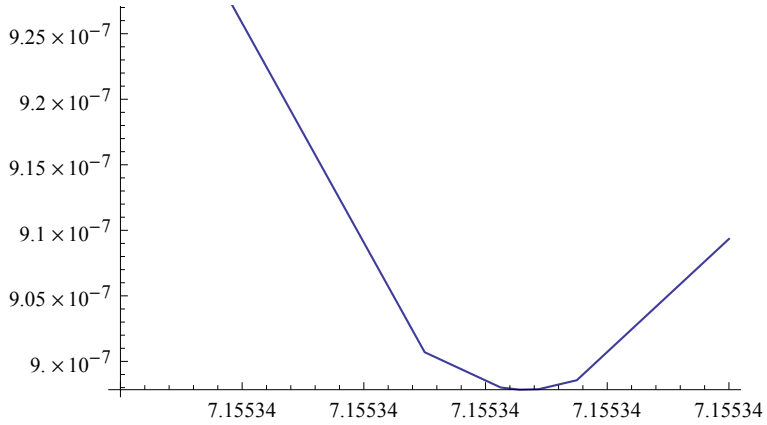

FIGURE 4.6.1. Plot of the largest singular value of the QR-decomposed matrix. A value near zero means that the matrix is quasi-singular and that we have found an eigenvalue. The principal eigenvalue of the unit hexagon corresponds to the pictured minimum.

remains an obstacle in its usage to compute Casimir energy or other spectral invariants. For example, while it takes only a few minutes to obtain the first 200 eigenvalues of a regular unit hexagon to 6 significant digits with MPSPack, this same computation would take hours using our method.

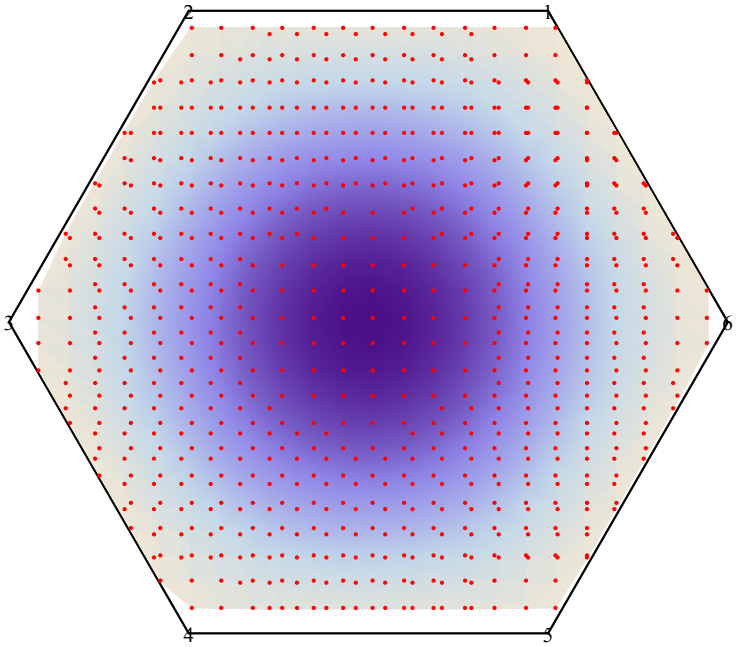

FIGURE 4.6.2. The first eigenfunction of the unit regular hexagon. The principal eigenvalue was computed to 20 significant figures using our Partition of Unity Method.

CHAPTER 5

Uniform Eigenfunction Estimate for Polygons

In what follows we will derive a uniform bound of Dirichlet eigenfunctions for polygonal domains without using heat equation methods. It has long been known (see eg. [**25**]) that using heat equation methods, it can be shown that Dirichlet eigenfunctions of the Laplacian on finite-volume domains in $\mathbb{R}^2$ satisfy the estimate

$$\|u_k\|_\infty^2 \leq \left(\frac{\mathrm{e}}{4\pi}\right)\lambda_k.$$

The proof uses only heat kernel domain monotonicity to bound the local heat trace by that of $\mathbb{R}^n$.

We will show a similar bound using the generalized maximum principle (Theorem 2.47). We will seek to bound the L^∞ norm of an eigenfunction by its L^2 norm, modulo a constant depending on the square root of the eigenvalue. The method we use (and the method used in Lemma 6 of [**36**]) suggest that it is possible to calculate this constant explicitly for a known domain (where the boundary is explicitly parametrised). We will estimate the norm of the eigenfunction by a constant times the square root of its eigenvalue, and this power is sharp by general theorems (see eg. [**41**]). We however do not claim that the constant is optimal. We will use an estimate by Safarov on the counting function of the Laplacian whenever x is far enough from the boundary. We will then follow the proof of [**36**] and use the generalized maximum principle (Theorem 2.47) to show that this estimate holds also when x is arbitrarily close to the boundary. The result of Safarov that we will use is the following:

THEOREM 5.1. *Let $e(x,y;\lambda)$ denote the spectral function of Δ_U. Then for all $x \in U$ and $\lambda > 0$, we have*

$$e(x,x,\lambda) \leq \frac{1}{4\pi}\lambda + \frac{(2\pi^{-1}v^2+v)}{d(x,\partial U)}\left(\lambda^{1/2} + \frac{v}{d(x,\partial U)}\right),$$

where $v = 4\times 3^{\frac{1}{4}}$.

PROOF. See [**64**]. □

THEOREM 5.2. *Suppose U is a polygonal domain and let d be the smallest distance between an edge of U and a vertex of U not contained in the edge. Let u be an L^2-normalized eigenfunction of Δ with eigenvalue $\lambda > \frac{1}{d^2}$. Then*

$$\|u\|_\infty^2 \leq \frac{1+4\pi}{4\pi}\lambda(2\pi^{-1}v^2+v)\,(1+v)\,,$$

where $v = 4\times 3^{\frac{1}{4}}$.

The proof of this theorem depends on the following Lemma, from which it follows directly.

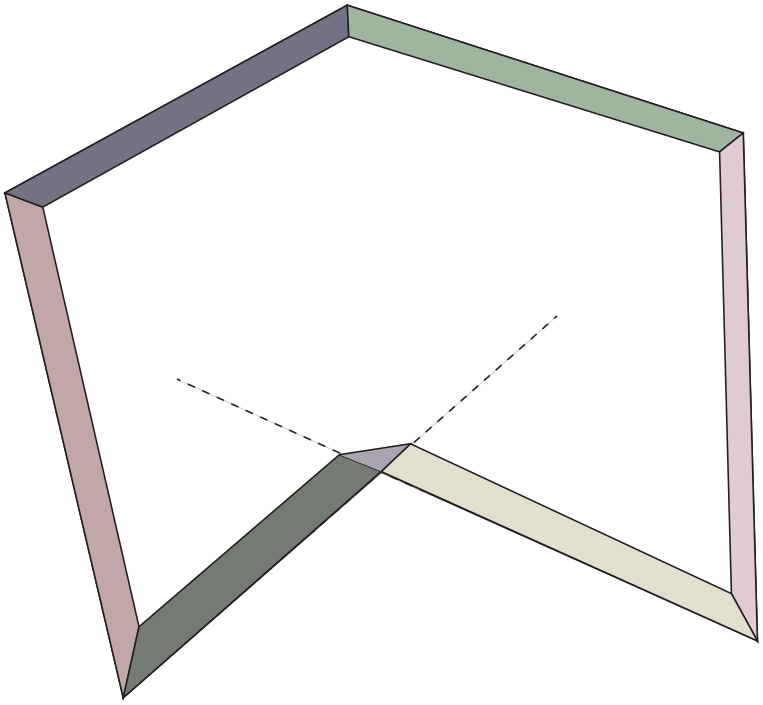

FIGURE 5.0.1. Decomposition of a polygon into "edges" and "vertices" near the boundary. The strip S is colored.

LEMMA 5.3. *Suppose U is a polygonal domain and let d be the smallest distance between an edge of U and a vertex of U not contained in the edge. Let u be an eigenfunction of Δ_U with eigenvalue $\lambda > \frac{1}{d^2}$. Then for $\mu = \sqrt{\lambda}$, we have*

$$\max_{x:d(x,\partial U)<\mu^{-1}} |u| \leq \max_{x:d(x,\partial U)=\mu^{-1}} |u|$$

PROOF. Consider a point $x \in U$. Let α be the angle of the vertex V of U nearest x. We will decompose the domain U into subdomains that are either near an edge or a vertex with angle greater than π. Below is an illustration of a decomposition for a polygon, where the shaded regions illustrate the strip S and how the decomposition is done:

Edges: We use these coordinates for all points whose nearest vertex has angle strictly less than π and for all points which are vertices. Let E be the edge closest to x. Local Cartesian coordinates can be given by letting y be the distance from x to E and z be a perpendicular coordinate in the same direction as E.

Consider the function $w(y,z) = \sin(\frac{\pi}{2} + \frac{3}{2}(\mu y - 1))$. Then $w > 0.07$ on the strip S defined by $\{(y,z) \in U : 0 \leq y \leq \mu^{-1}\}$ and we have $\frac{\partial^2}{\partial y^2} w = -\frac{9}{4}\mu^2 w(y,\theta) < 0$ on S and $\frac{\partial^2}{\partial z^2} w = 0$. In order to apply the Lemma, we need $(\Delta + \mu^2)w \leq 0$ on S, which is easily seen since

$$\begin{aligned}(\Delta+\mu^2)w &= -\frac{9}{4}\mu^2 w(y,z)+\mu^2 w(y,z)\\ &\leq -\frac{5}{4}\mu^2 w(y,z).\end{aligned}$$

Since w is strictly positive on S it follows that the conditions of Theorem 2.47 are satisfied. Therefore

$$\max_{x\in S}\frac{|u|}{w}\leq\max_{x\in\partial S}\frac{|u|}{w},$$

but since $u=0$ when $y=0$ and $w(y,z)=1$ when $y=\lambda^{-1}$ the claim follows since λ is large enough that S is entirely contained in U.

Corners: We use these coordinates for all points whose nearest vertex has angle strictly greater than π. In this case, the construction above fails in a sector because some points are nearer the vertex than the edges (for example when $\alpha=\frac{3}{2}\pi$ it fails for a sector of angle $\frac{\pi}{2}$). In this sector, we use polar coordinates with $r>0$ and the choice of function $w(r,\theta)=\sin(\frac{\pi}{2}+\frac{3}{2}(\mu r-1))$. The Laplace operator takes the form

$$\Delta_U=\frac{1}{r^2}\frac{d}{dr^2}+R(\frac{d}{dr}\frac{d}{d\theta},\frac{d^2}{d\theta^2}),$$

where the terms depending on θ are irrelevant since w does not depend on θ. This gives

$$(\Delta_U+\mu^2)w=-\frac{1}{r^2}\frac{5}{4}w(r,\theta)<0,$$

which is negative as required and well defined provided $r>0$, as we assumed (if $r=0$ then x lies on an edge and we can use the previous construction, which is nonsingular, instead).

We can therefore apply Theorem 2.47 and because $w(r,\theta)=1$ when $r=\lambda^{-1}$ and u vanishes on ∂U because it is a Dirichlet eigenfunction the result follows as λ is large enough that S is entirely contained in U. □

CHAPTER 6

Rigorous Error Estimates for Spectral Invariant Computations

In this section we derive some rigorous error bounds for the Casimir energy and spectral determinant when U is a polygonal domain in $\mathbb{R}^2$. These bounds will assume that error estimates for eigenvalues are also rigorous, which is not quite true in practice since the MPSPack error estimates are semi-rigorous. However, our estimates are package-agnostic in the sense that they do not depend on which method one uses to compute the eigenvalues so long as it comes with error estimates, so someone using a different package with rigorous error bounds to compute the spectrum can use our error estimates to get a rigorous estimate of the error he makes in computing the Casimir energy or spectral determinant.

Recall from (3.2.1) and Theorem 3.9 that to compute spectral zeta function one first analytically continues it and then splits the resulting integral into small-time and large-time components. For the small-time component we use heat trace asymptotics to obtain a result; for the large-time component we use the computed eigenvalues. This process introduces three sources of errors: One, the heat asymptotics are only true modulo some exponentially decaying function, which we can estimate using heat trace estimates for polygons. Two, we cannot compute all the eigenvalues and must therefore estimate the error we make by truncating the spectral sum. This is done using upper bounds of the spectral counting function. Finally, the eigenvalues themselves are not exact but approximate. Therefore we must estimate the error we make here as well, although admitedly this is just a question of summing over the individual errors as there are only finitely many of them.

6.1. Small time error bound

The error that we make by replacing the heat trace by its asymptotic expansion can be estimated by Theorem 7.6. Indeed, the difference between the heat trace and its asymptotic expansion is exponentially decaying as $t \to 0^+$, and so the remainder term in (3.2.1) and Theorem 3.9 are bounded. Namely, we have the following result, which is obvious by construction:

THEOREM 6.1. *(Spectral determinant heat trace approximation error) Let U be an n-sided polygonal domain in $\mathbb{R}^2$. Then for any $\epsilon > 0$, we have*

$$\int_0^\epsilon \left| \frac{\operatorname{Tr}(\mathrm{e}^{-\Delta_U t})}{t} - \sum_{j=1}^{3} a_n t^{-2+\frac{j}{2}} \right| dt \quad \leq \quad \int_0^\epsilon \frac{1}{t} R_U(t) dt,$$

where $R_U(t)$ is the heat trace estimate given either by the RHS of Theorem 2.55 or Theorem 7.7.

REMARK. What makes this rigorous and explicit error bound possible to obtain is that there are only three non-zero terms in the asymptotic expansion of the heat trace for polygons. For a more general domain (say, a disk), such error bounds using the same method are possible in principle but require careful control over the heat trace coefficients, which is in general not achievable. It is however possible to have semi-rigorous error bounds modulo some remainder of the form $O(\epsilon^n)$, where n depends on the number of known heat trace coefficients.

In practice we will use numerical integration to evaluate the remainder. Normally, our heat trace estimate (Theorem 7.7) will provide a slightly sharper error bound than the heat trace of van den Berg and Srisatkunarajah due to the better exponent. In practice we have observed that our estimate gives a heat trace error that is 5-10 times less in situations when the interior angles of the domain are not too acute. We will provide an example of this later on when computing the spectral determinant of a regular unit hexagon. For comparative purposes, we include both error formulas in the Mathematica notebook, available for download at http://bit.ly/Iq1hMh.

We now give the analogue of the preceding Theorem for the computation of Casimir energy, the proof of which is basically the same:

THEOREM 6.2. *(Casimir energy heat trace approximation error) Let U be an n-sided polygonal domain in $\mathbb{R}^2$ with heat coefficients $a_n, n = 1, 2, 3, \cdots$. Let R denote half the length of the shortest edge of U and γ its smallest angle. Recall that c_1 is a constant depending on universal eigenfunction estimates that we calculated in Corollary 5.2. Then for any $\epsilon > 0$, we have*

$$\int_0^\epsilon \left| \frac{\mathrm{Tr}(\mathrm{e}^{-\Delta_U t})}{t^{3/2}} - \sum_{j=1}^{3} a_n t^{-5/2+\frac{j}{2}} \right| dt \quad \leq \quad \int_0^\epsilon \frac{1}{t^{3/2}} R_U(t) dt,$$

where $R_U(t)$ is the heat trace estimate given either by the RHS of Theorem 2.55 or the RHS of Theorem 7.7.

6.2. Spectral Truncation Error

In this subsection we give the error bound for the error that is made by truncating the spectral sum, that is, by only considering finitely many eigenvalues.

THEOREM 6.3. *(Spectral determinant spectrum truncation error) Let U be an n-sided polygonal domain in $\mathbb{R}^2$ with Dirichlet Laplace eigenvalues $\lambda_k, k = 1, 2, 3, \cdots n$. Then for any $\epsilon > 0$, we have*

$$\int_\epsilon^\infty \left| \mathrm{Tr}(\mathrm{e}^{-\Delta_U t}) - \sum_{j=1}^{n} \mathrm{e}^{-\lambda_j t} \right| t^{-1} dt \leq 2\pi |U| (1+n) \Gamma(0, n\epsilon)$$

PROOF. Note that this integral on the LHS is precisely the spectral truncation error by virtue of (3.2.2). We can write the heat trace in terms of the counting function as follows (this is immediate from Theorem 2.28 since the spectral measure is a sum of delta distributions, the spectrum being discrete):

$$\mathrm{Tr}(\mathrm{e}^{-\Delta_U t}) = \int_0^\infty \mathrm{N}'(\lambda)\mathrm{e}^{-\lambda t} d\lambda$$

where $N(\lambda)$ is the counting function of Δ_U. Therefore we can express the difference between the real heat trace and the truncated one we obtain from the spectrum as

$$\begin{aligned}\mathrm{Tr}(\mathrm{e}^{-\Delta_U t}) - \sum_{j=1}^{n} \mathrm{e}^{-\lambda_j t} &= \int_n^\infty N'(\lambda)\mathrm{e}^{-\lambda t} d\lambda \\ &= -\lim_{\delta\to 0+} N(n+\delta)\mathrm{e}^{-nt} + t\int_n^\infty N(\lambda)\mathrm{e}^{-\lambda t} d\lambda\end{aligned}$$

where the last line follows by integrating by parts. We then use the Li-Yau estimate (Theorem 2.46), which says that

$$N(\lambda) \leq 2\pi|U|\lambda,$$

and substituting this estimate into the integral and integrating by parts gives

$$\begin{aligned}\mathrm{Tr}(\mathrm{e}^{-\Delta_U t}) - \sum_{j=1}^{n} \mathrm{e}^{-\lambda_j t} &\leq -\lim_{\delta\to 0+} N(n+\delta)\mathrm{e}^{-nt} + 2\pi|U|t\int_n^\infty \lambda \mathrm{e}^{-\lambda t} d\lambda \\ &= -\lim_{\delta\to 0+} N(n+\delta)\mathrm{e}^{-nt} + \frac{2\pi|U|\mathrm{e}^{-nt(1+nt)}}{t} \\ &\leq N(n)\mathrm{e}^{-nt} + \frac{2\pi|U|\mathrm{e}^{-nt(1+nt)}}{t} \\ &= 2\pi|U|\left(n\mathrm{e}^{-nt} + \frac{1}{t}\mathrm{e}^{-nt(1+nt)}\right) \\ &\leq 2\pi|U|\,(n+1)\,\mathrm{e}^{-nt}\end{aligned}$$

because the counting function is increasing. We make the last estimate to make the subsequent integral possible to evaluate in terms of special functions. Indeed, substituting gives

$$\int_\epsilon^\infty \left|\mathrm{Tr}(\mathrm{e}^{-\Delta_U t}) - \sum_{j=1}^{n} \mathrm{e}^{-\lambda_j t}\right| t^{-1} dt \leq 2\pi|U|(1+n)\Gamma(0, n\epsilon)$$

as required. □

For the Casimir energy the analogue is the following (the proof follows exactly the same lines):

THEOREM 6.4. *(Casimir energy spectrum truncation error) Let U be a polygonal domain in $\mathbb{R}^2$ with computed Dirichlet Laplace eigenvalues $\lambda_j, j = 1, 2, 3, \cdots n$. Then for any $\epsilon > 0$, we have*

$$\frac{1}{\Gamma(\frac{1}{2})}\int_{\epsilon}^{\infty}\left|\mathrm{Tr}(\mathrm{e}^{-\Delta_U t})-\sum_{j=1}^{n}\mathrm{e}^{-\lambda_j t}\right|t^{-3/2}dt \leq$$
$$\frac{1}{\Gamma(\frac{1}{2})}2\pi|U|(1+n)\left|\frac{2\mathrm{e}^{-n\epsilon}}{\sqrt{\epsilon}}-2\sqrt{n\pi}\mathrm{Erfc}\left(\sqrt{n\epsilon}\right)\right|.$$

PROOF. See above. □

6.3. Spectral Approximation Error

The spectral approximation error comes from using approximate eigenvalues instead of true eigenvalues. There are finitely many of these errors, one for each eigenvalue. We simply calculate the error for each eigenvalue and sum over all the errors to give an overall error. Again, because we truncate the spectrum, there are only finitely many such errors and therefore the sum is not a problem to implement. Suppose we have bounds on the individual errors given by $|\lambda_n - \tilde{\lambda_n}| \leq E_n$, where $\tilde{\lambda_n}$ is the approximate eigenvalue. The overall approximation error due to propagating the error of a single approximate eigenvalue is given by the remainder term of Taylor's Theorem:

$$Err(\lambda_n) \leq C_s E_n \int_{\epsilon}^{\infty} t^s \mathrm{e}^{-(\lambda_n - |E_n|)t}\mathrm{dt} \tag{6.3.1}$$

where s and C_s are constants depending on where the spectral zeta function is being evaluated. We then sum over all the approximate eigenvalues. Namely, s is zero for the spectral determinant and one for the Casimir energy, and C_s is one for the spectral determinant and $\frac{1}{\Gamma(\frac{1}{2})}$ for the Casimir energy. We then sum over all the errors. For the spectral determinant this was arrived directly from (3.2.2), for the Casimir energy it is clear. In practice, we obtain an estimate of the E_n directly from MPSPack.

CHAPTER 7

Heat Trace Estimate

We wish to know how much the diagonal of the heat kernel on a planar domain U differs from the diagonal of the unconstrianed, Euclidean heat kernel. This is useful in numerical applications, for if we are sufficiently far away from the boundary we can then replace the heat kernel on U by the Euclidean one, which is much easier to calculate, and the estimate gives us a rigorous error bound. Such estimates have come to be known as "not feeling the boundary" estimates, starting with M. Kac ([**45**]). These estimates were originally formulated in terms of path integrals and one obtained the estimate by replacing the heat kernel on U by a known heat kernel (i.e. a box) for small time. However, "small time" here means precisely the distance between the point x where we want the estimate, and the boundary. Using finite propagation speed we shall construct an estimate that depends on twice this distance, thereby improving the original estimate, which we now state for reference:

THEOREM 7.1. *(Original "not feeling the boundary" estimate,* [**73**]*) Let U be a bounded, open connected subset of $\mathbb{R}^2$, $x \in U$, and $t > 0$. Then we have that*

$$|k^U(x,x;t) - \frac{1}{4\pi t}| \leq \frac{1}{\pi t} e^{-\frac{d(x,\partial U)^2}{4t}}.$$

In particular, note that the difference between $k^U(x,x;t)$ and its Euclidean counterpart decays very fast as $t \to 0$ for all non-zero values of d.

7.1. Estimate of the Diagonal

Before we begin, we will need the following result.

PROPOSITION 7.2. *Let Δ_U be the Dirichlet Laplacian on a domain U with piecewise smooth, Lipschitz boundary. Furthermore, let $f : \sigma(\Delta) \to B(L^2(U))$ and $g : \sigma(\Delta) \to B(L^2(U))$ be continuous and have the following properties: f and g are $O(\lambda^{-N})$ for some $N > 0$ and $f(\lambda) \leq g(\lambda)$ for all $\lambda \in \sigma(\Delta)$. Then if $k_f(x,y)$ and $k_g(x,y)$ are the integral kernels of $f(\Delta)$ and $g(\Delta)$, respectively, then we have that for all $x \in U$,*

$$k_f(x,x) \leq k_g(x,x).$$

PROOF. We have that for $v \in D(\Delta)$,

$$\begin{aligned} \langle v, f(\Delta)v \rangle &= \int_U f(\lambda) d\langle v, E_\lambda v \rangle \\ &\leq \int_U g(\lambda) d\langle v, E_\lambda v \rangle \\ &= \langle v, g(\Delta)v \rangle . \end{aligned}$$

More explicitly:

$$\int_U \int_U k_f(x,y)v(y)v(x)dydx \leq \int_U \int_U k_g(x,y)v(y)v(x)dydx. \tag{7.1.1}$$

We may choose a sequence $v_n \in D(\Delta_U)$ of smooth, compactly supported bump functions centered at x of width ϵ . Because k_f and k_g are continuous (because f and g are $O(\lambda^{-N})$ by assumption), we have

$$\lim_{n\to\infty} \int \int_U k_f(x,y)v_n(y)v_n(x)dydx \to k_f(x,x),$$

in the sense of $D'(U)$ and also

$$\lim_{n\to\infty} \int \int_U k_g(x,y)v_n(y)v_n(x)dydx \to k_g(x,x).$$

But the bound (7.1.1), valid for all $v = v_n$, implies that $k_f(x,x) \leq k_g(x,x)$. □

Consider a point $x \in U$ and let $d = 2d(x, \partial U)$. Let Δ_0 be the Laplace operator on $H^2(\mathbb{R}^2)$. We begin by choosing an $\epsilon > 0$ and a cutoff function $\chi_\epsilon \in C^3(\mathbb{R})$ with the following properties:

(1) $\chi_\epsilon(s) = 0$ whenever $s < d - \epsilon$.
(2) $\chi_\epsilon(s) = 1$ whenever $s > d$.
(3) $\chi_\epsilon(s) = 3(\frac{s-d+\epsilon}{\epsilon})^2 - 2(\frac{s-d+\epsilon}{\epsilon})^3$ whenever $d - \epsilon \leq s \leq d$.

This choice of cutoff function will lead to the constants that appear in Theorem 7.5. We do not claim that our choice of cutoff function is optimal, and a different choice may produce slightly better constants. However, the discussion in [**68**] suggests that this particular cutoff function is optimal for at least some geometries, and we therefore expect it to be a very good choice.

Let x and $t > 0$ be real numbers. Then Lemma 2.62 implies that

$$\mathrm{e}^{-x^2 t} = \frac{1}{2\sqrt{\pi t}} \int_0^\infty \cos(xs)\mathrm{e}^{-\frac{s^2}{4t}} ds.$$

Using the Spectral Theorem for Unbounded operators (Theorem 2.28) we therefore have that the Pettis integral

$$\frac{1}{2\sqrt{\pi t}} \int_0^\infty \cos(\Delta_U^{\frac{1}{2}} s)\mathrm{e}^{-\frac{s^2}{4t}} ds$$

converges weakly to $\mathrm{e}^{-\Delta_U t}$ for U open (that is, it converges in the inner product when applied to test functions). Moreover, this integral converges in the norm (one can easily estimate the norm since the norm of the cosine factor is just one). Let $\mathrm{Tr}_x(A)$ denote the diagonal of the integral kernel of an operator A with continuous kernel. We have the identity

$$\begin{aligned}
\mathrm{Tr}_x(\mathrm{e}^{-\Delta_U t} - \mathrm{e}^{-\Delta_0 t}) &= \mathrm{Tr}_x\left(\frac{1}{2\sqrt{\pi t}}\int_0^\infty \cos(\Delta_U^{\frac{1}{2}}s)e^{-\frac{s^2}{4t}}ds - \frac{1}{2\sqrt{\pi t}}\int_0^\infty \cos(\Delta_0^{\frac{1}{2}}s)e^{-\frac{s^2}{4t}}ds\right)\\
&= \mathrm{Tr}_x(\frac{1}{2\sqrt{\pi t}}\int_0^\infty \cos(\Delta_U^{\frac{1}{2}}s)e^{-\frac{s^2}{4t}}\chi_\epsilon(s)ds\\
&- \frac{1}{2\sqrt{\pi t}}\int_0^\infty \cos(\Delta_0^{\frac{1}{2}}s)e^{-\frac{s^2}{4t}}\chi_\epsilon(s)ds\\
&+ \frac{1}{2\sqrt{\pi t}}\int_0^\infty \cos(\Delta_U^{\frac{1}{2}}s)e^{-\frac{s^2}{4t}}(1-\chi_\epsilon(s))ds\\
&- \frac{1}{2\sqrt{\pi t}}\int_0^\infty \cos(\Delta_0^{\frac{1}{2}}s)e^{-\frac{s^2}{4t}}(1-\chi_\epsilon(s))ds).\\
&= \mathrm{Tr}_x(I_1 - I_2 + I_3 - I_4).
\end{aligned}$$

By finite propagation speed (Corollary 2.61), $\mathrm{Tr}_x(I_3) = \mathrm{Tr}_x(I_4)$, so in fact $\mathrm{Tr}_x(\mathrm{e}^{-\Delta_U t} - \mathrm{e}^{-\Delta_0 t}) = \mathrm{Tr}_x(I_1 - I_2)$. This leaves us two terms:

(1) The contribution to the local trace from $\frac{1}{2\sqrt{\pi t}}\int_0^\infty \cos(\Delta_U^{\frac{1}{2}}s)e^{-\frac{s^2}{4t}}\chi(s)ds$, and
(2) The contribution to the local trace from $\frac{1}{2\sqrt{\pi t}}\int_0^\infty \cos(\Delta_0^{\frac{1}{2}}s)e^{-\frac{s^2}{4t}}\chi(s)ds$.

We will estimate the second term via Fourier analysis, the first using integration by parts and we will prove that both have continuous kernels.

LEMMA 7.3. *For any $0 < \epsilon < d$, the operator*

$$A_d(t) := \frac{1}{2\sqrt{\pi t}}\int_0^\infty \cos(\Delta_U^{\frac{1}{2}}s)e^{-\frac{s^2}{4t}}\chi_\epsilon(s)ds$$

has a continuous integral kernel $A_d(x,t)$, and moreover we have the estimate

$$|A_d(x,t)| \leq \frac{\zeta(3)\mathrm{Diam}(U)}{\sqrt{2}\pi^3\sqrt{t}\Gamma(3/2)}\left(\frac{30}{\epsilon^2} + \frac{32d}{\epsilon t} + 72\frac{(d-\epsilon)^2 - 2t}{t^2}\right)\mathrm{e}^{-\frac{(\mathrm{d}-\epsilon)^2}{4\mathrm{t}}},$$

where $\mathrm{Diam}(U)$ *is the diameter of U and ζ is the Riemann zeta function.*

PROOF. Let $x \in \mathbb{R} - 0$. Then

$$\int_0^\infty \cos(xs)e^{-\frac{s^2}{4t}}\chi_\epsilon(s)ds = -\int_0^\infty \frac{1}{x^3}\sin(xs)\left(e^{-\frac{s^2}{4t}}\chi_\epsilon(s)\right)'''ds$$

by integration by parts (the boundary terms vanish). The prime denotes differentiation in s. Therefore, if we denote by $A_d(x,t)$ the value of the integral kernel of

$$\frac{1}{2(\pi t)^{1/2}}\int_0^\infty \cos(\Delta_U^{\frac{1}{2}}s)e^{-\frac{s^2}{4t}}\chi_\epsilon(s)ds$$

at the point x, then we have that $A_d(x,t)$ is the same as the integral kernel of

$$\frac{1}{2(\pi t)^{1/2}}\int_0^\infty \frac{1}{\Delta_U^{3/2}}\sin(\Delta_U^{1/2}s)\left(e^{-\frac{s^2}{4t}}\chi_\epsilon(s)\right)'''ds$$

evaluated at the point x. However, because $\Delta_U^{-3/2}$ maps $H^s(U)$ to $H^{s+3}(U)$, it follows by a Sobolev embedding theorem (Corollary 2.17) that its integral kernel

must be continuous. Therefore, $A_d(x,t)$ has a continuous kernel since $\frac{1}{\Delta_U^{3/2}}$ has a continuous kernel as we showed above, $\sin(\Delta_U^{1/2}s)$ has a bounded kernel, and $e^{-\frac{s^2}{4t}}\chi_\epsilon(s)$ does not depend on x. Moreover, $f(\lambda)=\sin(\lambda^{\frac{1}{2}})$ satisfies the conditions for Proposition 7.2 when compared to $g(\lambda)=1$, and so we have:

$$A_d(x,t) \leq \frac{r(x,x)}{2(\pi t)^{1/2}} \int |\left(e^{-\frac{s^2}{4t}}\chi_\epsilon(s)\right)'''| ds,$$

where $r(x,x)$ is the integral kernel of $\Delta_U^{-3/2}$. We can use the Spectral Theorem for self-adjoint operators with compact resolvent (Theorem 2.29) to write this more explicitly in terms of the spectral zeta function:

$$\begin{aligned}
\Delta_U^{-3/2} f(x) &= \sum_{n=1}^{\infty} \frac{1}{\lambda_n^{3/2}} \langle \phi_n, f\rangle \phi_n \\
&= \zeta_U(\frac{3}{2}) \langle \phi_n, f\rangle \phi_n \\
&= \frac{1}{\Gamma(\frac{3}{2})} \int_0^\infty \int_U t^{\frac{1}{2}} k_U(x,y,t) f(y) dy dt,
\end{aligned}$$

using the Mellin transform to write the zeta function in terms of the heat kernel as in Theorem 3.5. Now, domain monotonicity implies that if $U \subset V$, then $k_U(x,x;t) \leq k_V(x,x;t)$. We can therefore estimate $k_U(x,x)$ by $k_S(x,x)$, where S is a square of side length $L = \frac{\mathrm{Diam}(U)}{\sqrt{2}}$ containing U. Thus, with coordinates for the square x_1 and x_2,

$$\begin{aligned}
r(x,x) &= \frac{1}{\Gamma(\frac{3}{2})} \int_0^\infty t^{\frac{1}{2}} k_U(x,x,t) dt \\
&\leq \frac{1}{\Gamma(\frac{3}{2})} \int_0^\infty t^{\frac{1}{2}} k_S(x,x,t) dt \\
&= \frac{1}{\Gamma(\frac{3}{2})} \int_0^\infty t^{\frac{1}{2}} \frac{4}{L^2} \sum_{k=1}^{\infty}\sum_{m=1}^{\infty} \mathrm{e}^{-\frac{\pi^2}{L^2}(m^2+k^2)t} \sin^2(\frac{\pi k x_1}{L}) \sin^2(\frac{\pi m x_2}{L}) dt \\
&\leq \frac{1}{\Gamma(\frac{3}{2})} \int_0^\infty t^{\frac{1}{2}} \frac{4}{L^2} \sum_{k=1}^{\infty}\sum_{m=1}^{\infty} \mathrm{e}^{-\frac{\pi^2}{L^2}(m^2+k^2)t} dt \\
&= \frac{4}{L^2\Gamma(\frac{3}{2})} \sum_{k=1}^{\infty}\sum_{m=1}^{\infty} \int_0^\infty t^{\frac{1}{2}} \mathrm{e}^{-\frac{\pi^2}{L^2}(m^2+k^2)t} dt \\
&= \frac{4}{\pi^{5/2}L^2\Gamma(\frac{3}{2})} \sum_{k=1}^{\infty}\sum_{m=1}^{\infty} \left(\frac{k^2+m^2}{L^2}\right)^{-\frac{3}{2}},
\end{aligned}$$

where the interchange can be done by Fubini's Theorem since the integrand is non-negative. The RHS is related to the number of ways that an integer can be written as a sum of two squares by Fermat's Theorem on the Sum of two Squares, and thus can be explicitly written in terms of the Dirichlet L-function to the character $\bmod 4$, $L(s,\chi_{-4}) := \frac{1}{1^s} - \frac{1}{3^s} + \frac{1}{5^s} - \frac{1}{7^s} + \cdots$. Making use of eg. the line preceding (12) in 8.1 of [**76**] we can thus evaluate the RHS explicitly:

$$\frac{4}{\pi^{5/2}L^2\Gamma(\frac{3}{2})}\sum_{k=1}^{\infty}\sum_{m=1}^{\infty}\left(\frac{k^2+m^2}{L^2}\right)^{-\frac{3}{2}} = \frac{4C}{2\pi^{5/2}L^2\Gamma(\frac{3}{2})}\sum_{k=1}^{\infty}\left(\frac{k^2}{L^2}\right)^{-\frac{3}{2}}$$

where

$$\begin{aligned} C &= \left(\frac{\zeta(\frac{3}{2})L(\frac{3}{2},\chi_{-4})-\zeta(3)}{\zeta(3)}\right) \\ &\approx 0.84\cdots \end{aligned}$$

so in fact we can replace C by 1. We can write this in terms of the Riemann zeta function:

$$\begin{aligned} \frac{4}{2\pi^{5/2}L^2\Gamma(\frac{3}{2})}\sum_{k=1}^{\infty}\left(\frac{k^2}{L^2}\right)^{-\frac{3}{2}} &= \frac{2}{\pi^{5/2}L^2\Gamma(\frac{3}{2})}\sum_{k=1}^{\infty}\left(\frac{k^2}{L^2}\right)^{-\frac{3}{2}} \\ &= 2\frac{L\zeta(3)}{\Gamma(\frac{3}{2})\pi^{5/2}}, \end{aligned}$$

using properties of the zeta function to simplify the expression (see eg. [**1**]). Now that we have estimated $r(x,x)$, we must estimate the other factor:

$$\int_0^{\infty}\left|e^{-\frac{s^2}{4t}}\chi_\epsilon(s)^{'''}\right|ds.$$

Note the following estimates on the L^∞ norm of the derivatives of χ_ϵ:

$$\|\chi_\epsilon\|_\infty \leq 1,$$

$$\|\chi_\epsilon^{'}\|_\infty \leq \frac{6}{\epsilon},$$

$$\|\chi_\epsilon^{''}\|_\infty \leq \frac{18}{\epsilon^2},$$

and

$$\|\chi_\epsilon^{'''}\|_\infty \leq \frac{30}{\epsilon^3}.$$

Now, using the product rule, we have that if $f,g\in C^3(\mathbb{R})$, then

$$\frac{d^3}{dx^3}(fg)(x) = f(x)g^{'''}(x)+3f^{'}(x)g^{''}(x)+3f^{''}(x)g^{'}(x)+f^{'''}(x)g(x).$$

We now find an estimate for each term, then we will add them together:

$$\begin{aligned} \int_0^{\infty}\chi_\epsilon(s)\frac{d^3}{ds^3}e^{-\frac{s^2}{4t}}ds &= \int_0^{\infty}\chi_\epsilon(s)s\left(\frac{6t-s^2}{8t^3}\right)e^{-\frac{s^2}{4t}}ds. \\ &\leq \int_{d-\epsilon}^{\infty}s\left(\frac{6t-s^2}{8t^3}\right)e^{-\frac{s^2}{4t}}ds \\ &= \frac{\left[2t-(d-\epsilon)^2\right]e^{-\frac{(d-\epsilon)^2}{4t}}}{4t^2}. \end{aligned}$$

Similarly, and using the fact that derivatives of χ_ϵ are supported on the interval $(d-\epsilon, d)$,

$$\begin{aligned}\int_0^\infty \chi_\epsilon^{'}(s)\frac{d^2}{ds^2}e^{-\frac{s^2}{4t}}ds &= \int_{d-\epsilon}^d \chi_\epsilon^{'}(s)\left(\frac{s^2-2t}{4t^2}\right)e^{-\frac{s^2}{4t}}ds \\ &\leq \|\chi_\epsilon^{'}\|_\infty\epsilon\left(\frac{d^2-2t}{4t^2}\right)e^{-\frac{(d-\epsilon)^2}{4t}} \\ &\leq 6\left(\frac{d^2-2t}{4t^2}\right)e^{-\frac{(d-\epsilon)^2}{4t}}.\end{aligned}$$

The other terms can be estimated similarly as follows:

$$\begin{aligned}\int_0^\infty \chi_\epsilon^{''}(s)\frac{d}{ds}e^{-\frac{s^2}{4t}}ds &= \int_{d-\epsilon}^d \chi_\epsilon^{''}(s)\left(\frac{s}{2t}\right)e^{-\frac{s^2}{4t}}ds \\ &\leq \|\chi_\epsilon^{''}\|_\infty\epsilon\left(\frac{d-\epsilon}{2t}\right)e^{-\frac{(d-\epsilon)^2}{4t}} \\ &= \frac{18}{\epsilon^2}\epsilon\left(\frac{d-\epsilon}{2t}\right)e^{-\frac{(d-\epsilon)^2}{4t}} \\ &= \frac{18(d-\epsilon)}{2\epsilon t}e^{-\frac{(d-\epsilon)^2}{4t}}.\end{aligned}$$

$$\begin{aligned}\int_0^\infty \chi_\epsilon^{'''}(s)e^{-\frac{s^2}{4t}}ds &= \int_{d-\epsilon}^d \chi_\epsilon^{'''}(s)e^{-\frac{s^2}{4t}}ds \\ &\leq \|\chi_\epsilon^{'''}\|_\infty\epsilon e^{-\frac{(d-\epsilon)^2}{4t}} \\ &= \frac{30}{\epsilon^2}e^{-\frac{(d-\epsilon)^2}{4t}}.\end{aligned}$$

Combining these results we obtain that

$$\begin{aligned}\int_0^\infty |\left(e^{-\frac{s^2}{4t}}\chi_\epsilon(s)\right)^{'''}|ds &\leq \left|\frac{30}{\epsilon^2}+3\times\frac{18(d-\epsilon)}{2\epsilon t}+3\times 6\left(\frac{d^2-2t}{4t^2}\right)+\frac{\left[2t-(d-\epsilon)^2\right]}{4t^2}\right|\mathrm{e}^{-\frac{(\mathrm{d}-\epsilon)^2}{4\mathrm{t}}} \\ &= \left|\frac{30}{\epsilon^2}+\frac{32d}{\epsilon t}+72\frac{(d-\epsilon)^2-2t}{t^2}\right|\mathrm{e}^{-\frac{(\mathrm{d}-\epsilon)^2}{4\mathrm{t}}}.\end{aligned}$$

Combined with the estimate for $r(x,x)$ this gives

$$\tilde{A}_d(x) \leq \frac{\sqrt{2}\zeta(3)\mathrm{Diam}(U)}{\pi^3\sqrt{t}\Gamma(3/2)}\left|\frac{30}{\epsilon^2}+\frac{32d}{\epsilon t}+72\frac{(d-\epsilon)^2-2t}{t^2}\right|\mathrm{e}^{-\frac{(\mathrm{d}-\epsilon)^2}{4\mathrm{t}}}$$

as required. □

Next we estimate the part of the integral relating to Δ_0. Namely, we have the following lemma:

LEMMA 7.4. *Denote by $A_d^0(t)$ the operator*

$$A_d^0(t) := \frac{1}{(\pi t)^{1/2}}\int_0^\infty \cos(\Delta_0^{1/2}s)\mathrm{e}^{-\frac{s^2}{4t}}\chi(s)ds$$

and let its integral kernel be denoted by $a_d^0(x,y;t)$. Then $a_d^0(t)$ is continuous and for any $0<\epsilon<d$,

$$a_d^0(x,x;t) \leq \left[4\left|\frac{30}{\epsilon^2}+\frac{32d}{\epsilon t}+72\frac{(d-\epsilon)^2-2t}{t^2}\right|+\frac{3\pi^2}{t}\right]\mathrm{e}^{-\frac{(d-\epsilon)^2}{4t}}$$

Proof. Let f be a bounded, smooth function. Using the identity $\Delta_0 f = \mathcal{F}^{-1}(\|\xi\|^2\hat{f})$, and the Spectral Theorem for unbounded operators (Corollary 2.30), we have that

$$f(\Delta_0) = \mathcal{F}^{-1} f(\|k\|^2)\mathcal{F}$$

where $\mathcal{F}$ is the Fourier transform and k is the transform variable. The kernel $F(x,y)$ of $f(\Delta_0)$ is therefore given by

$$F(x,y) = \frac{1}{(2\pi)^2}\int_{\mathbb{R}^2}\mathrm{e}^{-ik\cdot(x-y)}f(\|k\|^2)dk.$$

In polar coordinates and with $f(\lambda)=\cos(\Delta_0^{1/2})$ this integral becomes:

$$\begin{aligned}
a_d^0(x,x;t) &= \frac{1}{(\pi t)^{1/2}}\int_0^\infty\int_{\mathbb{R}^2}\cos(|k|s)\mathrm{e}^{-\frac{s^2}{4t}}\chi(s)dkds \\
&= 2\pi\frac{1}{(\pi t)^{1/2}}\int_0^\infty\int_0^\infty r\cos(rs)\mathrm{e}^{-\frac{s^2}{4t}}\chi(s)drds \\
&= 2\pi\frac{1}{(\pi t)^{1/2}}\int_0^\infty\int_0^{\frac{\pi}{2}} r\cos(rs)\mathrm{e}^{-\frac{s^2}{4t}}\chi(s)drds + \\
&+2\pi \quad \frac{1}{(\pi t)^{1/2}}\int_0^\infty\int_{\frac{\pi}{2}}^\infty r\cos(rs)\mathrm{e}^{-\frac{s^2}{4t}}\chi(s)drds \\
&= \tilde{I}_1+\tilde{I}_2,
\end{aligned}$$

where the point $r=\frac{\pi}{2}$ is chosen to simplify the estimate of I_1 but could in principle be any positive real number. The first term I_1 is easy to evaluate analytically. Specifically,

$$\begin{aligned}
\tilde{I}_1 &= \frac{2\pi}{(\pi t)^{1/2}}\int_0^\infty \mathrm{e}^{-\frac{s^2}{4t}}\chi(s)\int_0^{\frac{\pi}{2}} r\cos(rs)drds \\
&= \frac{2\pi}{(\pi t)^{1/2}}\int_0^\infty \mathrm{e}^{-\frac{s^2}{4t}}\chi(s)\left(\frac{\pi s\sin\left(\frac{\pi s}{2}\right)+2\cos\left(\frac{\pi s}{2}\right)-2}{2s^2}\right)ds.
\end{aligned}$$

Using the inequality

$$\pi s\sin\left(\frac{\pi s}{2}\right)+2\cos\left(\frac{\pi s}{2}\right)-2 \leq \pi s+4$$

and the properties we assumed of the cutoff function (namely, that $\chi(s) = 0$ whenever $s < d - \epsilon$), we have that

$$\begin{aligned} &\leq \frac{2\pi}{(\pi t)^{1/2}} \int_{d-\epsilon}^{\infty} \left(\frac{\pi s + 4}{2s^2} \right) \mathrm{e}^{-\frac{s^2}{4t}} ds \\ &\leq \frac{2\pi}{(\pi t)^{1/2}} \int_{d-\epsilon}^{\infty} \left(\frac{3\pi}{s} \right) \mathrm{e}^{-\frac{s^2}{4t}} ds \\ &= \frac{6\pi^2}{(\pi t)^{1/2}} \int_{d-\epsilon}^{\infty} \frac{1}{s} \mathrm{e}^{-\frac{s^2}{4t}} ds \\ &= \frac{3\pi^{3/2}}{t^{1/2}} \Gamma(0, \frac{(d-\epsilon)^2}{4t}) \\ &\leq \frac{3\pi^{3/2}}{t} \mathrm{e}^{-\frac{(d-\epsilon)^2}{4t}}. \end{aligned}$$

provided that $d > \epsilon$, which we assumed, where $\Gamma(0, x)$ is the incomplete gamma function.

The second term $\tilde{I}_2$ is a priori unbounded, as $r\cos(rs)$ is unbounded. However, using integration by parts and the properties of the cutoff function χ makes this integral converge. First, note that integrand is continuous in r and s and converges on compact sets, and thus we may change the order of integration to give

$$\begin{aligned} \tilde{I}_2 &= 2\pi \frac{1}{(\pi t)^{1/2}} \int_{\frac{\pi}{2}}^{\infty} \int_0^{\infty} r\cos(rs) \mathrm{e}^{-\frac{s^2}{4t}} \chi(s) ds dr \\ &= 2\pi \frac{1}{(\pi t)^{1/2}} \left\{ \int_{\frac{\pi}{2}}^{\infty} \left[\int_0^{\infty} \frac{1}{r^2} \sin(rs) \left(\mathrm{e}^{-\frac{s^2}{4t}} \chi(s) \right)''' ds \right] + B(r) dr \right\} \end{aligned}$$

where $B(r)$ are the boundary terms from integration by parts, given by

$$\begin{aligned} B(r,s) &= \left[\sin(rs) \mathrm{e}^{-\frac{s^2}{4t}} \chi(s) + \frac{\cos(rs)}{r} \left(\mathrm{e}^{-\frac{s^2}{4t}} \chi(s) \right)' \right]_0^{\infty} \\ &= 0, \end{aligned}$$

since the cutoff function χ vanishes at the boundary points. Therefore we may write $\tilde{I}_2$ as

$$\begin{aligned} |\tilde{I}_2| &= 2\pi \frac{1}{(\pi t)^{1/2}} \int_{\frac{\pi}{2}}^{\infty} \left[\int_0^{\infty} \left| \frac{1}{r^2} \sin(rs) \left(\mathrm{e}^{-\frac{s^2}{4t}} \chi(s) \right)''' \right| ds \right] dr \\ &\leq 2\pi \frac{1}{(\pi t)^{1/2}} \int_{\frac{\pi}{2}}^{\infty} \frac{1}{r^2} \left[\int_0^{\infty} \left| \left(\mathrm{e}^{-\frac{s^2}{4t}} \chi(s) \right)''' \right| ds \right] dr \\ &\leq 2\sqrt{\pi} \left(\int_{\frac{\pi}{2}}^{\infty} \frac{1}{r^2} dr \right) \left| \frac{30}{\epsilon^2} + \frac{32d}{\epsilon t} + 72 \frac{(d-\epsilon)^2 - 2t}{t^2} \right| \mathrm{e}^{-\frac{(d-\epsilon)^2}{4t}} \end{aligned}$$

by our previous estimate of $\int_0^{\infty} \left| \left(\mathrm{e}^{-\frac{s^2}{4t}} \chi(s) \right)''' \right| ds$ (see the proof of the previous lemma), and evaluating the integral in r this gives

$$\begin{aligned} |I_2| &\leq 2\pi^{1/2}\left(\frac{2}{\pi}\right)\left|\frac{30}{\epsilon^2}+\frac{32d}{\epsilon t}+72\frac{(d-\epsilon)^2-2t}{t^2}\right|\mathrm{e}^{-\frac{(d-\epsilon)^2}{4t}} \\ &\leq 4\left|\frac{30}{\epsilon^2}+\frac{32d}{\epsilon t}+72\frac{(d-\epsilon)^2-2t}{t^2}\right|\mathrm{e}^{-\frac{(d-\epsilon)^2}{4t}}, \end{aligned}$$

and combining this with our estimate for $\tilde{I}_1$ gives

$$|\tilde{I}_1+\tilde{I}_2| \leq \left[4\left|\frac{30}{\epsilon^2}+\frac{32d}{\epsilon t}+72\frac{(d-\epsilon)^2-2t}{t^2}\right|+\frac{3\pi^{3/2}}{t}\right]\mathrm{e}^{-\frac{(d-\epsilon)^2}{4t}},$$

as required. □

Combining the previous two lemmas gives our "not feeling the boundary" estimate. Recall that by definition $d = 2d(x, \partial U)$:

THEOREM 7.5. *"Not feeling the boundary" Let U be an open bounded subset of $\mathbb{R}^2$ with piecewise smooth, Lipschitz boundary. Let $x \in U$. Then for any $0 < \epsilon < 2d(x, \partial U)$, we have*

$$|k_t(x,x)-\frac{1}{4\pi t}| \leq \left[\left(\frac{\sqrt{2}\zeta(3)\mathrm{Diam}(U)}{\pi^3\sqrt{t}\Gamma(3/2)}+4\right)|\psi(\epsilon,t)|+\frac{3\pi^{3/2}}{t}\right]\mathrm{e}^{-\frac{(2d(x,\partial U)-\epsilon)^2}{4t}}$$

where

$$\psi(\epsilon,t)=\frac{30}{\epsilon^2}+\frac{32d}{\epsilon t}+72\frac{(d-\epsilon)^2-2t}{t^2}.$$

7.2. Full Heat Trace Estimate for Polygonal Domains

In the previous sections we have improved an error estimate for the heat trace known as "not feeling the boundary". In a 1988 paper [**75**], van den Berg and Srisatkunarajah used this estimate to derive an improved heat trace estimate for polygons. While it had been known for some time that the asymptotic expansion of the heat trace for polygons has only three terms (the rest is fast decaying as $t \to 0$), what was unknown was the uniform constant for the decaying part. What van den Berg and Srisatkunarajah proved is the following Theorem:

THEOREM 7.6. *Let U be a polygonal domain with n sides, γ_i the angles of its vertices, γ its smallest angle and R be half the length of its shortest edge. Then we have that*

$$\left|\mathrm{Tr}(\mathrm{e}^{-\Delta t})-\frac{|U|}{4\pi t}+\frac{|\partial U|}{8\sqrt{\pi t}}-\sum_{k=1}^{n}\frac{\pi^2-\gamma_i^2}{24\pi\gamma_i}\right| \leq \left(5n+\frac{20|U|}{R^2}\right)\frac{1}{\gamma^2}\mathrm{e}^{-(R\sin\gamma/2)^2/(16t)}.$$

PROOF. Theorem 1 in [**75**]. □

To prove this Theorem, the authors decompose U into subdomains of the following form: near corners they use Sommerfeld's heat kernel on an infinite wedge. Near edges they use the solution of a half-plane, and near the interior they use the Euclidean heat kernel. The estimate of not feeling the boundary provides an estimate in each of the subdomains and once the subdomains are suitably pieced together the authors obtain their global estimate.

To obtain an estimate based on our improved "not feeling the boundary" inequality, we simply replace occurences of the original "not feeling the boundary" estimate used in their proof by our own estimate (7.5). We are thus able to obtain a full heat trace estimate on polygonal domains too, but with a better exponent guaranteeing faster decay properties as $t \to 0^+$. Our proof is strictly algebraic manipulation, all the hard work having been already done by the authors of the original paper.

THEOREM 7.7. *(Full heat trace estimate for polygons) Let U be a polygonal domain with n sides, γ_i the angles of its vertices, γ its smallest angle and R be half the length of its shortest edge. Then we have that for $0 < \epsilon < 2R\sin(\frac{1}{2}\gamma)$:*

$$\left|\mathrm{Tr}(\mathrm{e}^{-\Delta t}) - \frac{|U|}{4\pi t} + \frac{|\partial U|}{8\sqrt{\pi t}} - \sum_{k=1}^{n} \frac{\pi^2 - \gamma_i^2}{24\pi\gamma_i}\right| \leq \left(n + \frac{19|D|}{R^2}\right)\left(\frac{(5+n)(72(R-\epsilon)^2|D|)}{\gamma^2\epsilon^2 t}\right)\mathrm{e}^{-(\mathrm{R}\sin\frac{1}{2}\gamma - \frac{1}{2}\epsilon)^2/4\mathrm{t}}$$

PROOF. In what follows we modify the argument of van den Berg and Srisatkunarajah ([**75**]), replacing occurences of Kac's original "not feeling the boundary" estimate with our own (Theorem 7.5)

(7.2.1)
$$|k_t(x,x) - \frac{1}{4\pi t}| \leq \left[\left(\frac{\sqrt{2}\zeta(3)\mathrm{Diam}(U)}{\pi^3\sqrt{t}\Gamma(3/2)} + 4\right)|\psi(\epsilon,t)| + \frac{3\pi^{3/2}}{t}\right]\mathrm{e}^{-\frac{(2d(x,\partial U)-\epsilon)^2}{4t}},$$

where

$$\psi(\epsilon,t) = \frac{30}{\epsilon^2} + \frac{32d}{\epsilon t} + 72\frac{(d-\epsilon)^2 - 2t}{t^2}.$$

In the following we display in parentheses the numbers of the lemmas/theorems in ([**75**]), so the reader can follow that paper and see clearly where we make the modifications. We also follow all the notation of that paper. □

LEMMA. *(Lemma 6) For $x \in B_i(R)$ and for any $0 < \epsilon < 2R$, we have*

$$|K_{\gamma_i}(x,x;t) - K(x,x;t)| \leq \left[\left(\frac{C(D)}{\sqrt{t}} + 4\right)|\psi(\epsilon,t)| + \frac{3\pi^{3/2}}{t}\right]\mathrm{e}^{-(R-\frac{1}{2}\epsilon)^2/t}$$

where

$$C(D) = \frac{\sqrt{2}\zeta(3)\mathrm{Diam}(U)}{\pi^3\sqrt{t}\Gamma(3/2)}$$

and

$$\psi(\epsilon,t) = \frac{30}{\epsilon^2} + \frac{32d}{\epsilon t} + 72\frac{(d-\epsilon)^2 - 2t}{t^2}.$$

PROOF. This is straightforward substitution of our formula instead of Kac's in the original proof (page 124). □

LEMMA. *(Lemma 7) For $A \in C(\frac{1}{2}R\sin\frac{1}{2}\gamma, R)$ and for any $0 < \epsilon < 2R\sin(\frac{1}{2}\gamma)$,*

$$|K(x,x;t) - \frac{1}{4\pi t}(1 - \mathrm{e}^{d^2(x,\partial U)/t})| \leq \left[\left(\frac{C(D)}{\sqrt{t}} + 4\right)|\psi(\epsilon,t)| + \frac{3\pi^2}{t}\right]\mathrm{e}^{-(\mathrm{R}\sin\frac{1}{2}\gamma - \frac{1}{2}\epsilon)^2/4\mathrm{t}},$$

where

$$C(D) = \frac{\sqrt{2}\zeta(3)\mathrm{Diam}(U)}{\pi^3\sqrt{t}\Gamma(3/2)},$$

$$\psi(\epsilon,t) = \frac{30}{\epsilon^2} + \frac{32d}{\epsilon t} + 72\frac{(d-\epsilon)^2 - 2t}{t^2}.$$

PROOF. This is also a straightforward substitution of our formula instead of Kac's in the original proof (page 124).

Combining these lemmas we arrive at the analogue of (4.2) of ([**75**]). For any $0 < \epsilon < R\sin(\frac{1}{2}\gamma)$, we have the inequality

$$\left|Z(t) - \int_{D(\frac{1}{2}R\sin\frac{1}{2}\gamma,R)} dx\frac{1}{4\pi t} - \int_{C(\frac{1}{2}R\sin\frac{1}{2}\gamma,R)} dx\frac{1}{4\pi t}(1 - \mathrm{e}^{-d^2(x,\partial D)/t}) - \sum_{i=1}^{n} Z_{\gamma_i}(t;R)\right| \leq |D|\left[\left(\frac{C(D)}{\sqrt{t}} + 4\right)\psi(\epsilon,t) + \frac{3\pi^{3/2}}{t}\right]\mathrm{e}^{-(\mathrm{R}\sin\frac{1}{2}\gamma - \frac{1}{2}\epsilon)^2/2\mathrm{t}}.$$

As in the original paper, we then use Corollary 3 and (4.1) of ([**75**]) to give:

$$\left|Z(t) - \frac{|D|}{4\pi t} + \int_{C(\frac{1}{2}R\sin\frac{1}{2}\gamma,R)} dx\frac{1}{4\pi t}\mathrm{e}^{-d^2(x,\partial D)/t} + \frac{nR^2}{2\pi t}\int_0^1 \mathrm{e}^{-\mathrm{R}^2\mathrm{y}^2/\mathrm{t}}(1-\mathrm{y}^2)^{\frac{1}{2}}\mathrm{dy} - \sum_{i=1}^{n}\frac{\pi^2 - \gamma_i^2}{24\pi\gamma_i}\right| \leq$$
$$C_0\left[\left(\frac{\sqrt{2}\zeta(3)\mathrm{Diam}(U)}{\pi^3\sqrt{t}\Gamma(3/2)} + 4\right)|\psi(\epsilon,t)| + \frac{3\pi^{3/2}}{t}\right]\mathrm{e}^{-(\mathrm{R}\sin\frac{1}{2}\gamma - \frac{1}{2}\epsilon)^2/4\mathrm{t}} + \left(\frac{|\partial D|}{4\pi\sin\frac{1}{2}\gamma} + \frac{nR^2}{2\pi t}\right)\mathrm{e}^{-(R\sin\frac{1}{2}\gamma - \frac{1}{2}\epsilon)^2/(2t)}$$

where $C_0 = \left[n(\frac{1}{4} + \frac{3}{64}\pi^2) + \frac{16\pi|D|}{eR^2}\right]\frac{1}{\gamma^2} \leq \left(n + \frac{19|D|}{R^2}\right)\frac{1}{\gamma^2}$. From Lemma 8 of [**75**], we have the estimate

$$|\partial D| \leq \frac{|D|}{R} + \frac{nR}{\sin\frac{1}{2}\gamma}$$

and substituting this into the above inequality and using (4.5) of ([**75**]) gives

$$|Z(t) - \frac{|D|}{4\pi t} + \frac{|\partial D|}{8(\pi t)^{\frac{1}{2}}} - \sum_{i=1}^{n} \frac{\pi^2 - \gamma_i^2}{24\pi\gamma_i}| \leq$$

$$C_0 \left[\left(\frac{\sqrt{2}\zeta(3)\mathrm{Diam}(U)}{\pi^3\sqrt{t}\Gamma(3/2)} + 4 \right) |\psi(\epsilon, t)| + \frac{3\pi^{3/2}}{t} \right] \mathrm{e}^{-(\mathrm{R}\sin\frac{1}{2}\gamma - \frac{1}{2}\epsilon)^2/4\mathrm{t}} +$$

$$\left(\frac{\frac{|D|}{R} + \frac{nR}{\sin\frac{1}{2}\gamma}}{4\pi\sin\frac{1}{2}\gamma} + \frac{nR^2}{2\pi t} \right) \mathrm{e}^{-(R\sin\frac{1}{2}\gamma - \frac{1}{2}\epsilon)^2/(2t)}$$

$$= A + B.$$

Simplifying B, using that $\sin(\frac{1}{2}\gamma) \leq \frac{\gamma}{3}$ since $\gamma \leq \frac{\pi}{2}$ gives

$$\begin{aligned} B &= \left(\frac{|D|}{4\pi R\sin\frac{1}{2}\gamma} + \frac{nR}{4\pi} + \frac{nR^2}{2\pi t} \right) \mathrm{e}^{-(R\sin\frac{1}{2}\gamma - \frac{1}{2}\epsilon)^2/(2t)} \\ &\leq \left(\frac{3|D|}{4\pi R} + \frac{nR}{4\pi} + \frac{nR^2}{2\pi t} \right) \frac{1}{\gamma^2} \mathrm{e}^{-(R\sin\frac{1}{2}\gamma - \frac{1}{2}\epsilon)^2/(2t)} \\ &= \left(\frac{3|D|t + nR^2(t+2n)}{4\pi Rt} \right) \frac{1}{\gamma^2} \mathrm{e}^{-(R\sin\frac{1}{2}\gamma - \frac{1}{2}\epsilon)^2/(2t)} \end{aligned}$$

so we have that

$$A + B \leq$$

$$\left(n + \frac{19|D|}{R^2} \right) \left(\left(\frac{\sqrt{2}\zeta(3)\mathrm{Diam}(U)}{\pi^3\sqrt{t}\Gamma(3/2)} + 4 \right) |\psi(\epsilon, t)| + \frac{3\pi^{3/2}}{t} \right) \frac{1}{\gamma^2} \mathrm{e}^{-(\mathrm{R}\sin\frac{1}{2}\gamma - \frac{1}{2}\epsilon)^2/4\mathrm{t}}$$

(7.2.2)

$$+ \left(\frac{3|D|t + nR^2(t+2n)}{4\pi Rt} \right) \frac{1}{\gamma^2} \mathrm{e}^{-(\mathrm{R}\sin\frac{1}{2}\gamma - \frac{1}{2}\epsilon)^2/2\mathrm{t}}.$$

While we will use this estimate for numerics, we can simplify it greatly at the expense of sharpness of the constants:

$$A + B \leq$$

$$\left(n + \frac{19|D|}{R^2} \right) \left(\frac{(5+n)(72(R-\epsilon)^2|D|)}{\gamma^2\epsilon^2 t} \right) \mathrm{e}^{-(\mathrm{R}\sin\frac{1}{2}\gamma - \frac{1}{2}\epsilon)^2/4\mathrm{t}}.$$

□

CHAPTER 8

Numerical Applications

In this chapter we apply our computational framework to calculate the spectral determinant and Casimir energy of various domains with rigorous error bounds, as well as investigating some extremal behavior. After showing some simple regular polygonal examples, we compute the spectral determinant and Casimir energy of an irregular, non-convex polygon (an arrowhead). Then, we look at the Casimir energy of special multiply connected polygonal domains we call cutouts as well as extremizers of spectral determinants within the class of n-sided polygons of fixed area. We use our methods to provide evidence that a regular polygon is a maximizer of the spectral determinant within its class.

In this chapter, when we refer to a "unit regular" n-gon, we mean the following:

DEFINITION 8.1. A unit regular n-gon is a polygon with n sides whose vertices z_i are placed at

$$z_i = \mathrm{e}^{\frac{2\pi i}{n}k}, \quad k = 1 \cdots n.$$

8.1. Unit Regular Pentagon

In this section, we compute the Casimir energy and spectral determinant of a unit regular pentagon, with rigorous theoretical error bounds. We use MPSPack to obtain the approximate first 892 eigenvalues, along with error estimates. These eigenvalues can be found at http://bit.ly/18dTfjd. We are then able to use our error bounds to place a theoretically rigorous estimate on our overall error. Below in Figure 8.1.1, we plot the difference between the heat trace obtained from the spectrum and the heat trace approximated by the heat expansion, for small time. The excellent agreement between these two quantities for a large range of time ensures a priori that our calculation will be stable with small changes of ϵ. It also suggests that the heat approximation error should be small, although this will of course be confirmed rigorously by our error estimate.

Using Theorems 3.7 and 3.9, we obtain that for P the regular unit pentagon,

$$\det \Delta_P \approx 0.461436914...$$

and

$$\zeta_P(-\frac{1}{2}) \approx 0.0421024....$$

We now compute the error bounds of these computations. The Mathematica notebook used to compute the determinant and zeta functions can be downloaded at http://bit.ly/Iq1hMh.

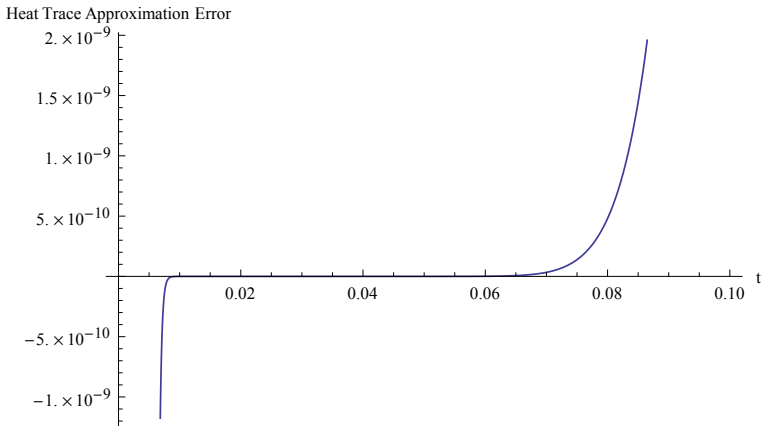

FIGURE 8.1.1. Agreement between the heat expansion and the heat trace computed from the spectrum, for small time (for a regular unit pentagon). The excellent agreement means that we can make small changes in ϵ without affecting the result.

8.1.0.1. *Spectral determinant error bounds.* For a choice of $\epsilon = 0.0063$, the heat trace approximation error (Theorem 6.1) is 7.22083×10^{-7}. The spectral truncation error, that is, the error from taking finitely many eigenvalues (see Theorem 6.3), is 2.4959×10^{-14}. The spectral approximation error, that is, the error we make by using approximated eigenvalues rather than their true values, is given by (6.3.1), and totals 1.00642×10^{-7}. The overall error estimate is therefore 8.22974×10^{-7}. For comparative purposes, the heat trace approximation error which we would obtain from using van den Berg and Srisatkunarajah's heat trace estimate with the same ϵ (Theorem 2.55) would be 0.0137543. This less optimal bound can also be computed using the same Mathematica notebook which we use for our computations (see above for download link).

In conclusion, using our error bound, we have the rigorous estimate

$$0.461436091 \leq \det \Delta_P \leq 0.461437737.$$

We can verify this using the computation of Aurell-Salomonson, which we implemented in Matlab using Driscoll's SC toolbox. This computation only applies to the spectral determinant, hence we cannot use it for the Casimir energy. The result of this computation is:

$$\det \Delta_P = 0.461436918986281 \cdots,$$

which is within the tolerance specified by our error bound.

8.1.0.2. *Casimir energy error bounds.* For a choice of $\epsilon = 0.0063$, the heat trace approximation error (Theorem 6.2) is 2.61007×10^{-6}. The spectral truncation error, that is, the error from taking finitely many eigenvalues (see Theorem 6.4), is 8.73681×10^{-10} The spectral approximation error, that is, the error we make by using approximated eigenvalues rather than their true values, is given by (6.3.1), and totals 5.56035×10^{-7}. Summing these errors up, we obtain the overall error estimate of 3.16697×10^{-6}. Therefore,

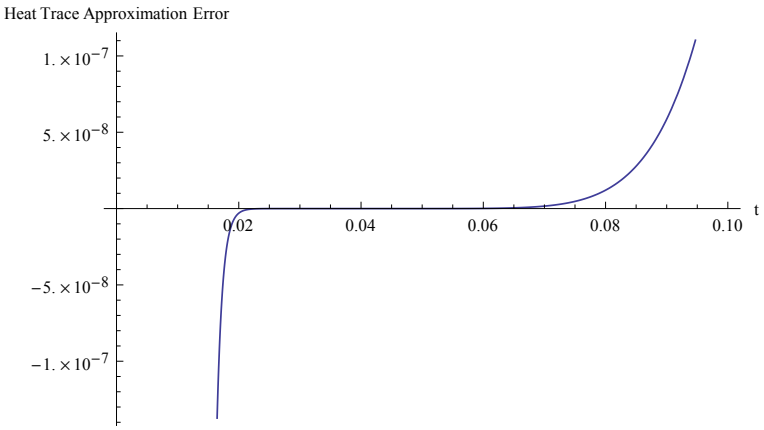

FIGURE 8.2.1. Agreement between the heat expansion and the heat trace computed from the spectrum, for small time (for a regular unit hexagon). The excellent agreement means that we can make small changes in ϵ without affecting the result.

$$0.0420992 \leq \zeta_P(-\frac{1}{2}) \leq 0.0421056.$$

8.2. Unit Regular Hexagon

In this section, we compute the Casimir energy and spectral determinant of a unit regular hexagon, with rigorous theoretical error bounds. We use MPSPack to obtain the approximate first 888 eigenvalues, along with error estimates. These eigenvalues can be found at http://bit.ly/18dTfjd. We are then able to use our error bounds to place a theoretically rigorous estimate on our overall error. Below in Figure 8.2.1, we plot the difference between the heat trace obtained from the spectrum and the heat trace approximated by the heat expansion, for small time. The excellent agreement between these two quantities for a large range of time ensures a priori that our calculation will be stable with small changes of ϵ. It also suggests that the heat approximation error should be small, although this will of course be confirmed rigorously by our error estimate.

Using Theorems 3.7 and 3.9, we obtain that for H the regular unit hexagon,

$$\det \Delta_H \approx 0.464460686...$$

and

$$\zeta_H(-\frac{1}{2}) \approx 0.0345513....$$

We now compute the error bounds of these computations. The Mathematica notebook used to compute the determinant and zeta functions can be downloaded at http://bit.ly/Iq1hMh.

8.2.0.3. *Spectral determinant error bounds.* For a choice of $\epsilon = 0.006$, the heat trace approximation error (Theorem 6.1) is 1.88299×10^{-7}. The spectral truncation error, that is, the error from taking finitely many eigenvalues (see Theorem 6.3), is 1.06684×10^{-9}. The spectral approximation error, that is, the error we make by using approximated eigenvalues rather than their true values, is given by (6.3.1), and totals 6.86279×10^{-6}. The overall error estimate is therefore 7.052160573×10^{-6}. For comparative purposes, the heat trace approximation error which we would obtain from using van den Berg and Srisatkunarajah's heat trace estimate (Theorem 2.55) would be 2.87487×10^{-5} , leading our overall error bound to increase slightly and requiring more eigenvalues to achieve the same accuracy. To obtain the same error bound would require a lower ϵ, and at least 40 additional eigenvalues would need to be computed, roughly a 15% increase in computational time. This less optimal bound can also be computed using the same Mathematica notebook which we use for our computations (see above for download link).

In conclusion, using our error bound, we have the rigorous estimate

$$0.464453634 \leq \det \Delta_H \leq 0.464467738.$$

Arguing non-rigorously, we can vary ϵ in the region $0.002 < \epsilon < 0.05$ without changing the value of our computation by more than 10^{-7}, so based on this information the first 6 decimal places should be correct. We can verify this using the computation of Aurell-Salomonson, which we implemented in Matlab using Driscoll's SC toolbox. This computation only applies to the spectral determinant, hence we cannot use it for the Casimir energy. The result of this computation is:

$$\det \Delta_H = 0.464460696610019 \cdots,$$

so in fact the first seven digits of our answer agree with it, and therefore we believe them to be correct.

8.2.0.4. *Casimir energy error bounds.* For a choice of $\epsilon = 0.006$, the heat trace approximation error (Theorem 6.2) is 6.9689×10^{-7}. The spectral truncation error, that is, the error from taking finitely many eigenvalues (see Theorem 6.4), is 3.8241×10^{-9} The spectral approximation error, that is, the error we make by using approximated eigenvalues rather than their true values, is given by (6.3.1), and totals 4.47107×10^{-5}. Summing these errors up, we obtain the overall error estimate of 4.54114×10^{-5}. Therefore,

$$0.0345059 \leq \zeta_H(-\frac{1}{2}) \leq 0.0345968.$$

8.3. Unit Regular Heptagon

In this section, we compute the Casimir energy and spectral determinant of a unit regular heptagon, with rigorous theoretical error bounds. We use MPSPack to obtain the approximate first 1031 eigenvalues, along with error estimates. These eigenvalues can be found at http://bit.ly/18dTfjd. We are then able to use our error bounds to place a theoretically rigorous estimate on our overall error. Below in Figure 8.3.1, we plot the difference between the heat trace obtained from the spectrum and the heat trace approximated by the heat expansion, for small time. The excellent agreement between these two quantities for a large range of time ensures a priori that our calculation will be stable with small changes of ϵ. It also

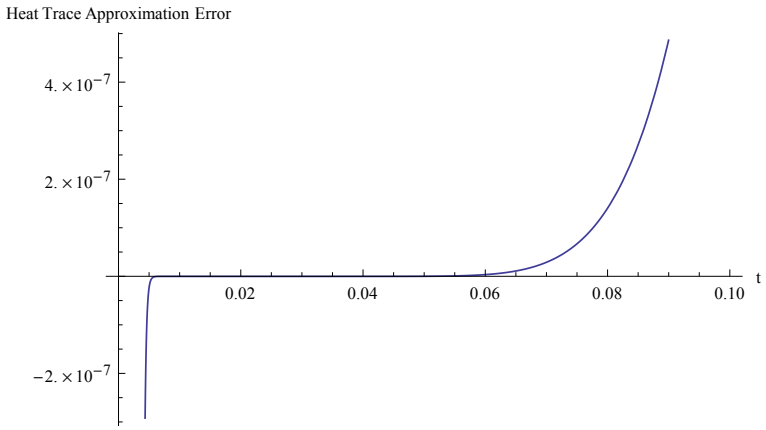

FIGURE 8.3.1. Agreement between the heat expansion and the heat trace computed from the spectrum, for small time (for a regular unit heptagon). The excellent agreement means that we can make small changes in ϵ without affecting the result.

suggests that the heat approximation error should be small, although this will of course be confirmed rigorously by our error estimate.

Using Theorems 3.7 and 3.9, we obtain that for H the regular unit heptagon,

$$\det \Delta_H \approx 0.466359979...$$

and

$$\zeta_H(-\frac{1}{2}) \approx 0.0300049....$$

We now compute the error bounds of these computations. The Mathematica notebook used to compute the determinant and zeta functions can be downloaded at http://bit.ly/Iq1hMh.

8.3.0.5. *Spectral determinant error bounds.* For a choice of $\epsilon = 0.0067$, the heat trace approximation error (Theorem 6.1) is 3.86096×10^{-7}. The spectral truncation error, that is, the error from taking finitely many eigenvalues (see Theorem 6.3), is 3.24326×10^{-11}. The spectral approximation error, that is, the error we make by using approximated eigenvalues rather than their true values, is given by (6.3.1), and totals 2.05578×10^{-7}. The overall error estimate is therefore $5.917065314 \times 10^{-7}$. For comparative purposes, the heat trace approximation error which we would obtain from using van den Berg and Srisatkunarajah's heat trace estimate (Theorem 2.55) would be 0.00756999 , several orders of magnitude greater, leading our overall error bound to increase and requiring almost double the number of eigenvalues to rigorously achieve the same precision. This would lead to an increase in computational time. This less optimal bound can also be computed using the same Mathematica notebook which we use for our computations (see above for download link).

In conclusion, using our error bound, we have the rigorous estimate

$$0.466359387 \leq \det \Delta_H \leq 0.466360570$$

We can verify this using the computation of Aurell-Salomonson, which we implemented in Matlab using Driscoll's SC toolbox. This computation only applies to the spectral determinant, hence we cannot use it for the Casimir energy. The result of this computation is:

$$\det \Delta_H = 0.466359978462963\cdots,$$

which is within the tolerance specified by our error margin.

8.3.0.6. *Casimir energy error bounds.* For a choice of $\epsilon = 0.0067$, the heat trace approximation error (Theorem 6.2) is 1.35287×10^{-6}. The spectral truncation error, that is, the error from taking finitely many eigenvalues (see Theorem 6.4), is 1.10185×10^{-10} The spectral approximation error, that is, the error we make by using approximated eigenvalues rather than their true values, is given by (6.3.1), and totals 1.15126×10^{-6}. Summing these errors up, we obtain the overall error estimate of 2.50424×10^{-6}. Therefore,

$$0.0300024 \leq \zeta_H(-\frac{1}{2}) \leq 0.0300074.$$

8.4. Unit Regular Octagon

In this section, we compute the Casimir energy and spectral determinant of a unit regular octagon, with rigorous theoretical error bounds. We use MPSPack to obtain the approximate first 1042 eigenvalues, along with error estimates. These eigenvalues can be found at http://bit.ly/1eKHXnJ. We are then able to use our error bounds to place a theoretically rigorous estimate on our overall error. Below in Figure 8.4.1, we plot the difference between the heat trace obtained from the spectrum and the heat trace approximated by the heat expansion, for small time. The excellent agreement between these two quantities for a large range of time ensures a priori that our calculation will be stable with small changes of ϵ. It also suggests that the heat approximation error should be small, although this will of course be confirmed rigorously by our error estimate.

Using Theorems 3.7 and 3.9, we obtain that for O the regular unit octagon,

$$\det \Delta_O \approx 0.467573753\cdots$$

and

$$\zeta_O(-\frac{1}{2}) \approx 0.0268804\cdots$$

We now compute the error bounds of these computations. The Mathematica notebook used to compute the determinant and zeta functions can be downloaded at http://bit.ly/Iq1hMh.

8.4.0.7. *Spectral determinant error bounds.* For a choice of $\epsilon = 0.006$, the heat trace approximation error (Theorem 6.1) is 2.09987×10^{-7}. The spectral truncation error, that is, the error from taking finitely many eigenvalues (see Theorem 6.3), is 1.10156×10^{-9}. The spectral approximation error, that is, the error we make by using approximated eigenvalues rather than their true values, is given by (6.3.1), and totals 1.8862×10^{-7}. The overall error estimate is therefore 3.99717×10^{-7}. For comparative purposes, the heat trace approximation error which we would obtain from using van den Berg and Srisatkunarajah's heat trace estimate (Theorem 2.55) would be 3.24538×10^{-5}, a slightly higher value, leading our overall error bound to

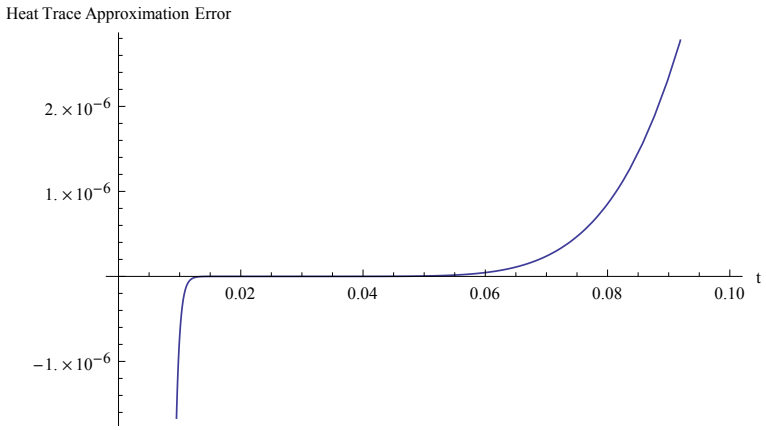

FIGURE 8.4.1. Agreement between the heat expansion and the heat trace computed from the spectrum, for small time (for a regular unit octagon). The excellent agreement means that we can make small changes in ϵ without affecting the result.

increase slightly as well. To obtain the same error bound as ours using their formula would therefore require the computation of more eigenvalues, at a computational cost. This less optimal bound can also be computed using the same Mathematica notebook which we use for our computations (see above for link).

In conclusion, using our error bound, we have the rigorous estimate

$$0.467573359 \leq \det \Delta_H \leq 0.467574158.$$

For verification purposes, the value computed using our Matlab implementation of Aurell-Salomonson's formula is

$$\det \Delta_H = 0.467573757402541\cdots$$

so in fact the first 8 decimal places of our approximation should be correct as they agree with the Aurell-Salomonson result. Again, note that the Aurell-Salomonson formula applies only tot he spectral determinant so we cannot use it to verify our Casimir energy estimate.

8.4.0.8. *Casimir energy error bounds.* For a choice of $\epsilon = 0.006$, the heat trace approximation error (Theorem 6.1) is 7.77156×10^{-7}. The spectral truncation error, that is, the error from taking finitely many eigenvalues (see Theorem 6.3), is 3.94851×10^{-9} The spectral approximation error, that is, the error we make by using approximated eigenvalues rather than their true values, is given by (6.3.1), and totals 1.09357×10^{-6}. Summing these errors up, we obtain the overall error estimate of 1.87471×10^{-6}. Therefore,

$$0.0268785 \leq \zeta_H(-\frac{1}{2}) \leq 0.0268822.$$

8.5. Arrowhead polygon

In this section, we compute the Casimir energy and spectral determinant of an irregular polygon shaped like an arrowhead, with rigorous theoretical error bounds.

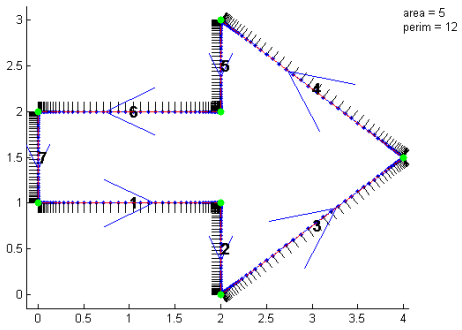

FIGURE 8.5.1. The geometry of the irregular arrowhead polygon, for which we compute spectral determinant and Casimir energy with explicit theoretical error bounds.

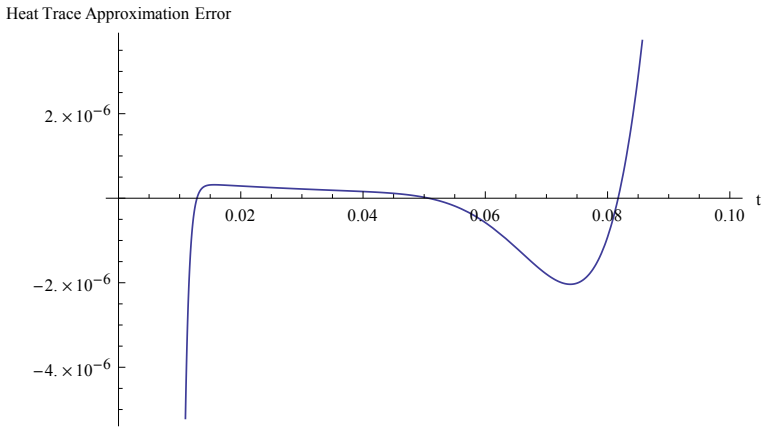

FIGURE 8.5.2. Agreement between the heat expansion and the heat trace computed from the spectrum, for small time (for the arrowhead shape). The agreement means that we can make small changes in ϵ without affecting the result.

The geometry can be seen in figure 8.5.1. We use MPSPack to obtain the approximate first 844 eigenvalues, along with error estimates. These eigenvalues can be found at http://bit.ly/1g25bcL. We are then able to use our error bounds to place a theoretically rigorous estimate on our overall error. Below in Figure 8.5.1, we plot the difference between the heat trace obtained from the spectrum and the heat trace approximated by the heat expansion, for small time. The excellent agreement between these two quantities for a large range of time ensures a priori that our calculation will be stable with small changes of ϵ. It also suggests that the heat approximation error should be small, although this will of course be confirmed rigorously by our error estimate.

Using Theorems 3.7 and 3.9, we obtain that for A the arrowhead shape in Fig. 8.5.1,

$$\det \Delta_A \approx 0.2042389\cdots$$

and

$$\zeta_A(-\frac{1}{2}) \approx 0.035252\cdots$$

We now compute the error bounds of these computations. The Mathematica notebook used to compute the determinant and zeta functions can be downloaded at http://bit.ly/Iq1hMh.

8.5.0.9. *Spectral determinant error bounds.* For a choice of $\epsilon = 0.008$, the heat trace approximation error (Theorem 6.1) is 7.9938×10^{-7}. The spectral truncation error, that is, the error from taking finitely many eigenvalues (see Theorem 6.3), is 2.82687×10^{-7}. The spectral approximation error, that is, the error we make by using approximated eigenvalues rather than their true values, is given by (6.3.1), and totals 5.9771×10^{-6}. The overall error estimate is therefore 7.05916×10^{-6}. For comparative purposes, the heat trace approximation error which we would obtain from using van den Berg and Srisatkunarajah's heat trace estimate (Theorem 2.55) would be 1.01917×10^{-4}, a few orders of magnitude worse than ours.

In conclusion, using our error bound, we have the rigorous estimate

$$0.204231080 \leq \det \Delta_H \leq 0.204245198$$

Using our Matlab implementation of Aurell-Salomonson's formula, we can check this, and find that the result using that formula is:

$$\det \Delta_H = 0.204238092020928\cdots$$

so in fact the first seven decimal places of our approximation agree with this.

8.5.0.10. *Casimir energy error bounds.* For a choice of $\epsilon = 0.008$, the heat trace approximation error (Theorem 6.1) is 2.56224×10^{-6}. The spectral truncation error, that is, the error from taking finitely many eigenvalues (see Theorem 6.3), is 8.74792×10^{-7} The spectral approximation error, that is, the error we make by using approximated eigenvalues rather than their true values, is given by (6.3.1), and totals 0.0000299471. Summing these errors up, we obtain the overall error estimate of 0.0000284463. Therefore,

$$0.0352236 \leq \zeta_H(-\frac{1}{2}) \leq 0.0352799.$$

We have varied ϵ within the region $0.0015 < \epsilon < 0.04$ and found that the first six significant digits of our spectral determinant and Casimir energy computations do not change. We therefore believe them to be correct.

8.6. L-Shaped Domain

In this section, we compute the Casimir energy and spectral determinant of an irregular polygon shaped like an arrowhead, with rigorous theoretical error bounds. The geometry can be seen in figure 8.6.1. We use MPSPack to obtain the approximate first 500 eigenvalues, along with error estimates. These eigenvalues can be found at http://bit.ly/1bFG6SO. We are then able to use our error bounds to place a theoretically rigorous estimate on our overall error. Below in Figure 8.6.1, we plot the difference between the heat trace obtained from the spectrum and the

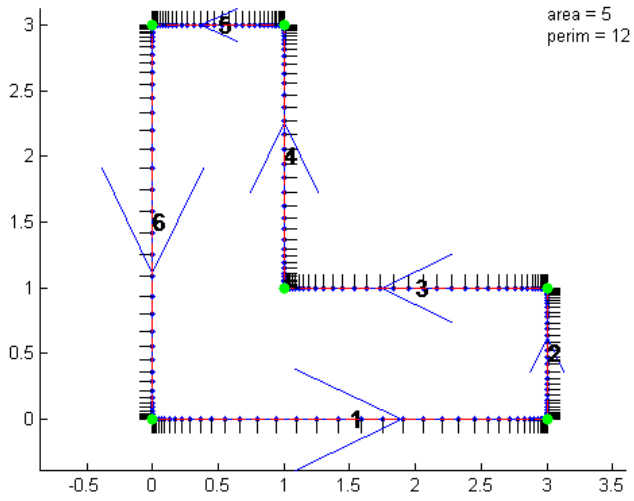

FIGURE 8.6.1. The geometry of the L-shaped domain for which we compute spectral determinant and Casimir energy with explicit theoretical error bounds.

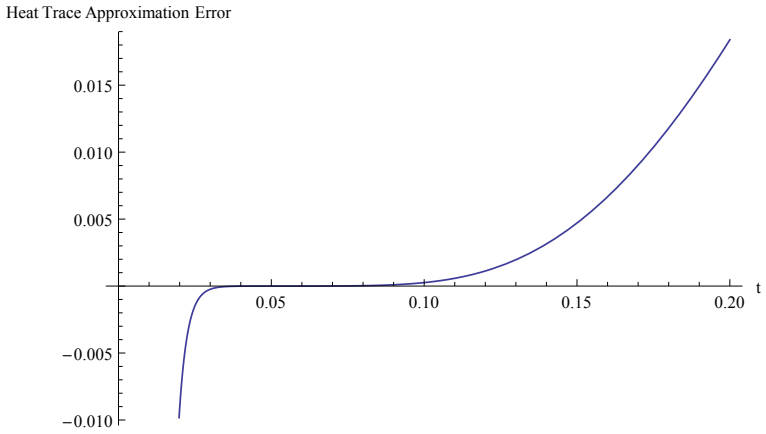

FIGURE 8.6.2. Agreement between the heat expansion and the heat trace computed from the spectrum, for small time (for the arrowhead shape). The agreement means that we can make small changes in ϵ without affecting the result.

heat trace approximated by the heat expansion, for small time. The excellent agreement between these two quantities for a large range of time ensures a priori that our calculation will be stable with small changes of ϵ. It also suggests that the heat approximation error should be small, although this will of course be confirmed rigorously by our error estimate.

Using Theorems 3.7 and 3.9, we obtain that for A the arrowhead shape in Fig. 8.6.1,

$$\det \Delta_A \approx 0.19412642\cdots$$

and

$$\zeta_A(-\frac{1}{2}) \approx -0.0795559\cdots$$

We now compute the error bounds of these computations. The Mathematica notebook used to compute the determinant and zeta functions can be downloaded at http://bit.ly/Iq1hMh.

8.6.0.11. *Spectral determinant error bounds.* For a choice of $\epsilon = 0.0028$, the heat trace approximation error (Theorem 6.1) is 2.35092×10^{-4}. The spectral truncation error, that is, the error from taking finitely many eigenvalues (see Theorem 6.3), is 3.40924×10^{-4}. The spectral approximation error, that is, the error we make by using approximated eigenvalues rather than their true values, is given by (6.3.1), and totals 7.45091×10^{-8}. The overall error estimate is therefore 0.000576091. For comparative purposes, the heat trace approximation error which we would obtain from using van den Berg and Srisatkunarajah's heat trace estimate (Theorem 2.55) would be 2.54982×10^{-4}, slightly worse than ours.

In conclusion, using our error bound, we have the rigorous estimate

$$0.19355 \leq \det \Delta_L \leq 0.194703.$$

Using our Matlab implementation of Aurell-Salomonson's formula, we can check this, the result according to this formula is:

$$\det \Delta_L = 0.194127996776785\cdots,$$

therefore the first five decimal places of our approximation agree with their formula and we believe them to be correct correct.

8.6.0.12. *Casimir energy error bounds.* For a choice of $\epsilon = 0.0029$, the heat trace approximation error (Theorem 6.1) is 4.53282×10^{-4}. The spectral truncation error, that is, the error from taking finitely many eigenvalues (see Theorem 6.3), is 5.48322×10^{-4} The spectral approximation error, that is, the error we make by using approximated eigenvalues rather than their true values, is given by (6.3.1), and totals 1.20390×10^{-7}. Summing these errors up, we obtain the overall error estimate of 0.00100172. Therefore,

$$-0.0805576 \leq \zeta_H(-\frac{1}{2}) \leq -0.0785542.$$

We have varied ϵ within the region $0.0015 < \epsilon < 0.04$ and found that the first six significant digits of our spectral determinant and Casimir energy computations do not change. We therefore believe them to be correct.

8.7. Extremal Properties of the Spectral Determinant in Polygons

We performed some numerical investigations into the extremal properties of the spectral determinant and within the class of n-sided polygons of fixed area. Namely, we tried to provide some numerical evidence to support the following conjecture:

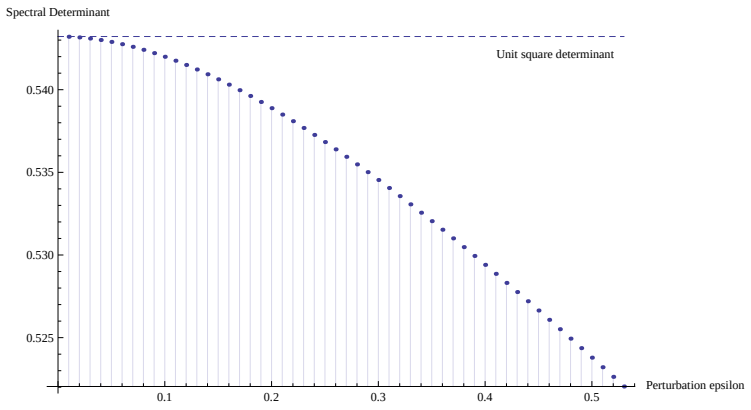

FIGURE 8.7.1. Spectral determinant for small perturbations of a unit square. As the perturbation gets smaller, the spectral determinant increases and converges to the spectral determinant of the unit square.

CONJECTURE 8.2. *In the class of n-sided polygons of fixed area, the spectral determinant is maximized by the regular polygon.*

There is some limited justification for this conjecture in the literature. For example, in [**58**] the authors show that within a conformal class the determinant is maximized by the sphere, leading to the speculation that maximal symmetry gives rise to maximum determinant. A close examination of the appendices of [**5**], where an explicit formula is provided for the spectral determinant of a polygon, shows that many terms in the formula are maximized for a regular polygon, although it is not clear whether this is true for all terms.

The experiment we made was to start with small perturbations of a square. The perturbation was achieved by moving one of the vertices (x, y) of the square a certain distance ϵ along the vector (x, y), with the magnitude of perturbation being defined to be ϵ. Computing values of the spectral determinant for various ϵ provides the plot in figure 8.7.1, that clearly shows that the spectral determinant is maximized when the magnitude of the perturbation is zero, i.e. for the square.

We then repeated the experiment for perturbations of various n-sided polygons for $3 \leq n \leq 10$. The results were the same in all cases with similarly shaped plots, which we will not produce here for the sake of brevity. In all cases we chose a suitable cutoff ϵ and computed sufficiently many eigenvalues for the error bound (computed like the previous section) of all computations to be accurate to within 10^{-4}. We verified this by computing the error estimate for the domain with the smallest γ (as this will produce the greatest error) and making sure that it was within the tolerance.

8.8. Casimir Energy of Cutouts

In this section we present some numerical results relating to the Casimir energy of cutouts. A **cutout** is a multiply connected Euclidean domain created by removing a smaller, possibly rotated copy of a simply connected Euclidean domain

from itself. For example, a square with a square-shaped hole in the middle. The question we will ask is: For what angle of rotation of the inner domain (the hole) is the Casimir energy minimized?

This question is interesting for applications because of the relationship that exists between the Casimir energy of solids corresponding to extruded planar domains, and the planar domains. More precisely, if one extrudes a cutout in the $x-y$ plane along the z axis, one obtains a multiply connected solid. For example, extruding a square with a square-shaped hole gives one a cuboid with a cuboid-shaped hole. Extruding a disk with a disk shaped hole (i.e. an annulus) produces an "empty cylinder" geometry. In practice it is possible to construct objects at the nano scale that are extruded cutouts, and thus to answer the question "which way should the hole be facing?" is important if one seeks to minimize Casimir interactions.

The relationship between the Casimir energy of the extruded solid and the one of the original planar domain is given by Theorem 8.3.

8.8.1. Casimir Energy of Extruded Planar Domains. Consider U an open, bounded subset of $\mathbb{R}^2$ with piecewise smooth, Lipschitz boundary. Now suppose we wish to compute the Casimir energy of its extrusion $M = S^1(L) \times U$ where $S^1(L) = \mathbb{R}/L\mathbb{Z}$. Such problems are interesting in nanophysics, where one extrudes a planar geometry, effectively extending it to have a cylindrical end. When one considers the problem on M, it is obvious that the energy will scale with the length L. Namely, the larger L, the larger the energy. Therefore we must consider the Casimir energy per unit length, that is, the Casimir energy as $L \to \infty$. It is natural to ask: how does $\zeta_M(-\frac{1}{2})$ relate to $\zeta_U(s)$, if at all? The answer is contained in the following Theorem, which we prove below for polygonal domains. Note that the same result holds true for more general domains, but the proof is trickier since one needs to be more careful about commuting limits and analytical continuation. In this special case, there are only three terms in the heat expansion, so the proof is technically simpler.

THEOREM 8.3. *Let D be a polygonal domain in $\mathbb{R}^2$ and $U = S^1(L) \times D$, where $S^1(L) = \mathbb{R}/L\mathbb{Z}$. Then for $s \in \mathbb{C} - \{1, \frac{3}{2}\}$, we have that*

$$\lim_{L\to\infty} \frac{\zeta_U(s)}{L} = \frac{\Gamma(s-\frac{3}{2})}{\Gamma(s)2\sqrt{\pi}}\zeta_D(s-\frac{1}{2}).$$

PROOF. Using the analytical continuation of the zeta function (Theorem 3.5), we have that for

$$\begin{aligned}\zeta_U(s) &= \frac{1}{\Gamma(s)}\int_0^\infty t^{s-1}(\mathrm{Tr}(\mathrm{e}^{-\Delta_U t}))dt \\ &= \frac{1}{\Gamma(s)}\int_0^\infty t^{s-1}(\mathrm{Tr}(\mathrm{e}^{-\Delta_D t})\mathrm{Tr}(\mathrm{e}^{-\Delta_{S^1(L)} t}))dt,\end{aligned}$$

and the factoring of the heat trace can be justified by noting that if λ_i are the eigenvalues of Δ_U and μ_i those of $\Delta^1_S(L)$, then the double sum

$$\mathrm{Tr}(\mathrm{e}^{-\Delta_U}) = \sum_k \sum_j \mathrm{e}^{-(\mu_k+\lambda_j)t}$$

is absolutely convergent and factors into the product of two sums corresponding to the individual heat traces of U and $S^1(L)$.

Now, we know the μ_i explicitly: $\mu_i = \frac{k^2\pi^2}{L^2}$. Therefore, we can write

$$\begin{aligned}\lim_{L\to\infty}\frac{\zeta_U(s)}{L} &= \lim_{L\to\infty}\frac{1}{L\Gamma(s)}\int_0^\infty t^{s-1}(\mathrm{Tr}(\mathrm{e}^{-\Delta_D t})\sum_{k=1}^\infty \mathrm{e}^{-\frac{k^2\pi^2}{L^2}t})dt\\ &= \lim_{L\to\infty}\frac{1}{L\Gamma(s)}\int_0^\infty t^{s-1}(\mathrm{Tr}(\mathrm{e}^{-\Delta_D t})(\frac{L}{\sqrt{\pi t}}\sum_{k=1}^\infty \mathrm{e}^{-\frac{L^2k^2}{\pi^2 t}} - \frac{L-\sqrt{\pi t}}{2\sqrt{\pi t}}))dt\end{aligned}$$

using the Poisson summation formula (Theorem 2.11). Now, partition the integral into two halves:

$$\begin{aligned}\lim_{L\to\infty}\frac{\zeta_U(s)}{L} &= \lim_{L\to\infty}\frac{1}{\Gamma(s)}\int_0^\epsilon t^{s-1}(\mathrm{Tr}(\mathrm{e}^{-\Delta_D t})(\frac{1}{\sqrt{\pi t}}\sum_{k=1}^\infty \mathrm{e}^{-\frac{L^2k^2}{\pi^2 t}t} - \frac{1-\sqrt{\frac{\pi t}{L^2}}}{2\sqrt{\pi t}}))dt\\ &\quad + \lim_{L\to\infty}\frac{1}{\Gamma(s)}\int_\epsilon^\infty t^{s-1}(\mathrm{Tr}(\mathrm{e}^{-\Delta_D t})(\frac{1}{\sqrt{\pi t}}\sum_{k=1}^\infty \mathrm{e}^{-\frac{L^2k^2}{\pi^2 t}t} - \frac{1-\sqrt{\frac{\pi t}{L^2}}}{2\sqrt{\pi t}}))dt\\ &= I_1(\epsilon)+I_2(\epsilon).\end{aligned}$$

Notice that $I_2(\epsilon)$ is convergent for all $s\in\mathbb{C}$ (see the proof of Theorem 3.5) and therefore

$$\begin{aligned}&\lim_{L\to\infty}\frac{1}{\Gamma(s)}\int_\epsilon^\infty t^{s-1}(\mathrm{Tr}(\mathrm{e}^{-\Delta_D t})(\frac{1}{\sqrt{\pi t}}\sum_{k=1}^\infty \mathrm{e}^{-\frac{L^2k^2}{\pi^2 t}t} - \frac{1-\sqrt{\frac{\pi t}{L^2}}}{2\sqrt{\pi t}}))dt\\ &\qquad = \frac{1}{2\sqrt{\pi t}\Gamma(s)}\int_\epsilon^\infty t^{s-\frac{3}{2}}(\mathrm{Tr}(\mathrm{e}^{-\Delta_D t}))dt\end{aligned}$$

by interchanging limits.

For $I_1(\epsilon)$, we can use the the heat expansion on D to obtain convergence in some half-plane, that we can make wider and wider by taking more terms in the asymptotic expansion. This will lead to an analytical continuation like the one we performed in the proof of Theorem 3.5, and will be meromorphic with poles at $s=1$ and $s=\frac{3}{2}$. For s outside these values, we can interchange limits to obtain the same equality:

$$I_1(\epsilon) = \frac{1}{2\sqrt{\pi t}\Gamma(s)}\int_0^\epsilon t^{s-\frac{3}{2}}(\mathrm{Tr}(\mathrm{e}^{-\Delta_D t}))dt.$$

Comparing with Theorem 3.5 completes the proof. □

8.8.2. Computation. The computation, which is not difficult, uses the rotational symmetry to reduce the three-dimensional problem to two dimensions, where it is far more tractable. In particular, the Casimir energy of the extruded solid depends on $\zeta(-1)$ of the original planar domain, and therefore in the following we compute this quantity instead of $\zeta(-1/2)$ for various angles of rotation of the hole geometry. We will be doing this on a cutout that is obtained by cutting a square out of a square. Due to difficulties in obtaining complete sets of eigenvalues from MPSPack for multiply connected domains it proved very difficult to perform more numerics for different geometries and the square was the only one that seemed to

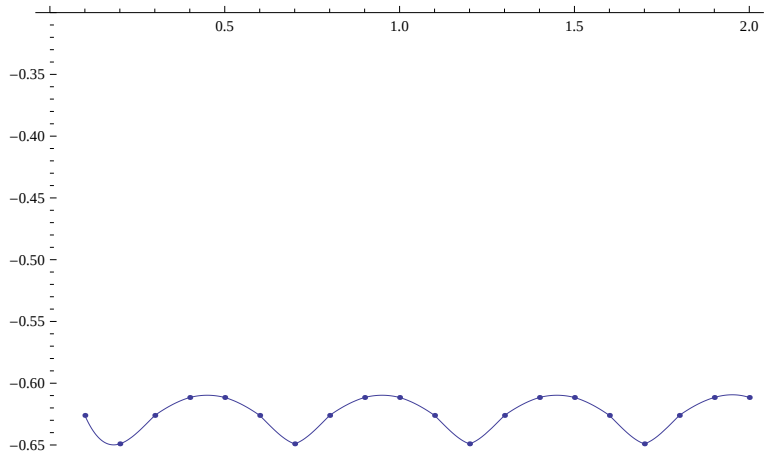

FIGURE 8.8.1. Plot of Casimir energy vs. rotation angle of inner square (as a multiple of π) with an interpolating curve. The geometry that minimized the Casimir energy is shown below. All points are accurate to within 0.003777.

work. The theoretical error estimates from MPSPack were especially large, and so the overall error of our calculation for all points was similarly increased. Its maximum value was 0.003777 according to our error estimates, so the computations below are only accurate to within this tolerance. Below is a plot of the geometry:

As the following plot shows, the Casimir interaction is minimized when the angle of rotation is $\pi/4$. The geometry of the object the minimizes the Casimir energy is shown in a further plot.

The geometry that minimized the Casimir energy is shown below:

8.9. Summary of Numerical Results

Below we summarize the examples of planar domains for which we computed the spectral determinant and $\zeta(-\frac{1}{2})$. In view of Theorem 8.3 we also add the values of

$$Z_U := \lim_{s\to-\frac{1}{2}} \left(\frac{\Gamma(s-\frac{3}{2})}{\Gamma(s)2\sqrt{\pi}} \zeta_U(s-\frac{1}{2}) \right)$$

as they can be used to directly compute the Casimir energy of the extruded solid. Note that because the residue of the simple pole of the Gamma function at a negative integer n is given by $\frac{(-1)^n}{n!}$, we have that

$$Z = \frac{1}{4\sqrt{\pi}\Gamma(-\frac{1}{2})} \int_0^\infty t^{-2} \mathrm{Tr}(\mathrm{e}^{-\Delta_U t}) dt.$$

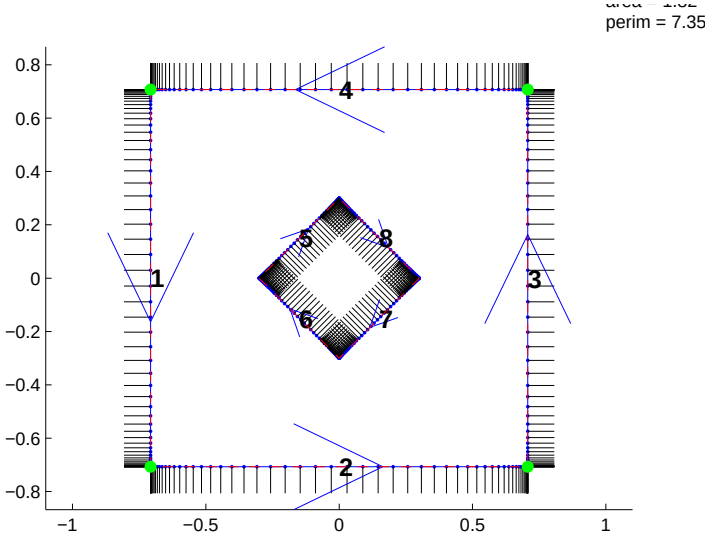

FIGURE 8.8.2. When rotating the inner square, an angle of $\pi/4$ minimized the Casimir energy.

TABLE 1. Summary of numerical results

Polygon	Spectral Determinant	$\zeta(-\frac{1}{2})$	Z
Unit Regular Pentagon	$0.461436914\cdots$	$0.0421024\cdots$	$0.00125292\cdots$
Unit Regular Hexagon	$0.464460686\cdots$	$0.0345513\cdots$	$0.000723416\cdots$
Unit Regular Heptagon	$0.466359979\cdots$	$0.0300049\cdots$	$0.000391465\cdots$
Unit Regular Octagon	$0.467573753\cdots$	$0.0268804\cdots$	$0.000145477\cdots$
Arrowhead Domain	$0.2042389\cdots$	$0.035252\cdots$	$0.352499\cdots$
L-Shaped Domain	$0.19412642\cdots$	$-0.0795559\cdots$	$-0.018441\cdots$

CHAPTER 9

Conclusion and future study

It was the objective of this thesis to develop a computational framework for the spectral determinant and Casimir energy for planar domains. Additionally, we provide rigorous error bounds in the case that the domain is polygonal. To improve the error estimate, we build on van den Berg and Srisatkunarajah's heat trace estimate for polygons ([**75**]), improving the constant in the exponent. Our Mathematica and Matlab tools also support automatic computation of any regular value of the spectral zeta function, and our error estimates can be easily modified to accomodate for this increased generality.

We also attempted to create an eigenvalue solver for polygonal domains using a partition of unity method. While the method allows for statement of the problem with greatly reduced complexity, as well as accurate computation of eigenvalues (we obtained the first 20 digits for the principal eigenvalue of the unit regular hexagon, in agreement with Alex Barnet's MPSPack up to machine precision), the efficiency of the algorithm was unexpectedly poor and greatly outperformed by existing packages, namely MPSPack, which was up to 40 times faster. Further study should be done to determine whether this is due to an inefficient implementation or whether the method itself is theoretically bound to be slower than boundary element methods.

Finally, we applied our tools to investigate extremal properties of the Casimir energy and spectral determinant. We provide some evidence to support the conjecture that within the class of n-sided polygons of fixed area, the regular polygon maximizes the spectral determinant. We also investigate the behavior of the Casimir energy of various "cutout" geometries, that is, a polygonal domain with a smaller polygonal domain cut out of its interior. We investigate optimal rotation angles when the cutout is a scaled version of the larger domain's and what happens to the Casimir energy when the smaller domain is placed closer and closer to the boundary of the larger domain. These are both problems interesting in physics.

Bibliography

[1] M. Abramowitz and I. Stegun. *Handbook of Mathematical Functions*. Dover books, 1970.

[2] R.A. Adams. *Sobolev Spaces*. Academic Press, 1975.

[3] K. Aehlig, H. Dietert, T. Fischbacher, and J. Gerhard. Casimir Forces via Worldline Numerics: Method Improvements and Potential Engineering Applications.

[4] Phillip R. Atkins, Qi I. Dai, Wei E. I. Sha, and Weng C. Chew. Casimir Force for Arbitrary Objects Using the Argument Principle and Boundary Element Methods. *Progress In Electromagnetics Research*, 142:615–624, 2013.

[5] E. Aurell and P. Salomonson. On Functional Determinants of Laplacians in Polygons and Simplices, February 2008. arXiv:hep-th/9304031v1.

[6] R. Aurich, M. Sieber, and F. Steiner. Quantum Chaos of the Hadamard-Gutzwiller Model. *Physical Review Letters*, 61:483–487, 1988.

[7] I. Babuska. Error-bounds for finite element method. *Numerische Mathematik*, 16:322–333, 1971.

[8] I. Babuska. The partition of unity finite element method: basic theory and applications. *Computer methods in applied mechanics and engineering*, 1996.

[9] I. Babuska and J.M. Melenk. The partition of unity finite element method. *Internat. J. Numer. Methods Engrg.*, 40:727–758, 1997.

[10] R. E. Bank and M. J. Holst. A new paradigm for parallel adaptive mesh refinement. *SISC*, 22(4):1411–1443, 2000.

[11] A. Barnett and T. Betcke. Stability and convergence of the method of fundamental solutions for Helmholtz problems on analytic domains. *J. Comp. Phys.*, 2008.

[12] A. H. Barnett and T. Betcke. An exponentially convergent nonpolynomial finite element method for time-harmonic scattering from polygons. *SIAM Journal on Scientific Computing*, 32(3):1417–1441, 2010.

[13] J.D. Barrow. *The book of nothing: vacuums, voids, and the latest ideas about the origins of the universe*. Pantheon Books, 2000.

[14] T. Betcke and L. Trefethen. Reviving the method of particular solutions. *SIAM Review*, pages 469–491, 2005.

[15] P.H.G.M Blockland and J.T.G Overbeek. Van der Waals forces between objects covered with a chromium layer. *J. Chem. Soc. Far. Trans. I*, 74:2637–2651, 1978.

[16] G. Bressi, G. Carugno, R. Onofrio, and Ruoso G. Measurement of the casimir force between parallel metallic surfaces. *Phys. Rev. Lett.*, 88, 2002.

[17] J.K. Brooks. Representations of Weak and Strong Integrals in Banach Spaces. *PNAS*, 63:266–270, 1969.

[18] F. Capasso, J.N. Munday, D. Ianuzzi, and H.B. Chan. Casimir forces and quantum electrodynamical torques: Physics and nanomechanics. *IEEE J. Selected Topics in Quant. Elec*, 13:400–415, 2007.

[19] H.B.G Casimir. On the attraction between two perfectly conducting plates. *Proc. Kon. Nederland. Akad. Wetensch*, B51:793, 1948.

[20] G. Chardon and L. Daudet. Low-complexity computation of plate eigenmodes with Vekua approximations and the Method of Particular Solutions. arXiv:1301.0908.

[21] R. Courant. Variational methods for the solution of problems of equilibrium and vibrations. *Bull. Amer. Math. Soc.*, 1943.

[22] T. A. Cruise and F. J Rizzo. A direct formulation and numerical solution of the general transient elastodynamic problem. *Journal of Mathematical Analysis and Applications*, 22(1):244–259, 1968.

[23] B. Dacorogna. *Introduction to the Calculus of Variations*. Imperial College Press, 2004.

[24] D. Dalvit, P. Milonni, D. Roberts, and F. da Rosa. *Casimir Physics*. Springer, 2011.
[25] E.B. Davies. *Heat Kernels and Spectral Theory*. Cambridge University Press, 1989.
[26] J. Demmel, M. Gu, and S. Eisenstat. Computing the singular value decomposition with high relative accuracy. *Linear Algebra and its Applications*, 299:21–80, 1999.
[27] S.J Dilworth and M. Girardi. Nowhere Weak Differentiability of the Pettis Integral. *Quaestiones Math.*, pages 365–380, 1995.
[28] J. Dowker and J. Apps. Further Functional Determinants. *Class. Quant. Grav.*, 12:1363–1383, 1995.
[29] H. Epstein, V. Glaser, and A. Jaze. *Nuovo Cimento*, 36, 1965.
[30] Lawrence C. Evans. *Partial Differential Equations*. American Mathematical Society, 1998.
[31] H. Fox, P. Henrici, and C. Moler. Approximations and bounds for eigenvalues of elliptic operators. *SIAM Journal on Numerical Analysis*, 4:89–102, 1967.
[32] D. Gilbarg and N.S. Trudinger. *Elliptic Partial Differential Equations*. Springer, 1998.
[33] Peter B. Gilkey. *Invariance Theory, the Heat Equation, and the Atiyah-Singer Index Theorem*. CRC Press, 1994.
[34] C. Gordon, D.L. Webb, and S. Wolpert. One Cannot Hear the Shape of a Drum. *Bulletin of the AMS*, 27:134–138, 1992.
[35] M. Griebel and M.A. Schweitzer. A particle-partition of unity method for the solution of elliptic, parabolic, and hyperbolic PDEs. *SISC*, 22:853–890, 2000.
[36] D. Grieser. Uniform bounds for eigenfunctions of the Laplacian on manifolds with boundary.
[37] P. Grisvard. *Elliptic Problems in Nonsmooth Domains*. Pitman, 1985.
[38] G.H. Hardy and J.E. Littlewood. Contributions to the Theory of the Riemann Zeta-Function and the Theory of the Distribution of Primes. *Acta Mathematica*, 41:119Ũ196, 1916.
[39] A. Hassell. Lectures on the Wave Equation. 2005.
[40] A. Hassell and A.H. Barnett. Estimates on Neumann eigenfunctions at the boundary, and the ŞMethod of Particular SolutionsT̃ for computing them. *Spectral Geometry*, 84:195, 2012.
[41] L. Hormander. The spectral function of an elliptic operator. *Acta Math.*, 121:193–218, 1968.
[42] L. Hormander. *The analysis of linear partial differential operators I*. Grundl. Math. Wissenschaft., 1983.
[43] F. Intravia. Strong Casimir force reduction through metallic surface nanostructuring. *Nature Communications*, 4, 2013.
[44] M.A. Jawson. Integral equation methods in potential theory-I. *Proc. R. Soc. A*, 1963.
[45] M. Kac. Can One Hear the Shape of a Drum? *American Mathematical Monthly*, 73:1–23, 1966.
[46] D. Kammler. *A First Course in Fourier Analysis*. Prentice Hall, 2000.
[47] C. Klein, A. Kokotov, and D. Korotkin. Extremal properties of the determinant of the Laplacian in the Bergman metric on the moduli space of genus two Riemann surfaces. *Mathematische Zeitschrift*, 261:72–108, 2009.
[48] V. A. Kondratiev. Boundary-value problems for elliptic equations in domains with conical or angular points. *Trans. Moscow Math. Soc.*, 16:227–313, 1967.
[49] E. Kreyszig. *Introductory Fuctional Analysis with Applications*. Wiley, 1989.
[50] H. Kumagai. The determinant of the Laplacian on the n-sphere. *Acta Arithmetica*, 3:199–208, 1999.
[51] S.K. Lamoreaux. Demonstration of the casimir force in the 0.6 to 6 microm range. *Phys. Rev. Lett.*, 78, 1997.
[52] P.D. Lax and R.D. Richtmayer. Survey of the stability of linear finite difference equations. *Communications on Pure and Applied Mathematics*, 9:267–293, 1956.
[53] P Li and S.T Tau. On the Schrodinger Equation and the Eigenvalue Problem. *Comm. Math. Phys*, 88:309–318, 1983.
[54] E. Lieb and M. Loss. *Analysis*. American Mathematical Society, 1997.
[55] Daryl Logan. *A First Course in the Finite Element Method*. Cengage Learning, 2012.
[56] J. Lussange, R. Gurout, and A. Lambrecht. Casimir energy between nanostructured gratings of arbitrary periodic profile. *Physical Review A*, 86, 2012.
[57] R. Onofrio. Casimir forces and non-Newtonian gravitation. *New J. Phys.*, 8:237, 2006.
[58] R. Phillips, B. Osgood, and P. Sarnak. Extremals of Determinants of Laplacians. *Journal of Functional Analysis*, 80:148–211, 1988.
[59] M.H. Protter and H.F. Weinberger. *Maximum Principles in Differential Equations*. Springer, 1984.

[60] D.B. Ray and I.M. Singer. R-Torsion and the Laplacian on Riemannian Manifolds. *Advances in Mathematics*, 7:145–210, 1971.
[61] M. Reed and B. Simon. *Methods of Modern Mathematical Physics*. Academic Press, 1980.
[62] Z. Rodriguez, F. Zou, and Z. Marcet. Geometry-dependent casimir forces on a silicon chip.
[63] S. Rosenberg. *The Laplacian on a Riemannian Manifold*. Cambridge University Press, 1997.
[64] Y. Safarov. Fourier Tauberian Theorems and Applications. *Journal of Functional Analysis*, 185:111–128, 2001.
[65] M.J. Sparnaay. *Physica*, 24:751, 1958.
[66] Y. N. Srivastava, A. Widom, S. Sivasubramanian, and M. Pradeep Ganesh. Static and Dynamic Casimir Effect Instabilities. *Phys. Rev. A*, 2005.
[67] K. Stewartson and R. Waechter. On hearing the shape of a drum: further results. *Math. Proc. Camb. Philos. Soc.*, 69:353–363, 1971.
[68] A. Strohmaier and V. Uski. An Algorithm for the Computation of Eigenvalues, Spectral Zeta Functions and Zeta-Determinants on Hyperbolic Surfaces. *Communications in Mathematical Physics*, 317:827–869, 2013.
[69] T. Sunada. Riemannian coverings and isospectral manifolds. *Annals of Mathematics*, 121:169–186, 1985.
[70] G.T. Symm. Integral equation methods in potential theory. *Proc. R. Soc. Lond. A*, 1963.
[71] M.E. Taylor. *Partial Differential Equations*. Springer.
[72] L.N. Trefethen and D. Bau. *Numerical Linear Algebra*. SIAM, 1997.
[73] M. van den Berg. Bounds on Green's Functions of second-order differential equations. *J. Math. Phys*, 22:2452–2487, 1981.
[74] M. van den Berg. Heat Equation and the Principle of Not Feeling the Boundary. *Proc. Royal Soc. Edinburgh*, 122A:257–262, 1989.
[75] M. van den Berg and S. Srisatkunarajah. Heat Equation for a Region in R2 with a polygonal boundary. *J. London Math. Soc.*, 37:119–127, 1988.
[76] I. Varma. *Sums of Squares, Modular Forms, and Hecke Characters*. PhD thesis, Leiden University, 2010.
[77] H. Weyl. ber die asymptotische Verteilung der Eigenwerte. *Nachrichten der Kniglichen Gesellschaft der Wissenschaften zu Gttingen*, pages 110–117, 1911.
[78] L. C. Wrobel and M. H. Aliabadi. *The Boundary Element Method*. Wiley, 2002.
[79] B.F. Zalewski, R.L. Mullena, and R.L. Muhanna. Interval Boundary Element Method in the Presence of Uncertain Boundary Conditions, Integration Errors, and Truncation Errors. *Engineering Analysis with Boundary Elements*, 33:508–513, 2009.
[80] S. Zelditch. Inverse spectral problem for analytic plane domains II: Z_2-symmetric domains. *Annals of Mathematics*, 70:205–269, 2009.
[81] O. C. Zienkiewicz, R. L. Taylor, and J. Z. Zhu. *The Finite Element Method: Its Basis and Fundamentals*. Butterworth-Heinemann, 2005.
[82] M. Zlamal. On the finite element method. *Numerische Mathematik*, 1968.
[83] Z. Rodriguez A.W. Reid M.T.H McCauley A.P. Kravchenko I.I. Lu T. Bao Y. Johnson S.G. Chan H.B. Zou, F. Marcet. Geometry-dependent Casimir forces on a silicon chip. *http://arxiv.org/abs/1207.6163*.